Fakultät Wissenschaftszentrum Weihenstephan für Ernährung,
Landnutzung und Umwelt

Professur für Ökoklimatologie

Climate extremes and variability, and their ecological impacts

Michael Christian Matiu

Vollständiger Abdruck der von der Fakultät Wissenschaftszentrum Weihenstephan für Ernährung, Landnutzung und Umwelt der Technischen Universität München zur Erlangung des akademischen Grades eines

Doktors der Naturwissenschaften (Dr. rer. nat.)

genehmigten Dissertation.

Vorsitzender:		Prof. Dr. Thomas Knoke
Prüfer der Dissertation:	1.	Prof. Dr. Annette Menzel
	2.	Prof. Donna Ankerst, Ph.D.

Die Dissertation wurde am 27. Juni 2017 bei der Technischen Universität München eingereicht und durch die Fakultät Wissenschaftszentrum Weihenstephan für Ernährung, Landnutzung und Umwelt am 24. Juli 2017 angenommen.

Contents

Abstract

Climate change leads to increasing global mean temperatures and with higher mean temperatures also different extreme temperatures are expected in the future. These extremes have larger impacts on ecology than a gradual rise of mean temperatures. However, whether the change in temperature extremes has been in line with changes in mean temperature or accompanied with additional changes in variability and symmetry is not yet clear. Moreover, climate extremes are multifactorial: Drought, for instance, depends on precipitation and temperature, and identifying impacts strongly depends on interactions between the critical causing variables.

In this thesis, the changes in temperature mean, variability, and extremes were quantified simultaneously. Futhermore, impacts of climate variability on global crop yields were identified. And finally, the ecological succession after an extreme event was monitored. For this purpose, statistical methods were used, such as quantile regression, mixed effects models, and generalized additive models, with a focus on interactions and adequate error covariance structures, as well as automated image analysis.

The obtained results led to the conclusion that temperature changed asymmetrically, that is changes in hot or cold extremes were not identical and also not linked to mean temperature changes. Regarding the effects of climate variability, interactions played a key role for crop yields: Temperature and drought interactions caused a significantly different temperature effect depending on moisture conditions, such that, depending on crop, low water availability exacerbated or high water availability diminished the effect of high temperatures. Thus, effects of temperature would be over- or underestimated if interactions were not considered. The succession in a spruce forest after a major wind-throw was monitored using a combination of digital photography, remote sensing, and turbulent CO_2 exchange. The increased productivity shown in the CO_2 flux footprint was mirrored in trends of camera greenness and remotely sensed vegetation indices.

Zusammenfassung

Klimawandel bedeutet einen Anstieg der globalen Durchschnittstemperatur. Dieser Anstieg, sprich höhere Temperaturen, wird Auswirkungen auf die zu erwartenden Temperaturextreme in der Zukunft haben. Genau diese Extreme wirken sich stärker auf die Ökologie aus als ein kontinuierlicher Anstieg der mittleren Temperatur. Zu klären bleibt, ob sich die Temperaturextreme analog zur mittleren Temperatur verändert haben oder ob sich zusätzlich die Variabilität und Symmetrie der Temperaturverteilung verändert haben und welchen Einfluss all dies auf Extreme hat. Zudem sind Klimaextreme multifaktoriell: Dürre, zum Beispiel, hängt vom Niederschlag und der Temperatur ab. Somit bedingen sich die damit zusammenhängenden Auswirkungen durch die Wechselwirkungen zwischen den verursachenden Faktoren.

Die vorliegende Dissertation hat zum einen die Quantifizierung der Änderungen im Mittelwert, Variabilität und Extreme der Temperaturverteilung zum Thema. Zum anderen werden die Einflüsse von Klimavariabilität hinsichtlich globaler Ernteerträge bestimmt, sowie die Sukzession nach einem klimatischen Extremereignis. Hierfür finden statistische Methoden, insbesondere Quantilregression, gemischte Modelle und generalisierte addivitive Modelle, sowie eine neuartige Bildverarbeitung Anwendung. Ein besonderes Augenmerk liegt dabei auf Interaktionen zwischen Erklärvariablen und einer passenden Modellierung der Fehlerkovarianz.

Die Ergebnisse zeigen, dass sich Temperatur asymmetrisch verändert hat, das heißt die Änderungen der kalten und warmen Extreme sind nicht identisch und stehen nicht im Einklang mit den Veränderungen der mittleren Temperatur. Hinsichtlich der Klimavariabilität waren Wechselwirkungen zwischen Temperatur und Dürre entscheidend für deren Einfluss auf Ernteerträge. Der Effekt von zu hohen Temperaturen war, abhängig von der Feldfrucht, größer bei trockenen Bedingugnen und schwächer bei feuchten Bedingungen. Werden die Wechselwirkungen nicht berücksichtigt, kommt es zu einer Über- beziehungsweise Unterschätzung des Temperatureffektes. Schließlich wurde die ökologische Sukzession in einem Fichtenwald nach einem Windwurf mithilfe von Digitalfotografie, Fernerkundung und turbelentem CO_2-Austausch nachverfolgt. Die erhöhte Produktivität des Waldes, basierend auf den Messungen der CO_2-Flüsse, wurde ebenfalls durch Trends in Vegetationsindizes, die aus Kamera- und Fernerkundungsdaten berechnet wurden, wiedergegeben.

1. Introduction

Scientists divide the history of our planet into epochs such as the Pleistocene, the Pliocene and the Miocene. Officially, we live in the Holocene epoch. Yet it may be better to call the last 70,000 years the Anthropocene epoch: the epoch of humanity. For during these millennia Homo sapiens *became the single most important agent of change in the global ecology.*
— Yuval Noah Harari, *Homo Deus*

The planet earth has seen many revolutions in its ecology during the 4.6 billion years of its existence. The first large one was the emergence of cyanobacteria 2.1 billion years ago, which were capable of producing their own food through photosynthesis with oxygen as by-product. Consequently, the amount of oxygen in the atmosphere increased from basically none to ~10% in a very short period of time, ecologically speaking. This is one of the first examples that "living things" brought massive change to their own environment. Cyanobacteria changed the atmosphere, almost eliminated competitors, which could not survive with oxygen in the atmosphere, and changed the course of what life on earth would become.

Today, it is *Homo sapiens* that brings massive change to the global ecology at - speaking in ecological time frames - the speed of light. Technology has increased the speed of change such that for an adult now it becomes unimaginable how the world will look like when he will die - contrary to the previous hundreds and thousand of years, where change happened slowly.

In contrast to previous ecological revolutions, the current agent of change, *Homo sapiens*, also has the awareness of what he is doing. Anthropogenic climate change is a fact, and even climate change deniers cannot deny how humans have changed the planet. Since the earth provides the very foundation for human life, its future should be treated with responsibility. Globalization unified humans across the planet, economically, culturally, and personally. From tribes of hunters and gatherers to ancient city states to national states to supranational entities, the next logical step would be a global community of *Homo sapiens*, which is required to deal with the global problems humankind currently faces.

For such a community to take appropriate actions, a solid and unbiased information basis is required, which science can provide. As such, science needs to engage in open communication with society, elaborating on what is already known, and what is

still unknown. The following thesis deals with the already known on climate change, and elaborates on the still unknown of the changes in climate variability and extremes, and their impacts on selected ecological systems.

1.1. Changes in temperature variability and extremes

Climate is what we expect, weather is what we get.
— Robert A. Heinlein

Temperature is one of the main factors in ecological studies, because it is a direct driving force for many ecological systems and is closely linked to other driving parameters (Nemani et al. 2003). Thus it can serve as a versatile proxy. Impacts from the hot tail of the temperature distribution operate through heat waves, which contribute to human mortality (Patz et al. 2005) and crop failure (Olesen and Bindi 2002). At the cold tail, increased variability affects species distribution (Gloning, Estrella, and Menzel 2013) and population growth (Roland and Matter 2012). Correct assessment of climate variability and extremes is important for the tools and methods required for applied climate impact research, including the downscaling of climate model outputs, risk assessment, and the determination of ecological climate change experimental settings (Thompson et al. 2013).

How have the expectations on weather changed so far? With increasing mean global temperatures, more warm and less cold weather should be expected, that is more hot extremes and less cold extremes. The theoretical motivation to infer changes in temperature extremes from the changes in mean and variability of the temperature distribution gained much attraction through the IPCC (Intergovernmental Panel on Climate Change) reports, especially since the third report (Folland et al. 2001).

This concept of the relationship between changes in mean, variance and extremes is illustrated with schematic graphs of probability density functions (see Figure 1). If only the mean temperature increases and variability stays constant, more warm extremes and less cold extremes are expected. If, additional to the increase in mean temperature, variability increases as well, much more warm extremes are expected than with only an increase in mean temperature, and the change in cold extremes is less.

In 2012 the SREX (Special Report on Extreme Events), published by the IPCC, see IPCC (2012), extended the concept by including the possibility of changes in the symmetry (Figure 2). Such changes in symmetry would result in changes of extremes,

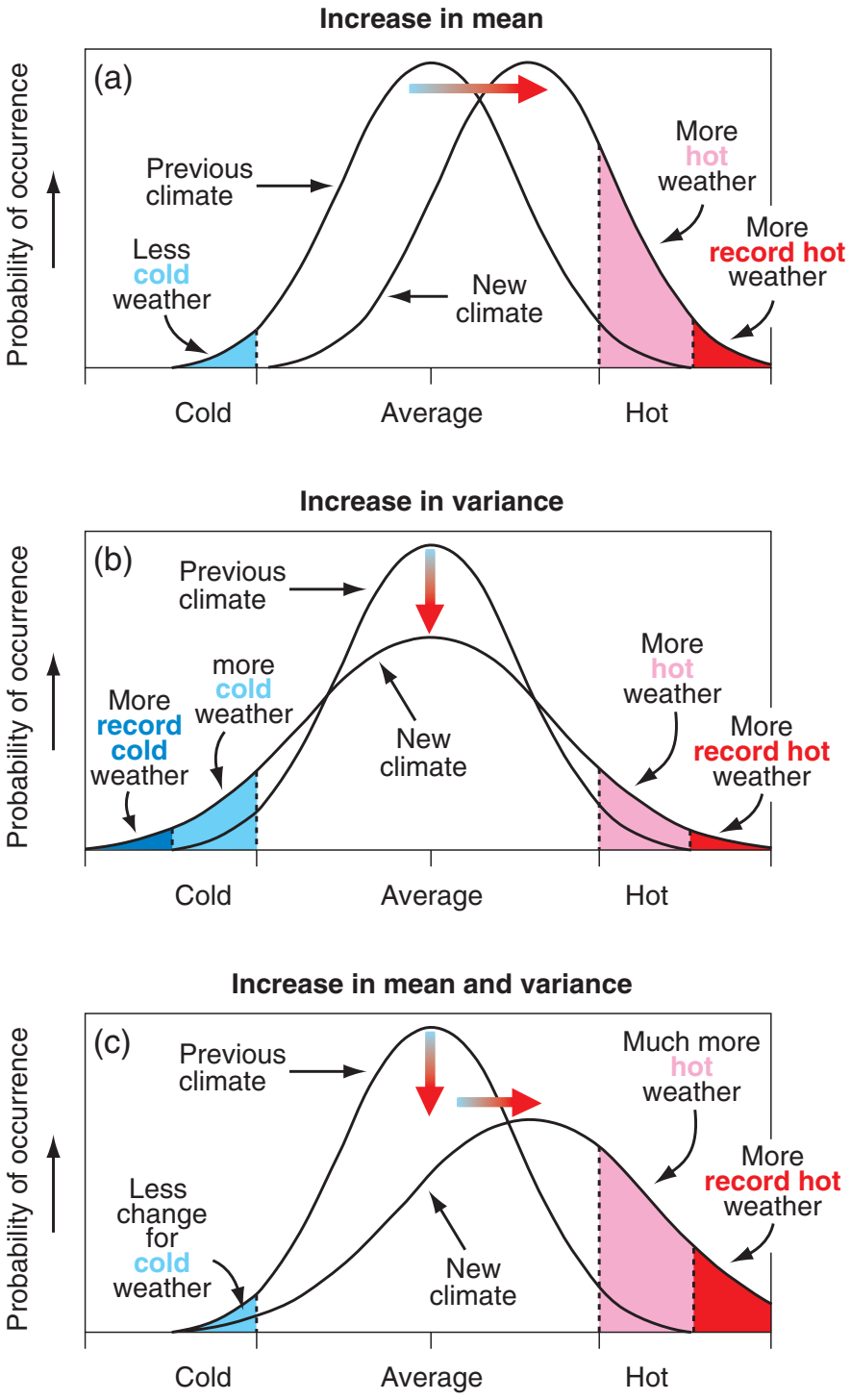

Figure 1 Schematic showing the effect on extreme temperatures for a normal distribution of temperature when (a) the mean temperature increases, (b) the variance increases, and (c) when both the mean and variance increase. Figure and caption are Figure 2.32 in Folland et al. (2001).

even if the mean stayed constant. Depending on how the symmetry changed, more cold or warm extremes would be expected.

Following the IPCC reports, many studies examined trends in the variability of the observed temperature changes (see Matiu, Ankerst, and Menzel (2016) for an overview of published literature until 2014). They differed in multiple aspects:

1. Variability metric: Mostly used was the SD (Standard Deviation), which assumes normality, or robust quantile-based metrics, and rarely other metrics.
2. Time base for variability metric: Seasonal, annual, or decadal.
3. Underlying data resolution: Mostly daily and monthly temperature values.
4. Time frame to detect trends: From several decades to up to more than 100 years.
5. Spatial extent: While trends could be calculated on a per station basis, some studies aggregated over similar climatic regions.

All these differences make a unifying assessment difficult, which is why the debate on how temperature variability has changed is ongoing (Alexander and Perkins 2013). While extremes can be predicted from the mean, SD, and skewness of the temperature probability density function (Ballester, Giorgi, and Rodó 2010), it is a rather cumbersome approach to assess changes in extremes. Another approach would be looking at the whole temperature distribution and the changes thereof, for example with quantile regression (Barbosa, Scotto, and Alonso 2011; Lee, Baek, and Cho 2013; Reich 2012; Rhines et al. 2016).

But why is climate variability so important? Because at the very edge of climate variability lie climate extremes, which have large impacts on socio-economies (Easterling et al. 2000), human health (O'Neill and Ebi 2009), and terrestrial ecosystems (Reyer et al. 2013).

The study of extremes is complicated mainly by two issues. First, an extreme event is multifactorial, which means it is an interplay of multiple causing factors. In the example of drought, it is a lack of water, primarily caused by a lack of precipitation (Mishra and Singh 2010). However, high temperatures and strong winds increase evaporation and transpiration rates, together called evapotranspiration, leading to increased loss of water. Moreover soil properties might accelerate or slow down the rate of water loss (Qin, Hu, and Oenema 2015). Second, an extreme cause can have an extreme impact, or not. The impacts depend on the system studied, whether it is from society, economy or ecology, and how adapted and resilient the system is.

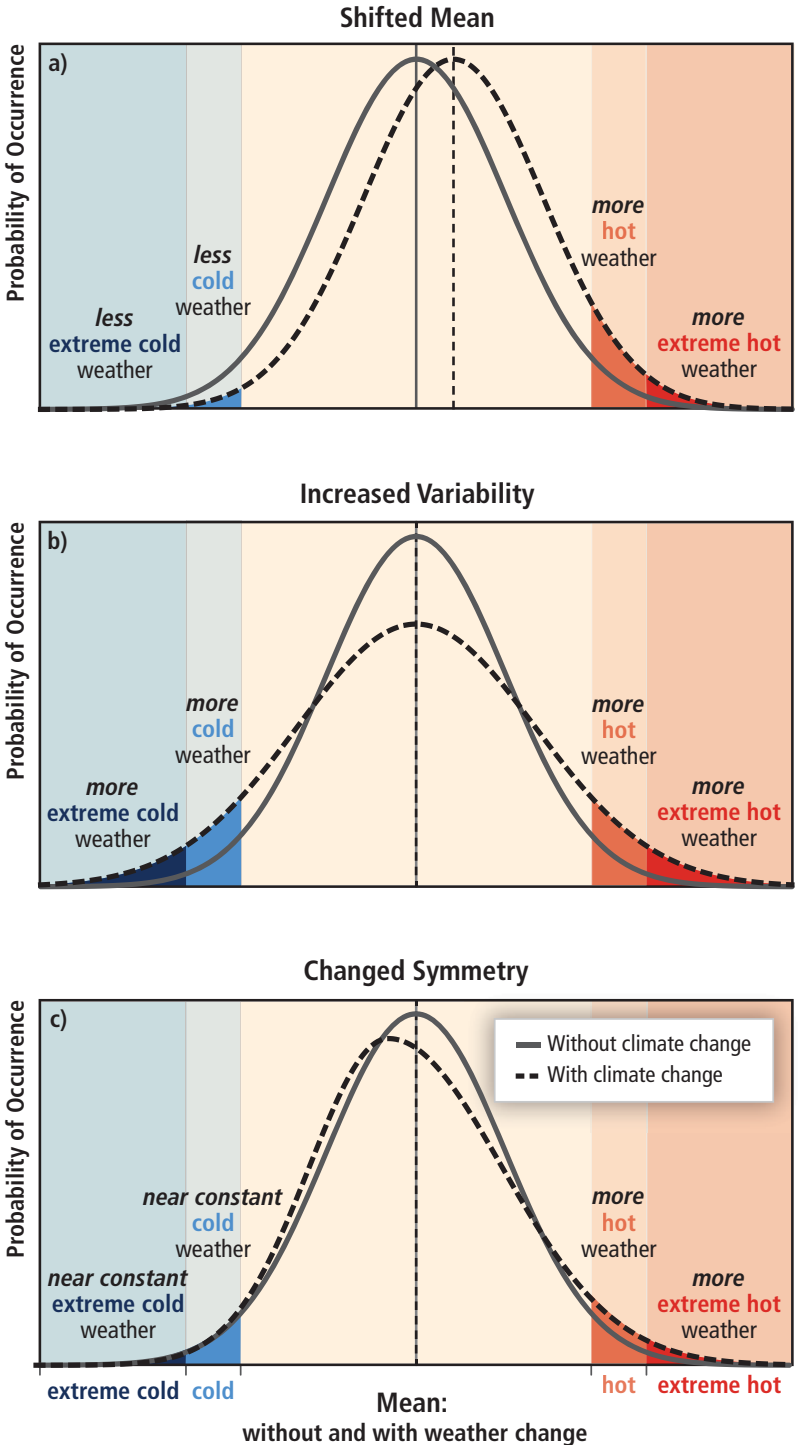

Figure 2 The effect of changes in temperature distribution on extremes. Different changes in temperature distributions between present and future climate and their effects on extreme values of the distributions: (a) effects of a simple shift of the entire distribution toward a warmer climate; (b) effects of an increase in temperature variability with no shift in the mean; (c) effects of an altered shape of the distribution, in this example a change in asymmetry toward the hotter part of the distribution. Figure and caption are Figure SPM.3 in IPCC (2012).

Continuing the drought example from before and focusing on impacts on crop yields, a drought of the same intensity can lead to a large range of yield losses depending on, for example, whether irrigation is provided (Troy, Kipgen, and Pal 2015), how adapted the crops are to drought conditions, or in what developmental stage the crops are.

1.2. Impacts of climate variability and extremes

> *Changes in temperature, water availability and atmospheric composition will affect most plants, animals and micro-organisms in some way. Any increase in climate variability, especially in extreme events, would have greater ecological effects than a change in mean conditions.*
>
> — Ecological Society of Australia

Extremes and variability have impacts on a wide range of systems, both natural and man-made, and giving an extensive account on all possible impacts would be beyond the limits of this thesis. Consequently, selected impacts will be presented, first on crop yields (Section 1.2.1), which are important in a global context, and second the ecological succession of a forest ecosystem (Section 1.2.2), which is representative for a wider array of impacts.

1.2.1. Crop yields

Agriculture is the foundation for feeding the 7.5 billion people living on the planet as of 2017. The associated concept of *food security* was defined by the World Summit on Food Security in 2009 held at the FAO (Food and Agriculture Organization of the United Nations) as follows (FAO 2009):

> "Food security exists when all people, at all times, have physical, social and economic access to sufficient, safe and nutritious food to meet their dietary needs and food preferences for an active and healthy life. The four pillars of food security are availability, access, utilization and stability."

Climate affects all four pillars, but with different magnitudes (Porter et al. 2014). The largest influence is on food availability or supply. Here, the supply of staple crops, such as maize, rice, soybeans, and wheat is the most important, since they represent approximately 75% of the calories in human diets (Cassman 1999; Roberts and Schlenker 2013).

At the same time, crop yields are largely affected by climate (Lobell, Schlenker, and

Costa-Roberts 2011) and climate variability (Ray et al. 2015). Current estimates suggest that a third of the global yield variability can be explained by climate variability, and in substantial breadbaskets of the world this percentage can exceed 60% (Ray et al. 2015).

The most important climate variables globally are temperature and precipitation (Lobell and Field 2007; Lobell, Schlenker, and Costa-Roberts 2011; Lobell et al. 2011; Lobell et al. 2013; Ray et al. 2015; Schlenker and Roberts 2009; Welch et al. 2010) and to a lesser extent also radiation (Leng et al. 2016). Interactions between temperature and precipitation, which can lead to varying effects of temperature depending on moisture conditions, are important issues that need to be addressed (Hawkins et al. 2013; Leng et al. 2016; Ray et al. 2015; Urban, Sheffield, and Lobell 2015).

1.2.2. Ecological succession after natural disturbances

Anthropogenic climate change is closely linked to the level of CO_2 in the atmosphere. Atmospheric CO_2 is a part of the global carbon cycle, in which forests play an important role. Intact forests act as strong carbon sinks (Grünwald and Bernhofer 2007), and together with longer vegetation seasons induced by climate change (Dragoni et al. 2011), they are regarded as one possibility to mitigate climate change impacts of CO_2 emissions. At the same time, natural disturbances such as fire, insect outbreaks and storms are expected to increase with climate change, which would negatively impact the forest performance regarding the carbon cycle (Seidl, Schelhaas, and Lexer 2011; Seidl et al. 2014).

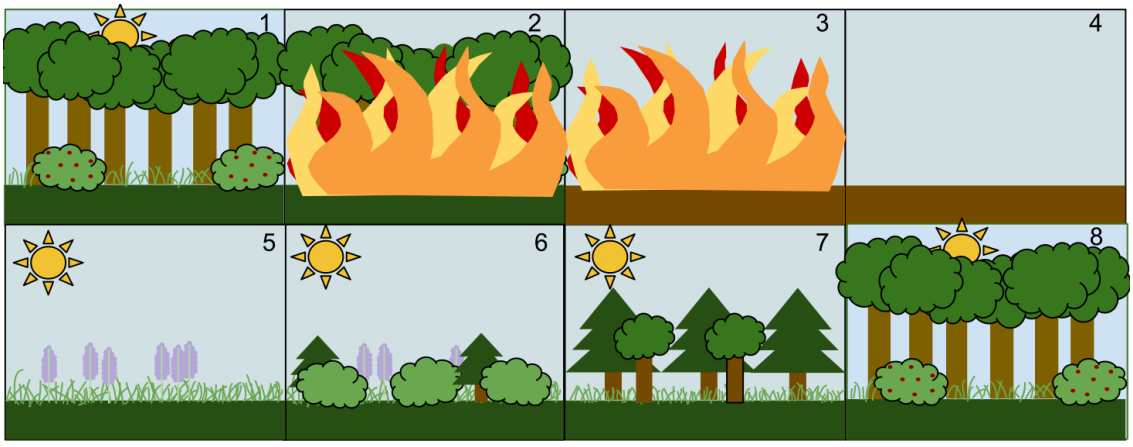

Figure 3 This is an example of Secondary Succession by stages: 1. A stable deciduous forest community 2. A disturbance, such as a wild fire, destroys the forest 3. The fire burns the forest to the ground 4. The fire leaves behind empty, but not destroyed, soil 5. Grasses and other herbaceous plants grow back first 6. Small bushes and trees begin to colonize the area 7. Fast growing evergreen trees develop to their fullest, while shade-tolerant trees develop in the understory 8. The short-lived and shade intolerant evergreen trees die as the larger deciduous trees overtop them. The ecosystem is now back to a similar state to where it began. Figure source is Murphy (2012).

After a disturbance, succession sets in, which can lead to the recovery of an ecosystem to nearly pre-disturbance conditions. In the example of a wild fire (see Figure 3), which has left bare soil, grasses grow back first, followed by small bushes and trees, until a stable forest community has developed back again.

Monitoring the succession after a natural disturbance, for instance, a major storm in a forest is made easier with digital repeat photography, which provide a continuous signal of the change. Images allow quantifying the successional change and can be combined with turbulent CO_2 measurements to identify the carbon balance of the region. Using long-term series, the duration of processes can be estimated, such as the time for the land cover to change and the time it needs for the area to switch from carbon source to sink.

2. Methods overview

An overview of the methods used in the publications will be given here, separated in statistics, image analysis, and software used. The statistics part includes quantile regression (Section 2.1.1), mixed effects models (Section 2.1.2), interactions (Section 2.1.3), generalized additive models (Section 2.1.4), and spatio-temporal modelling (Section 2.1.5). The image analysis part comprises repeated digital photography (Section 2.2.1) and thermography (Section 2.2.2). Finally, the software used for the previously introduced methods will be presented (Section 2.3).

2.1. Statistics

...the statistician knows...that in nature there never was a normal distribution, there never was a straight line, yet with normal and linear assumptions, known to be false, he can often derive results which match, to a useful approximation, those found in the real world.
— George E. P. Box

Selected statistical methods that are particularly useful in climatological and ecological studies will be presented in the following sections.

2.1.1. Quantile regression

Quantile regression (Koenker 2005; Koenker and Bassett 1978) is a regression technique originating from the econometrics field, which does not assume a Normal or any kind of distribution for the errors. In addition, it allows quantifying different effect sizes of explanatory variables depending on the level of the response. Compared to normal linear regression, which models solely the mean response, Quantile Regression shifts the focus to all parts of the distribution by looking at multiple quantiles thereof. Thus, it inherently enables the study of changing distributional properties, such as for example variance or skewness. For a more mathematical description of the basics of quantile regression, see Appendix A.

Coefficients from multiple quantile regression can be summarized in slope-quantile plots (Figure 4). Higher coefficients for higher quantiles, for example, hint to heteroscedasticity, whereas if coefficients are similar for all quantiles (nearly horizontal line in the slope-quantile plot), the covariate effect is the same over the whole distribution.

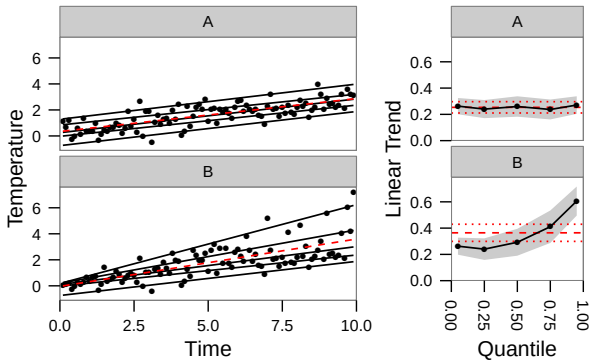

Figure 4 Left: Quantile regression (solid black lines; 0.05, 0.25, 0.5, 0.75 and 0.95 quantile levels) and ordinary least squares regression (OLS, dashed red line) for a set of 99 synthetic temperatures assuming constant variance (top) versus a one-sided increase in variance for higher temperatures (bottom). Right: Linear trend values for quantile regression estimated at five distinct quantiles 0.05, 0.25, 0.5, 0.75 and 0.95 (connected points with shaded 95% confidence bands) versus trend values for OLS regression (dashed red line with dotted red lines representing 95% confidence bands).

The standard algorithm estimates quantile trends separately for each quantile and thus could lead to the crossing of quantile trends. This is problematic, because crossing quantile trend lines would contradict the definition of quantiles, for example if the 0.95 quantile trend line crossed the 0.90 quantile trend line at a certain time, then for some years the estimated temperature at the 0.95 quantile would be below the temperature at the 0.90 quantile, which is impossible via definition. A workaround solution is constraining the estimation (Bondell, Reich, and Wang 2010).

2.1.2. Mixed effects models

Mixed effects models are a tool to analyze grouped data, such as longitudinal data, repeated measures, or multilevel data (Pinheiro and Bates 2000). Such grouped data arise in many observational studies or experimental designs, and require special modelling of the within-group correlation.

Accounting for this withing-group correlation allows estimating the population level response to covariates with much less error than ignoring the inherent structure (see Figure 5).

In its simplest form, the data has an inherent grouping structure with, for example $i = 1..m$ higher level groups - let's call them subjects for clarity - each having $j = 1..n_i$ observations. If the interest was in estimating the influence of variable x on response y, a mixed linear model would be

$$y_{ij} = \beta_0 + \beta_1 x_{ij} + b_{0,i} + b_{1,i} x_{ij} + \epsilon_{ij},$$

with β_0 the population intercept, β_1 the population response to x, $b_{0,i}$ the subject

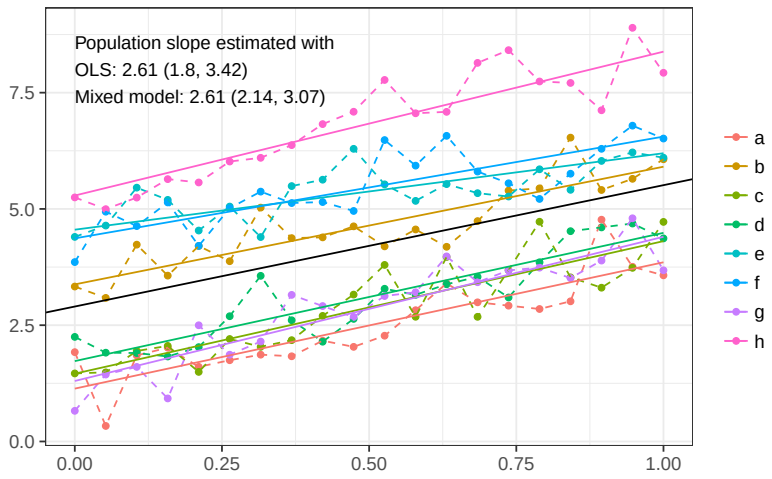

Figure 5 Synthetic data showing the benefits of mixed effects model versus ordinary least squares (OLS). By accounting for the inherent grouping structure and within-group correlation, the population slope (black) can be estimated with less uncertainty. Note that population slope estimates are identical for OLS and mixed model, only the uncertainty is reduced.

intercepts that are normally distributed with $b_{0,i} \sim \mathcal{N}(0, \sigma_0^2)$, $b_{1,i}$ the subject response modifiers with $b_{1,i} \sim \mathcal{N}(0, \sigma_1^2)$, and errors $\epsilon_{ij} \sim \mathcal{N}(0, \sigma^2)$. So the subject effects b are not estimated individually, as opposed to using the subjects as factorial variables, but the spread of the subject effects is estimated as variance of the normal distribution.

This could be rearranged to

$$y_{ij} = (\beta_0 + b_{0,i}) + (\beta_1 + b_{1,i})x_{ij} + \epsilon_{ij},$$

thus showing more clearly the relationship between the so-called fixed effects β and random effects b.

Further generalizations include the modelling of the error term ϵ, allowing, for example, for different error variances per group

$$Var(\epsilon_{ij}) = \sigma^2 \delta_i,$$

with $\delta_1 = 1$ and $\delta_2..\delta_m$ the variance ratios respective to the first group; or for errors depending on covariates

$$Var(\epsilon_{ij}) = \sigma^2 \exp(2\delta x_{ij}),$$

with δ estimated coefficient for the exponential variance relationship; and combinations of the two and more (Pinheiro and Bates 2000).

2.1.3. The importance of interactions for extremes

Since extremes are multifactorial, the impacts depend on the interaction of multiple variables. The statistical estimation of interactions with, for example, linear regressions requires product terms. Consider the following example of y being regressed on x_1 and x_2 and their interaction term:

$$y = \beta_0 + \beta_1 x_1 + \beta_2 x_2 + \beta_3 x_1 x_2 + \epsilon$$

The estimated coefficients of such a regression are hard to interpret on their own, because no coefficient can be looked at independently. For instance, the effect of x_1 depends on β_1, β_2, β_3 and x_2.

So with interaction terms, visualization is a key component to judge the estimated effects. One possibility is to use heatmaps or levelplots, however, it is not trivial to visualize confidence intervals in these plots. It is possible to use additional separate panels for heatmaps, or intermediate lines in levelplots, but both are not very intuitive. Another option is to condition the interaction on one variable, say x_2 and then plot the effect of x_1 conditionally on some meaningful values of x_2 (see Figure 6).

In the above example, the effect of x_1 on y for a given x_2, say $x_2 = c$, would be

$$y(x_1) = \beta_0 + \beta_2 c + (\beta_1 + \beta_3 c) x_1.$$

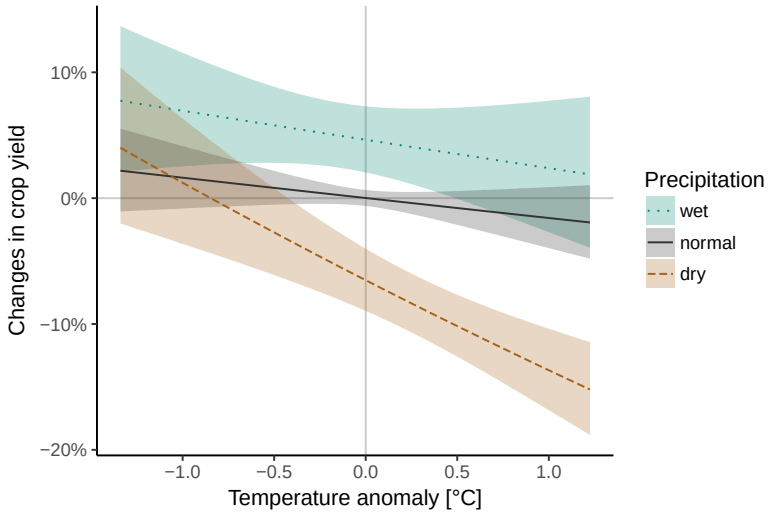

Figure 6 Scheme showing the visualization from an linear regression with an interaction term. The example has crop yield as response and two covariates (temperature and precipitation) that are included with an interaction. Shown is the effect of temperature conditioned on three levels of precipitation, which could be, for example, based on representative quantiles.

2.1.4. Generalized additive models

In the framework of "let the data speak for itself", imposing any functional relationship between a response variable and some predictors is already a fundamental choice. The widely used linearity works well because most processes can be considered linear with the right focus and a sufficiently small scale. However, in certain situations, more flexible solutions are desired.

Instead of estimating the linear slope in ordinary least squares regression, GAMs (generalized additive models) allow estimating a semi-parametric functional relationship between y and x,

$$y = f(x) + \epsilon,$$

by using a penalized spline basis for f and determining the appropriate smoothness of f using, for instance, cross-validation (Wood 2006). Contrary to polynomial or spline-based functions, which require a specification of the exact degrees of freedom (df), GAMs require only the maximum df to be specified. While this is still a choice to be made, it is less severe than specifying the exact degree, since using a too high maximum value will not have any impact compared to lower values. Only when the maximum df supplied is close to the actual determined df, differences may arise. See Figure 7 for a comparison of various polynomial fits to GAM models.

GAMs can also include multiple explanatory variables, functions with multiple arguments, for instance latitude and longitude, and parametric terms. Options for the smooth functions are to use cyclic functions, for instance to determine seasonality, adaptive smoothers that allow a varying df depending on the covariate, and more (see, for example, documentation in R-package mgcv).

All the benefits of GAMs come with a caveat: While uncertainty and formal hypothesis testing exist, covariate effects still need to visualized in every case and no simple coefficients, for example linear slopes, can be provided.

2.1.5. Analysis of spatio-temporal raster data

Special attention has to be given to both spatial and temporal correlation, when dealing with spatio-temporal raster data. The spatial correlation manifests itself through the fact that observations close in space have values more similar than observations far away. With 2-dimensional isotopic data, this correlation is identified with respect to the distance between observations. It can be measured with variograms, which plot the variance of the observations depending on distance, and summarized with coefficient such as Geary's C or Moran's I (Cressie 1993), similar to Pearson correlation

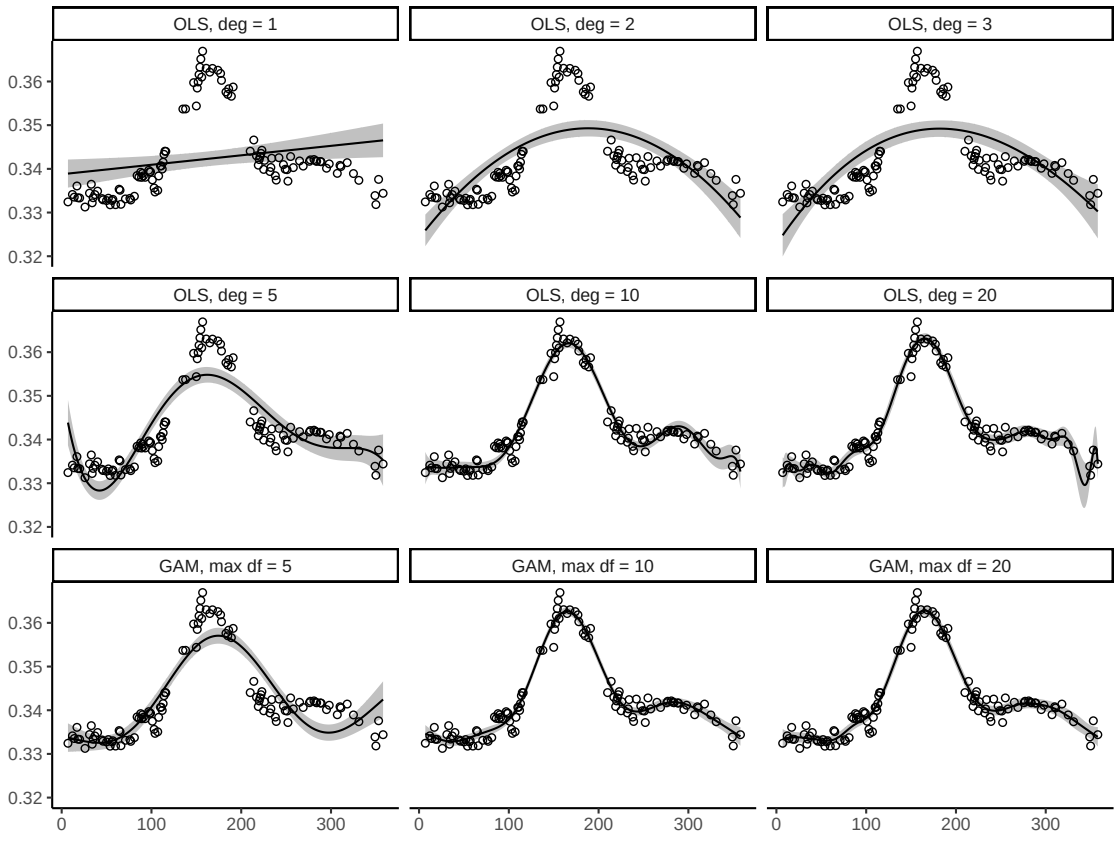

Figure 7 Comparison of ordinary least squares (OLS) regression with various polynomials to generalized additive models (GAM). Points show sample data from image greenness depicting a year of observations of grass. In each panel a different regression is shown with lines and 95% confidence intervals as shaded areas. The first six depict OLS regression using polynomials with different degrees. The last three show GAM fits with maximum degrees of freedom specified as 5, 10, and 20 - the actual degrees of freedom were 3.99, 8.65, and 11.96, respectively. So in the first two GAM models, the actual degrees of freedom are close to the maximum - 1 (for the intercept), signifying that more might be appropriate. Nevertheless, GAMs fit the underlying data better than OLS, and especially the problems of OLS polynomials at their tails are not present for GAMs.

coefficient for standard bivariate data.

Temporal data can have autocorrelation, which is similar to spatial autocorrelation in that observations close by in time have values that are more similar than observation farther away in time. Climatological data such as temperature or snow further often have some sort of seasonality.

With these two issues, identifying relationships between variables in a spatio-temporal raster setting is not possible with simple regression techniques, since the assumption of independent observations is violated. One possibility to deal with this is to account for the spatial and temporal autocorrelation in the residuals with generalized least squares (Pinheiro and Bates 2000). However, this is computationally often not feasible with raster data, which, since the advent of satellite remotely sensed variables, has large number of observations.

Other options for dealing with spatial correlation include, but are not limited to:

- Removing the spatial correlation from the observed values. Side effects could be that what gets removed in this process is related to topography, or other variables of interest.
- Modelling the spatial correlation with other variables, such as latitude, longitude, and altitude.
- Taking subsamples of the data, sufficiently small, so that no spatial correlation exists any more. While this reduces the number of observations available, this is rarely an issue with raster data, and has the additional benefit of having independent validation data.

Similar options exist in the case of temporal autocorrelation and seasonality:

- Removing the temporal correlation from the observed values with for example autoregressive or moving average models (ARMA).
- Removing the seasonality for example with Fourier approximations or cyclic penalized splines.
- Stratifying the data in the temporal domain, and analyzing each stratum separately.

Sample spatial raster data from northern Italy is shown in Figure 8, depicting the spatial correlation of deseasonalized climate values.

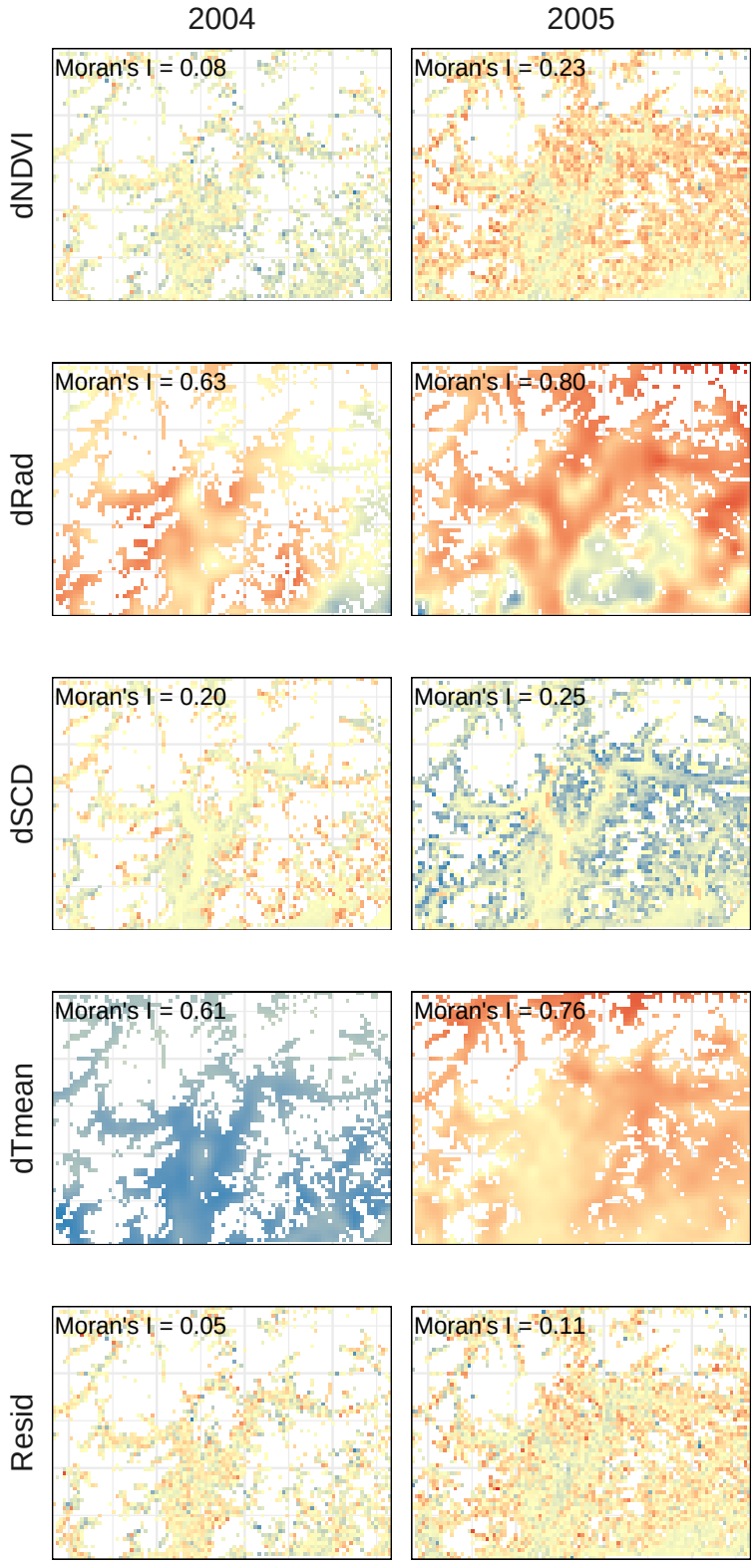

Figure 8 Sample spatial data from April 2004 and 2005 from South Tyrol (northern Italy) with Moran's I. Maps show deseasonalized values (denoted with prefix d) of NDVI (Normalized Difference Vegetation Index), Radiation (Rad), Snow cover duration (SCD), mean temperature (Tmean), and residuals (Resid) of modelling dNDVI depending on the aforementioned variables interacted with topography. Red indicates higher than average values, and blue lower than average. Moran's I is a measure of spatial autocorrelation, where 0 means independence, 1 perfect autocorrelation, and -1 perfect dispersion. 2004 is a year colder than average with a little more snow cover; while 2005 is a year warmer than average with a lot less snow cover, especially at higher altitudes, leading to higher than average NDVI values.

2.2. Image analysis

The greatest value of a picture is when it forces us to notice what we never expected to see.
— John W. Tukey

Image data is becoming increasingly available and popular since the advent of cheap sensors, ease of wireless transmission, and satellite remote sensing. Digital images are discrete quantifications of natural observations, and in the following two applications will be outlined, one is images in the visible red-green-blue spectrum (Section 2.2.1), and the other in the invisible infra-red spectrum (thermal images, Section 2.2.2).

2.2.1. Repeated digital photography

Digital cameras offer a new possibility of monitoring the phenological development by taking repeated images of the same scene each day using stationary cameras (Richardson et al. 2007; Sonnentag et al. 2012). This allows to quantify the spring green-up and fall coloring by calculating *mean greenness* of a specific ROI (Region of Interest). In order to calculate mean greenness, the digital numbers (DN) of each color channel of an RGB-image are extracted, and then the green DN is standardized with the sum over all other DNs (red + green + blue), resulting in the so-called GCC (Green Chromatic Coordinate).

But first, the images have to be preprocessed to remove low quality images that are affected by fog, rain, or are otherwise flawed. This can be done manually, however, as usually large amounts of image have to processed, also automatically using the blue channel or envelopes with certain standard deviations (Filippa et al. 2016). Additionally, for sites that are prone to snow, snowy images have to be masked out, since this would bias the GCC in ways unrelated to phenology. Beside manually going through all images or identifying snow with nearby meteorological stations measuring snow depth, the BCC (blue chromatic coordinate = blue / (red + green + blue)) can be used to create a classifier with a threshold around 0.30 depending on site and field of view.

Another issue is the unintended movement of the camera which can change the field of view. If these movements are not too large, images can be registered (pixels mapped onto each other), so that a continuous scene is shown. Then the scene available during the whole study period needs to be cropped.

Spring green-up and fall coloring is then determined by fitting various kinds of double-log functions with different flexibility in modelling the greenness that is present in deciduous forest, evergreen forests, grass- and croplands. From these functions, phenophases are extracted that correspond to the start and end of season (Gu et al. 2009; Klosterman et al. 2014; White, Thornton, and Running 1997). Figure 9 shows an example of different fitting functions and different methods to extract phenophases.

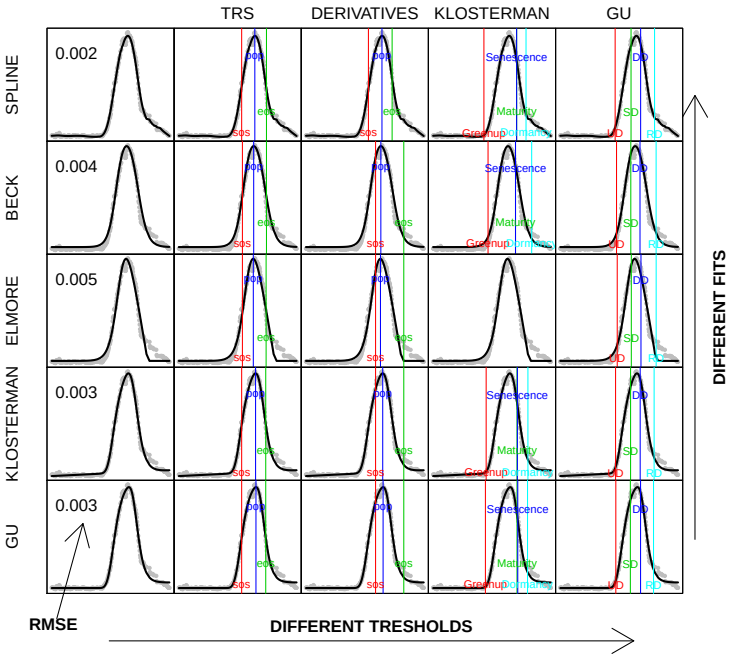

Figure 9 Comparison of functions fitted to image greenness, and phenophase extraction methods. Image taken from the vignette of R-package phenopix.

If the images have a complicated composition, such as many different species, or vegetation interspersed with buildings or roads, manually choosing a ROI by drawing polygons can be tedious and inaccurate. Recent advances allow a data-driven solution, which splits the image in a pre-defined number of clusters using only the information available in the images (Bothmann et al. 2017).

2.2.2. Quantifying thermal images of leaves and needles

Thermal imaging is a non-destructive method to measure drought stress in trees, in contrast to other available methods that are time-consuming and/or destructive. Thermal imaging uses the fact that evapotranspiration reduces surface temperature, and thus under reduced water availability, evapotranspiration decreases and temperature increases (Maes and Steppe 2012).

To calculate leaf or needle temperature for a tree or seedling requires identifying the

ROI and more specifically the pixels that correspond to leaves or needles (Seidel et al. 2016). Pixels at the edge of a leaf or needle then show a temperature which is a mixture of the surrounding pixels. If these show other leaves or needles, it is not problematic. However, if these show soil, sky, or another type of background, then including these edge-pixels when calculating the temperature will introduce bias. Thus, besides removing the background, it is also necessary to remove edge-pixels.

Image processing software offers some tools to achieve this automatically. For instance, automatic thresholding can remove the background pixels, and edge finding algorithms can detect edges. The edge finding works best if the image is as sharp as possible, so an option is to sharpen the image beforehand. Then the background and edge pixels can be removed, and the remaining pixels can be used to calculate the mean temperature of all visible leaves or needles (Figure 10).

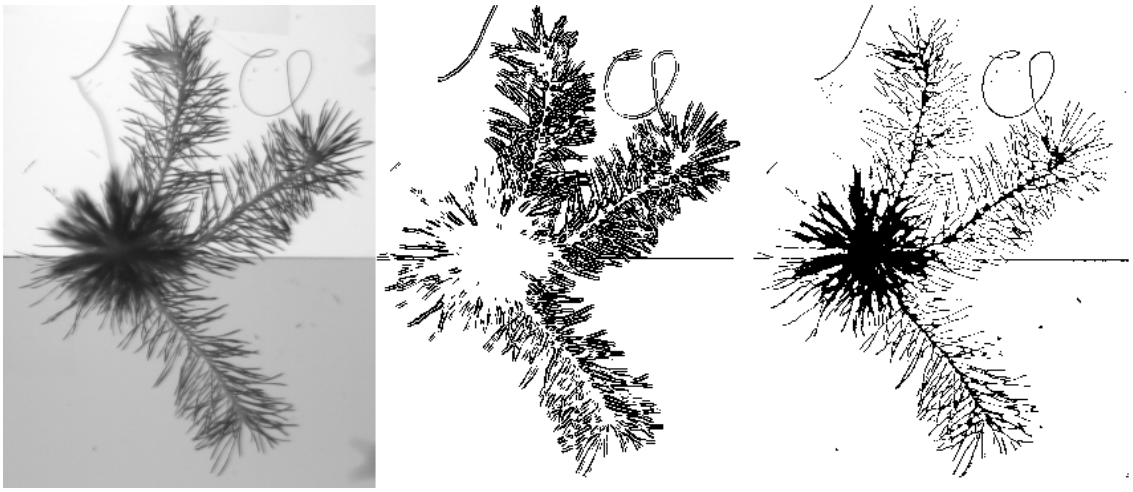

Figure 10 Separating background and needle-edge pixels in a thermal image of a spruce seedling. Left is a greyscale thermography image of spruce seedling looking from the top, where lighter colour means higher temperature (the background is two heating plates that were mounted directly above the pot around the tree-trunk to ease separation of the background). Middle image shows the pixels that were identified as needle-edges by first sharpening the image and then applying an edge-finding algorithm. Right image shows the remaining pixels after edges and background were removed. These pixels were used to calculate the mean temperature. Note that on the right there are still some pixels that are not plant material, such as a cable that was incidentally photographed and the intersection of the two heating plates (horizontal line in the middle).

This procedure has been applied in Seidel et al. (2016) in order to assess drought responses in scots pine seedlings from various provenances in Europe.

2.3. Software used

For the statistical parts, the R programming language was used, and especially the following packages:

- `nlme` (Pinheiro et al. 2017)

- `ggplot2` (Wickham, Chang, and RStudio 2016)
- `effects` (Fox et al. 2016) and `lsmeans` (Lenth 2017)
- `sp` (Pebesma et al. 2016) and `raster` (Hijmans et al. 2016)

The image analysis was done in Fiji, using custom Jython scripts, and with following packages in R:

- `EBImage` (Pau et al. 2010) from the Bioconductor suite of tools
- `phenopix` (Filippa et al. 2016) and `phenofun` (Bothmann et al. 2017)

3. Publications: Summaries and contributions

In God we trust. All others must bring data.
— W. Edwards Deming

The following publications provide the basis for this thesis:

(i) Michael Matiu, Donna P. Ankerst, and Annette Menzel (2016). "Asymmetric Trends in Seasonal Temperature Variability in Instrumental Records from Ten Stations in Switzerland, Germany and the UK from 1864 to 2012". *International Journal of Climatology* 36.1, pp. 13–27. DOI: 10.1002/joc.4326

(ii) Michael Matiu, Donna P. Ankerst, and Annette Menzel (2017). "Interactions between Temperature and Drought in Global and Regional Crop Yield Variability during 1961-2014". *PLOS ONE* 12.5, e0178339. DOI: 10.1371/journal.pone.0178339

(iii) Michael Matiu, Ludwig Bothmann, Rainer Steinbrecher, and Annette Menzel (2017). "Monitoring Succession after a Non-Cleared Windthrow in a Norway Spruce Mountain Forest Using Webcam, Satellite Vegetation Indices and Turbulent CO2 Exchange". *Agricultural and Forest Meteorology* 244–245, pp. 72–81. DOI: 10.1016/j.agrformet.2017.05.020

In the following, a summary of the obtained results along with details on the particular contributions are given. In the contributions, authors are abbreviated with their initials, for example, Michael Matiu as MM.

The entire articles can be found in Appendix C.

3.1. Observed changes in temperature variability and extremes

Michael Matiu, Donna P. Ankerst, and Annette Menzel (2016). "Asymmetric Trends in Seasonal Temperature Variability in Instrumental Records from Ten Stations in Switzerland, Germany and the UK from 1864 to 2012". *International Journal of Climatology* 36.1, pp. 13–27. DOI: 10.1002/joc.4326

Summary

The increases in mean temperature associated to climate change are widely acknowledged, but the question how variability and extremes have changed has remained unanswered so far. In the present article, nine stations from the Alpine region in Europe and one from the UK with long-term daily temperature data were analyzed. Measures of variability, that is the spread of the temperature distribution, were compared, such as the SD, and multiple quantile ranges. Additionally, quantile regression was used to identify the simultaneous changes in the whole temperature distribution. Increases in the mean or median of temperature showed uniformly accelerating warming in all stations, seasons, and time frames, except for Tmin in winter in the recent period (1973-2012). Variability changes were not as ubiquitous. Long-term trends (1864-2012) showed increases in Tmax and Tmin variability in summer and decreases in Tmin variability in the other seasons. However, during the recent 40 years (1973-2012), summer variability did not change, but winter and spring variability increased for Tmin and Tmax, and fall variability decreased for Tmin. More importantly, changes in variability were asymmetric, that is either in the part above or below the median, thus making predictions of the extreme changes based alone on mean and variability inadequate. With quantile regression, it could be shown that the increases of winter variability during 1973-2012 were mainly because of increase in the warmer tail of the distribution, and no changes in temperature below the median. Similarly, for spring, all temperatures above the .25 quantile increased uniformly, while coldest temperature changed little if at all.

Contributions

MM downloaded and prepared the data. DPA suggested the statistical methods. MM analyzed the data and wrote the manuscript together with DPA. DPA and AM discussed and commented on the manuscript.

3.2. Impacts of climate variability on global crop yields

Michael Matiu, Donna P. Ankerst, and Annette Menzel (2017). “Interactions between Temperature and Drought in Global and Regional Crop Yield Variability during 1961-2014”. *PLOS ONE* 12.5, e0178339. DOI: 10.1371/journal.pone.0178339

Summary

Climate change alters crop yields and crop distribution globally, whereas climate variability is the most important factor determining year-to-year crop yield variability. In this study, country-level crop yields were merged with crop area adjusted growing season temperature and SPEI (Standardized Precipitation Evapotranspiration Index) in order to quantify the effects of climate variability and interactions on yields of top-producing countries and global yields. For this, yields and climate variables were detrended, then yields were regressed on quadratic forms of temperature, SPEI, and interaction terms using mixed effects models in order to estimate global sensitivites from country-level variables and country-level sensitivities from sub-country data. It could be shown that heat and dryness was damaging to maize, soybeans, and wheat yields, and to a lesser extent also for rice yields. But as a result of interactions, heat was more damaging in dry than in wet conditions. For global maize and soybeans yields, temperature effects were insignificant at average SPEI levels, but high temperatures under extreme dry conditions were associated to yield reductions of 11.6% and 12.4%, respectively. For the USA, sub-country data at the state level was used to estimate the country-level sensitivities, showing that temperature effects on maize and soybeans yields were stronger in dry than in normal conditions, and for soybeans also less in wet than in normal. Another type of interactions considered were effects of consecutive dry or hot years, which reduced yields further for rice and soybeans in Viet Nam and soybeans in the USA.

Contributions

MM downloaded and prepared the data. DPA assisted in the choice of analytical methods. MM analyzed the data and wrote the manuscript. DPA and AM discussed and commented on the manuscript.

3.3. Monitoring succession in a wind-throw disturbed forest

Michael Matiu, Ludwig Bothmann, Rainer Steinbrecher, and Annette Menzel (2017). "Monitoring Succession after a Non-Cleared Windthrow in a Norway Spruce Mountain Forest Using Webcam, Satellite Vegetation Indices and Turbulent CO2 Exchange". *Agricultural and Forest Meteorology* 244–245, pp. 72–81. DOI: 10.1016/j.agrformet.2017.05.020

Summary

Extreme events disturb forest ecosystems in their productivity and possibility to capture atmospheric CO_2. In this study, the succession after a major wind-throw was observed using digital repeat photography and compared to satellite-derived vegetation indices, NDVI, EVI (Enhanced Vegetation Index), and PPI (Plant Phenology Index) as well as flux tower measurements of GPP (Gross Primary Production). Webcam ROIs were automatically defined using a data-driven approach, identifying three distinct regions showing spruce, grass, and a transition region which initially showed grass and became overgrown by spruce. Satellite measurements displayed a clear break after the storm and had increasing trends afterwards. These trends were mirrored in image greenness (GCC) of the transition ROI and GPP. Measured NEE (Net Ecosystem Exchange) identified the time it took for the ecosystem to switch from carbon source to carbon sink to be eight years. Estimates of SOS (Start of Season) and EOS (End of Season) were derived from GCC, GPP, satellite indices, and compared to climatological growing season indices and traditional phenological observations. Satellite SOS was most similar to the grass ROI, while GPP-SOS was most similar to PPI and the grass ROI. Some climatological indices identified spruce and grass SOS, while phenological observations matched to some extent GPP-SOS. Estimates of EOS showed almost no correspondence.

Contributions

The image data was available at the chair from a previous study, flux data was provided by RS, and ancillary data organized by MM. MM analyzed the data, with assistance from LB for the image data, and RS for the flux data. MM wrote the manuscript. RS, LB and AM commented and discussed on the manuscript.

4. Discussion

Man is an animal who more than any other can adapt himself to all climates and circumstances.
— Henry David Thoreau, *Walden*

In the following chapter, the findings of the four presented studies are set in a broader perspective. Futhermore, main results are discussed and hints to future directions are mentioned.

4.1. Changes in temperature variability and extremes

Global mean temperatures have increased by 0.85 °C since 1880 (IPCC 2013). In the same period, temperatures in Europe have increased by 1.5 °C (European Environment Agency 2017). Other regions in the world have experienced other warming rates. These regional differences arise because of different warming rates of sea and land, ice-albedo feedbacks, and because of climate change induced changes in weather patterns. In addition to these regional differences, warming has not been uniform across seasons (Cohen et al. 2012) and differed between minimum and maximum temperatures (Caesar, Alexander, and Vose 2006).

A plethora of climate indices can be derived from daily temperature and precipitation measurements, such as percentile-based temperature and precipitation extremes, duration of cold/warm/dry/wet spells, and threshold indices, for example, ice days, frost days, summer days, and tropical nights (Alexander et al. 2006). Each of these indices is useful for particular sectors of ecology or society.

But not every index is meaningful for all climates, and similarly, the global mean temperature is not meaningful for all regions. It is difficult to synthesize the findings on all climate indices into a complete picture, and at the same time difficult to infer changes in climate indices and extremes from trends in temperature means and variances.

The findings of Matiu, Ankerst, and Menzel (2016, Section 3.1) corroborate these claims. By using quantile regression, changes in the whole temperature distribution were quantified simultaneously. The most striking findings were that (1) variability has changed indeed and (2) the changes in variability were asymmetric. The integrated view helped gaining a better understanding of the past changes, but will not solve the quest for answering the variability issue (Alexander and Perkins 2013).

However, the asymmetries found in the changes of the temperature variability argue against using symmetric measures of variability, such as the commonly used SD (Beniston and Goyette 2007; Collins et al. 2000; Donat and Alexander 2012; Griffiths et al. 2005; Parker et al. 1994; Rusticucci and Barrucand 2004; Scherrer et al. 2005; Song, Pei, and Zhou 2014). With symmetric measures it is impossible to detect particular features, such as changes in either the hot or cold tail of temperatures but not both (Matiu, Ankerst, and Menzel 2016; Reich 2012; Rhines et al. 2016).

The climate stations used in the study of Matiu, Ankerst, and Menzel (2016, see Section 3.1) were the Hadley Centre Central England Temperature series and multiple stations from the European Alps covering a large altitudinal range from 273 to 2502 m a.s.l. These provide only a limited regional assessment based on a small number of stations, similar to other studies in Europe (Barbosa, Scotto, and Alonso 2011) and South Korea (Lee, Baek, and Cho 2013). However, Rhines et al. (2016) showed the potential of quantile regression for large scale application. Their study covered 3220 stations in North America, and results from the single stations were spatially smoothed with thin-plate regression splines to provide geographically explicit changes at the continental scale. Results indicate large reductions in winter variability due to arctic amplification as well as asymmetric changes in spring, summer, and fall for both daily minimum and maximum temperatures (Rhines et al. 2016).

Another finding from Matiu, Ankerst, and Menzel (2016) concerned the differences in variability trends between time periods, that is linear trends from 1864 to 2012, 1933 to 2012, and 1973 to 2012. While mean temperatures did not change linearly in the recent 150 years (Trenberth et al. 2007), using linear trends provides an appoximation of the speed of change during the respective period. However, with changes in variability, trends did not only differ in size, but also in sign, compared to the trends in mean temperature, which were all positive, and only showed accelerating warming with more recent periods. This implies that changes in mean and variability were not linked consistently during the recent 150 years, but the type of linkage changed, too.

Impacts from changes in temperature variability also depend on the differences between minimum, mean, and maximum temperatures. Extreme daily maximum and minimum temperatures have stronger impacts than extreme mean temperatures. But, interestingly, trends differed for minimum and maximum temperatures. Such a mismatch could have severe consequences, for example, in the case of late frost damage of plants (Menzel, Helm, and Zang 2015). For instance, higher temperatures lead to a faster development of plants and earlier flowering (Menzel et al. 2006). But if trends

in minimum temperature extremes do not match, then late frost events could lead to major damages and even crop failures, if the frost event falls into the critical flowering period.

4.2. Impacts of climate variability on global crop yields

Since the 1960s the agricultural productivity increased steadily through the adoption of modern varieties (Evenson and Gollin 2003, also called the green revolution), fertilizers, pesticides, and mechanization. Agricultural management and inputs thus played a key role in determining past yield trends and will most likely remain important also in the future (Pradhan et al. 2015). Furthermore, yield trends were influenced by climate change (Lobell, Schlenker, and Costa-Roberts 2011). Projections of climate change effects on yields indicate largely yield reductions and only limited benefits (Gregory, Ingram, and Brklacich 2005; Porter et al. 2014). But while the influence of climate trends on past yield trends is small compared to the other inputs, such as varieties, fertilizers, and pesticides, climate variability is the main driving force for year-to-year yield variability.

Yield variability is linked to the stability of food prices (Reidsma et al. 2010), and thus of crucial importance in the context of food security. The study presented in Section 3.2 quantified the climate variability effects associated to yield variability. Of particular importance were the interactions between temperature and SPEI (a drought index), which are summarized in Table 1. The effects of temperature and SPEI were not independent such that the yield effects of hot and dry conditions were not simply the sum of the individual effects.

For maize yields, the sum of individual hot and dry effects would have been -8.9%, but the actually estimated effects with interactions were -11.6%. For wheat yields, the difference was slightly less with -8.2% and -9.2%, respectively, as for rice yields with -1.1% and -2.0%. For soybeans yields, interaction effects were opposite, that is the combined effect of hot and dry conditions -12.4% was less than the sum of individual effects -14.2%. Thus not accounting for interaction effects would underestimate the effect of combined heat and drought for maize, rice, and wheat yields and overestimate it for soybeans yields.

On the other hand, for hot and wet conditions, effects without interaction would have been overestimated for maize and underestimated for rice, soybeans, and wheat. For wheat, yield reductions due to hot conditions (-4.2%) were reduced under wet

conditions to an insignificant -2.8%, although wet conditions in average temperatures were also insignificant. Soybeans profited most from wet conditions under average temperatures (7.1%) compared to the other crops and yield effects even increased to 8.1% under hot conditions, albeit hot temperatures had negative effects in average and dry conditions.

Table 1 Climate variability effects on global crop yields. Summary of the effects presented in Section 3.2, hereby focusing on the importance of interactions for assessing the impacts of hot and dry, as well as hot and wet conditions on global crop yields. The column <hot + dry> is simply the sum of the values in columns <hot> and <dry>, while the column <hot & dry> shows the actual effects of hot and dry conditions because of interactions; hot and wet analogously.

Crop	**Effects of**			
	hot	**dry**	**hot + dry**	**hot & dry**
	given avg. wetness	given avg. temperature	sum of hot and dry effects, assuming no interactions	combined hot and dry effects because of interactions
Maize	-1.1% (-2.9 0.7)	-7.8% (-10.7, -4.9)	-8.9%	-11.6% (-14.3 -8.9)
Rice	-0.7% (-2.5, 1.1)	-0.4% (-2.2, 1.4)	-1.1%	-2.0% (-4.2, 0.2)
Soybeans	-3.5% (-7.4, 0.5)	-10.7% (-13.6, -7.7)	-14.2%	-12.4% (-17.1, -7.4)
Wheat	-4.2% (-6.8, -1.6)	-4.0% (-6.8, -1.1)	-8.2%	-9.2% (-12.4, -5.9)
	hot	**wet**	**hot + wet**	**hot & wet**
	given avg. wetness	given avg. temperature	sum of hot and wet effects, assuming no interactions	combined hot & wet effects because of interactions
Maize	-1.1% (-2.9 0.7)	5.2% (1.9, 8.7)	4.1%	3.0% (-1.1, 7.4)
Rice	-0.7% (-2.5, 1.1)	0.4% (-1.4, 2.3)	-0.3%	0.6% (-1.8, 3.1)
Soybeans	-3.5% (-7.4, 0.5)	7.1% (3.8, 10.6)	3.6%	8.1% (1.3, 15.5)
Wheat	-4.2% (-6.8, -1.6)	-1.2% (-4.3, 2.0)	-5.4%	-2.8% (-7.0, 1.7)

Maize yields were shown to depend strongly on drought and hot temperatures. The yield increases in the Midwest-USA during 1995 and 2012 were accompanied by an increased susceptibility to drought, even after accounting for agronomic changes (Lobell et al. 2014). Rainfed maize crucially depended on precipitation during the reproductive and grain-filling stages (Nielsen, Vigil, and Benjamin 2009). Additionally, heat stress, which was quantified by excess degrees above a certain threshold, was shown to be detrimental for USA maize (Lobell et al. 2013) and French maize (Hawkins et al. 2013). The present study (Section 3.2) also identified strong effects of drought, but not such a strong dependence on heat. This might be because the SPEI already includes potential evapotranspiration and thus heat induced water loss.

Moreover, because of interactions between temperature and SPEI, their single independent effects were not as strong as combined.

Previous global studies of rice yields also coped with small effect sizes and high uncertainties (Lobell and Field 2007; Lobell, Schlenker, and Costa-Roberts 2011), as found in Section 3.2. These difficulties might stem from the sometimes questionable data quality in the reports found in the FAO data. Moreover, while maize, rice, and wheat can all be grown in multiple seasons, maize and wheat yields from the secondary growing season were only minor compared to the main growing season (Lobell, Schlenker, and Costa-Roberts 2011), however, for rice, the second season contributed large parts to the annual yields, and up to 50% are not uncommon (Matthews et al. 1995).

Water availability was the main limiting factor for soybean yields in Brazil (Sentelhas et al. 2015; Zanon, Streck, and Grassini 2016) and northern China (Yin et al. 2016). For other main producing regions, it was water availability combined with temperature that was associated best to soybean yields, such as in the USA (Leng et al. 2016; Ray et al. 2015), Argentina (Llano and Vargas 2016; Penalba, Bettolli, and Vargas 2007), southern China (Zhang et al. 2015), and India (Lal et al. 1999). However, the interactions between temperature and water availability responsible for positive temperature effects under wet conditions, as found in Section 3.2, were not reported for soybean yields before.

Wheat is heavily irrigated in the top producing countries India and China (see Figure 11), where wheat yield variability was mainly associated to temperature variability (Lobell, Sibley, and Ivan Ortiz-Monasterio 2012; Rao et al. 2015). Whereas in other top producing countries, it was precipitation variability or drought, for instance in Russia (Alcamo et al. 2007; Licker et al. 2013), the USA (Maltais-Landry and Lobell 2012), and France (Ceglar et al. 2016; Licker et al. 2013). For global averages as in Section 3.2, both temperature and drought had similar effect sizes.

The presented effects of climate variability on crop yields concern the availability pillar of food security. However, crop yields also feed intro crop prices, which influence the access pillar of food security. The real prices of food, that is adjusted for inflation, have decreased steadily since the 1960s, mainly because of the reasons that yields have increased. However, food crises and hunger arise because of unexpected price spikes. How prices respond to supply and demand is measured by price elasticities (Roberts and Schlenker 2013).

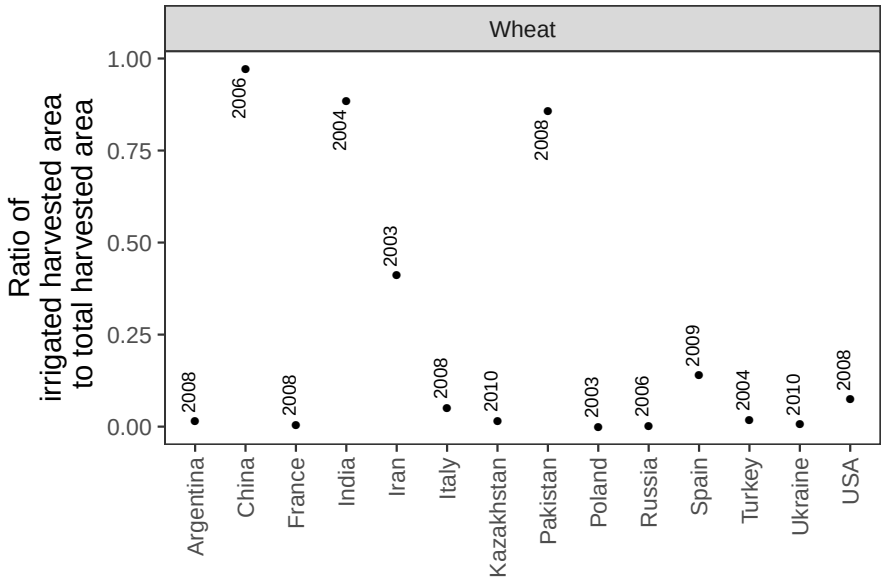

Figure 11 Irrigation rates for wheat in major producing countries. Shown are rates of irrigated area to total harvested area. The small numbers indicate the year of the last report. Source of the data is FAO (2016)

The economic market on staple crops was largely inelastic, since the demand for food cannot change rapidly, but supply could be modulated through stocks (Wright 2011). The introduction of biofuels caused some mixture of the elastic fuel market with the inelastic food market (Wright 2014), which was used to explain recent food price spikes. While price spikes also increase incomes of farmers (Swinnen and Squicciarini 2012), they mainly contribute to hunger in the already food insecure countries. Besides biofuels, other explanations for price spikes include low stocks, harvest failures, and food commodity speculation (Piesse and Thirtle 2009).

The impact of climate variability on price variability of staple crops is an interesting research question. In theory, climate variability leads to yield variability, which leads to price variability. One question would be whether economic responses such as using trading networks (Bren d'Amour et al. 2016; Wu and Guclu 2013) could dampen or completely undermine the effects of climate on food prices. For instance, in the case of wheat and soybeans, inter-hemispheric trade was shown to reduce production shocks by 25-50% (Lybbert, Smith, and Sumner 2014). But climate variability could influence prices also directly, for instance, if price expectations changed because of the expected consequences of severe drought or other extreme events. Prices respond stronger to yield changes, if stocks are low (Wright 2011). Since stock ratios have declined recently, it becomes more likely that climate induced yield variability might be feeding into price variability. However, a rigorous scientific evaluation is yet lacking.

4.3. Ecological succession following an extreme storm in a forest ecosystem

The advent of cheap digital cameras enabled continuous monitoring of phenology in a vast array of locations (Henneken et al. 2013; Julitta et al. 2014; Keenan et al. 2014; Klosterman et al. 2014; Menzel, Helm, and Zang 2015; Toomey et al. 2015; Wingate et al. 2015). In the study in Section 3.3 such a phenocam was used in an innovative way to monitor the succession after a major wind-throw. This was made possible with new statistical developments that allowed a data-driven approach to select ROIs (Bothmann et al. 2017) and thus enabled to identify the successional processes.

In course of the succession GPP increased. This was mirrored in trends of webcam greennees and remotely sensed vegetation indices. These common trends lead to positive correlations between seasonal GPP and proxies. Such a correlation was not observed in non-disturbed evergreen forests using webcam (Toomey et al. 2015) or satellite vegetation indices (Verma et al. 2014).

With the webcam images it was possible to distinguish between grass and spruce trees, while GPP measurements provide an integrated signal over the whole ecosystem. The seasonality of GPP was most similar to the remotely sensed vegetation indices, which also provide an integrated signal, but also to the ROI that showed grass or the grass-to-spruce transition ROI. An interesting question that was not part of the study of Matiu et al. (2017) would be whether it is possible to infer the contributions of the various species to the CO_2 fluxes inside an ecosystem, for instance using webcam imagery.

Soon after the wind-throw, the forest area had become infested with bark beetles, and this resulted in large cuttings to prevent a further spreading. While bark beetle induced tree mortality can be tracked using remotely sensed vegetation indices (Bright, Hicke, and Meddens 2013), in the present study no such links were observed. This is most probably because the successional processes outweigh any bark beetle damages.

For forest managers, knowledge of the timing of bark beetle flights is of crucial importance. Usually, the first flight occurs when daytime temperatures reach a certain threshold (16.5 °C) and weather conditions are suitable for flying (Baier, Pennerstorfer, and Schopf 2007). However, Zang et al. (2015) showed that phenology can be used as proxy to predict onset of bark beetle flight, in some cases even better

than with complex bark beetle models. The findings of Matiu et al. (2017) corroborate these results, since phenological observations on spruce May sprouting were strongly related to timing of the first bark beetle flight in four out of six years. Compared to climatological indices, which had no relationship at all to bark beetle flight, phenology was thus superior, however, it should be noted that the sample size was small consisting of only six years.

Large differences between the three remotely sensed vegetation indices, NDVI, EVI, and PPI were identified in Matiu et al. (2017). The study site has two characteristics that complicate observations by vegetation indices. First, it was covered almost completely with spruce trees before the storm, and afterwards with a mixture of spruce, grass and dead wood. Such a dense cover with evergreen needleleaf leads, for instance, to saturation in NDVI (Huete et al. 2002). Second, due to its location, the study site usually has a continuous snow cover from December to March hampering the validness of vegetation indices. The PPI has been proposed as an alternative especially for these two issues (Jin and Eklundh 2014). Matiu et al. (2017) found that out of the three mentioned indices, the PPI performed best in terms of correspondence to GPP and camera derived greenness (GCC).

With climate change, extreme events are expected to increase (Seneviratne et al. 2012). It then becomes increasingly important to monitor the impacts and recovery of natural systems. Remote sensing is ideally suited, since it provides a continuous signal and also allows, to a certain amount, to look at past conditions. However, the spatial and temporal resolution of remote sensing is yet limited. Webcams provide a much closer look at our environment, with higher detail and dense temporal coverage. The vast array of publicly available cameras (for example see `http://amos.cse.wustl.edu/` for cameras mainly located in the USA) is supplemented by selected high-quality imagery (`http://www.foto-webcam.eu/`) - also freely available. The study in Section 3.3 provides a proof-of-concept of how webcams and remote sensing can be combined to monitor ecological processes.

5. Conclusion

Each organism interacts with its environment. It not only shapes its environment but it also gets shaped by it. Interactions between climatic factors as well as between climatic and non-climatic factors are crucial for a better understanding of the influence of climate variability and extremes on ecology.

The results obtained in this thesis led to a better understanding of climate change induced distributional changes in temperature. Because of the asymmetries involved, it is not trivial to infer changes in temperature extremes from changes in mean and variability. In order to understand the evolution of temperature a wholesome approach is needed, such as quantile regression, which models the whole distribution simultaneously.

Regarding impacts of climate variability on crop yields, the importance of interactions between temperature and drought was elaborated. These interactions prevented an over- or underestimation of the combined influence of temperature and drought on crop yields. Consequently, adaptation measures need to take these interactions into account. Specifically, the importance of temperature varies not only by region, but also by present and future conditions of moisture availability.

Furthermore, climate variability encapsulates extremes, which have far more severe consequences on ecosystems than changing mean conditions. For the first time, impacts of such an extreme event have been monitored using digital repeat photography in combination with remote sensing and turbulent CO_2 measurements. Specifically, the ecological succession in a forest after a major wind-throw. This opens up new opportunities to observe successional processes and enables a more precise estimation of their duration. As a result, the obtained findings are useful for the understanding and managing of disturbed forest areas.

To sum up, the conducted research in course of this dissertation presented statistical techniques and image analysis methods that were used to solve climatological and ecological issues. More importantly, these methods and techniques enlarge the methodological scope and thus represent further opportunities for related research.

In the long run, we only hit what we aim at.
— Henry David Thoreau, *Walden*

References

Alcamo, Joseph, Nikolai Dronin, Marcel Endejan, Genady Golubev, and Andrei Kirilenko (2007). "A New Assessment of Climate Change Impacts on Food Production Shortfalls and Water Availability in Russia". *Global Environmental Change* 17.3–4, pp. 429–444. DOI: 10.1016/j.gloenvcha.2006.12.006.

Alexander, L. V., X. Zhang, T. C. Peterson, J. Caesar, B. Gleason, A. M. G. Klein Tank, M. Haylock, D. Collins, B. Trewin, F. Rahimzadeh, A. Tagipour, K. Rupa Kumar, J. Revadekar, G. Griffiths, L. Vincent, D. B. Stephenson, J. Burn, E. Aguilar, M. Brunet, M. Taylor, M. New, P. Zhai, M. Rusticucci, and J. L. Vazquez-Aguirre (2006). "Global Observed Changes in Daily Climate Extremes of Temperature and Precipitation". *Journal of Geophysical Research: Atmospheres* 111.D5, p. D05109. DOI: 10.1029/2005JD006290.

Alexander, Lisa and Sarah Perkins (2013). "Debate Heating up over Changes in Climate Variability". *Environmental Research Letters* 8.4, p. 041001. DOI: 10.1088/1748-9326/8/4/041001.

Baier, Peter, Josef Pennerstorfer, and Axel Schopf (2007). "PHENIPS—A Comprehensive Phenology Model of Ips Typographus (L.) (Col., Scolytinae) as a Tool for Hazard Rating of Bark Beetle Infestation". *Forest Ecology and Management* 249.3, pp. 171–186. DOI: 10.1016/j.foreco.2007.05.020.

Ballester, Joan, Filippo Giorgi, and Xavier Rodó (2010). "Changes in European Temperature Extremes Can Be Predicted from Changes in PDF Central Statistics". *Climatic Change* 98.1-2, pp. 277–284. DOI: 10.1007/s10584-009-9758-0.

Barbosa, S. M., M. G. Scotto, and A. M. Alonso (2011). "Summarising Changes in Air Temperature over Central Europe by Quantile Regression and Clustering". *Nat. Hazards Earth Syst. Sci.* 11.12, pp. 3227–3233. DOI: 10.5194/nhess-11-3227-2011.

Beniston, Martin and Stéphane Goyette (2007). "Changes in Variability and Persistence of Climate in Switzerland: Exploring 20th Century Observations and 21st Century Simulations". *Global and Planetary Change* 57.1, pp. 1–15. DOI: 10.1002/joc.1118.

Bondell, Howard D., Brian J. Reich, and Huixia Wang (2010). "Noncrossing Quantile Regression Curve Estimation". *Biometrika* 97.4, pp. 825–838. DOI: 10.1093/biomet/asq048.

Bothmann, Ludwig, Annette Menzel, Bjoern H. Menze, Christian Schunk, and Göran Kauermann (2017). "Automated Processing of Webcam Images for Phenological Classification". *PLOS ONE* 12.2, e0171918. DOI: 10.1371/journal.pone.0171918.

Bren d'Amour, Christopher, Leonie Wenz, Matthias Kalkuhl, Jan Christoph Steckel, and Felix Creutzig (2016). "Teleconnected Food Supply Shocks". *Environmental Research Letters* 11.3, p. 035007. DOI: 10.1088/1748-9326/11/3/035007.

Bright, Benjamin C., Jeffrey A. Hicke, and Arjan J. H. Meddens (2013). "Effects of Bark Beetle-Caused Tree Mortality on Biogeochemical and Biogeophysical MODIS Products". *Journal of Geophysical Research: Biogeosciences* 118.3, pp. 974–982. DOI: 10.1002/jgrg.20078.

Caesar, John, Lisa Alexander, and Russell Vose (2006). "Large-Scale Changes in Observed Daily Maximum and Minimum Temperatures: Creation and Analysis of a New Gridded Data Set". *Journal of Geophysical Research: Atmospheres* 111.D5, p. D05101. DOI: 10.1029/2005JD006280.

Cassman, Kenneth G. (1999). "Ecological Intensification of Cereal Production Systems: Yield Potential, Soil Quality, and Precision Agriculture". *Proceedings of the National Academy of Sciences* 96.11, pp. 5952–5959. DOI: 10.1073/pnas.96.11.5952.

Ceglar, Andrej, Andrea Toreti, Rémi Lecerf, Marijn Van der Velde, and Frank Dentener (2016). "Impact of Meteorological Drivers on Regional Inter-Annual Crop Yield Variability in France". *Agricultural and Forest Meteorology* 216, pp. 58–67. DOI: 10.1016/j.agrformet.2015.10.004.

Cohen, Judah L., Jason C. Furtado, Mathew Barlow, Vladimir A. Alexeev, and Jessica E. Cherry (2012). "Asymmetric Seasonal Temperature Trends". *Geophysical Research Letters* 39.4, p. L04705. DOI: 10.1029/2011GL050582.

Collins, DA, PM Della-Marta, N Plummer, and BC Trewin (2000). "Trends in Annual Frequencies of Extreme Temperature Events in Australia". *Australian Meteorological Magazine* 49.4, pp. 277–292.

Cressie, Noel A. C. (1993). *Statistics for Spatial Data*. New York, USA: J. Wiley.

Donat, Markus G. and Lisa V. Alexander (2012). "The Shifting Probability Distribution of Global Daytime and Night-Time Temperatures". *Geophysical Research Letters* 39.14, p. L14707. DOI: 10.1029/2012GL052459.

Dragoni, Danilo, Hans Peter Schmid, Craig A. Wayson, Henry Potter, C. Susan B. Grimmond, and James C. Randolph (2011). "Evidence of Increased Net Ecosystem Productivity Associated with a Longer Vegetated Season in a Deciduous Forest in South-Central Indiana, USA". *Global Change Biology* 17.2, pp. 886–897. DOI: 10.1111/j.1365-2486.2010.02281.x.

Easterling, D. R., J. L. Evans, P. Ya Groisman, T. R. Karl, K. E. Kunkel, and P. Ambenje (2000). "Observed Variability and Trends in Extreme Climate Events: A Brief Review". *Bulletin of the American Meteorological Society* 81.3, pp. 417–425. DOI: 10.1175/1520-0477(2000)081<0417:OVATIE>2.3.CO;2.

European Environment Agency (2017). *Climate Change, Impacts and Vulnerability in Europe 2016*. Publication EEA Report No 1/2017. Copenhagen.

Evenson, R. E. and D. Gollin (2003). "Assessing the Impact of the Green Revolution, 1960 to 2000". *Science* 300.5620, pp. 758–762. DOI: 10.1126/science.1078710.

FAO (2009). "Declaration of the World Food Summit on Food Security". *Rome: Food and Agriculture Organization of the United Nations*.

FAO (2016). *AQUASTAT Main Database*. http://www.fao.org/nr/water/aquastat/main/index.stm.

Filippa, Gianluca, Edoardo Cremonese, Mirco Migliavacca, Marta Galvagno, Matthias Forkel, Lisa Wingate, Enrico Tomelleri, Umberto Morra di Cella, and Andrew D. Richardson (2016). "Phenopix: A R Package for Image-Based Vegetation Phenology". *Agricultural and Forest Meteorology* 220, pp. 141–150. DOI: 10.1016/j.agrformet.2016.01.006.

Folland, TR Karl, JR Christy, RA Clarke, GV Gruza, J Jouzel, ME Mann, J Oerlemans, MJ Salinger, and S-W Wang (2001). "Observed Climate Variability and Change". *Climate Change 2001: The Scientific Basis. Contribution of Working Group I to the Third Assessment Report of the Intergovernmental Panel on Climate Change*. Ed. by JT Houghton, Y Ding, DJ Griggs, M Noguer, PJ Van der Linden, X Dai, K Maskell, and CA Johnson. Cambridge, United Kingdom and New York, NY, USA: Cambridge University Press.

Fox, John, Sanford Weisberg, Michael Friendly, Jangman Hong, Robert Andersen, David Firth, and Steve Taylor (2016). *Effects: Effect Displays for Linear, Generalized Linear, and Other Models*. R-package.

Gloning, Philipp, Nicole Estrella, and Annette Menzel (2013). "The Impacts of Climate Change on the Winter Hardiness Zones of Woody Plants in Europe". *Theoretical and Applied Climatology* 113.3-4, pp. 683–695. DOI: 10.1007/s00704-012-0817-5.

Gregory, P. J., J. S. I. Ingram, and M. Brklacich (2005). "Climate Change and Food Security". *Philosophical Transactions of the Royal Society of London B: Biological Sciences* 360.1463, pp. 2139–2148. DOI: 10.1098/rstb.2005.1745.

Griffiths, G. M., L. E. Chambers, M. R. Haylock, M. J. Manton, N. Nicholls, H.-J. Baek, Y. Choi, P. M. Della-Marta, A. Gosai, N. Iga, R. Lata, V. Laurent, L. Maitrepierre, H. Nakamigawa, N. Ouprasitwong, D. Solofa, L. Tahani, D. T. Thuy, L. Tibig, B. Trewin, K. Vediapan, and P. Zhai (2005). "Change in Mean Temperature as a Predictor of Extreme Temperature Change in the Asia–Pacific Region". *International Journal of Climatology* 25.10, pp. 1301–1330. DOI: 10.1002/joc.1194.

Grünwald, Thomas and Christian Bernhofer (2007). "A Decade of Carbon, Water and Energy Flux Measurements of an Old Spruce Forest at the Anchor Station Tharandt". *Tellus B* 59.3. DOI: 10.3402/tellusb.v59i3.17000.

Gu, Lianhong, Wilfred Post, Dennis Baldoucchi, Andrew Black, Andrew Suyker, Shashi Verma, and Timo Vesala (2009). “Characterizing the Seasonal Dynamics of Plant Community Photosynthesis Across a Range of Vegetation Types”. *Phenology of Ecosystem Processes: Applications in Global Change Research*. New York, NY: Springer New York.

Hawkins, Ed, Thomas E. Fricker, Andrew J. Challinor, Christopher A. T. Ferro, Chun Kit Ho, and Tom M. Osborne (2013). “Increasing Influence of Heat Stress on French Maize Yields from the 1960s to the 2030s”. *Global Change Biology* 19.3, pp. 937–947. DOI: 10.1111/gcb.12069.

Henneken, Raimund, Volker Dose, Christoph Schleip, and Annette Menzel (2013). “Detecting Plant Seasonality from Webcams Using Bayesian Multiple Change Point Analysis”. *Agricultural and Forest Meteorology* 168, pp. 177–185. DOI: 10.1016/j.agrformet.2012.09.001.

Hijmans, Robert J., Jacob van Etten, Joe Cheng, Matteo Mattiuzzi, Michael Sumner, Jonathan A. Greenberg, Oscar Perpinan Lamigueiro, Andrew Bevan, Etienne B. Racine, and Ashton Shortridge (2016). *Raster: Geographic Data Analysis and Modeling*. R-package.

Huete, A, K Didan, T Miura, E. P Rodriguez, X Gao, and L. G Ferreira (2002). “Overview of the Radiometric and Biophysical Performance of the MODIS Vegetation Indices”. *Remote Sensing of Environment*. The Moderate Resolution Imaging Spectroradiometer (MODIS): a new generation of Land Surface Monitoring 83.1–2, pp. 195–213. DOI: 10.1016/S0034-4257(02)00096-2.

IPCC (2012). “Summary for Policymakers”. *Managing the Risks of Extreme Events and Disasters to Advance Climate Change Adaptation*. Ed. by C.B. Field, V. Barros, T.F. Stocker, D. Qin, D.J. Dokken, K.L. Ebi, M.D. Mastrandrea, K.J. Mach, G-K. Plattner, S.K. Allen, M. Tignor, and P.M. Midgley. A Special Report of Working Groups I and II of the Intergovernmental Panel on Climate Change (IPCC). Cambridge, UK, and New York, NY, USA: Cambridge University Press, pp. 3–21.

IPCC (2013). “Summary for Policymakers”. *Climate Change 2013: The Physical Science Basis. Contribution of Working Group I to the Fifth Assessment Report of the Intergovernmental Panel on Climate Change*. Ed. by TF Stocker, D Qin, G-K Plattner, M Tignor, SK Allen, J Boschung, A Nauels, Y Xia, V Bex, and PM Midgley. Cambridge, United Kingdom and New York, NY, USA: Cambridge University Press.

Jin, Hongxiao and Lars Eklundh (2014). “A Physically Based Vegetation Index for Improved Monitoring of Plant Phenology”. *Remote Sensing of Environment* 152, pp. 512–525. DOI: 10.1016/j.rse.2014.07.010.

Julitta, Tommaso, Edoardo Cremonese, Mirco Migliavacca, Roberto Colombo, Marta Galvagno, Consolata Siniscalco, Micol Rossini, Francesco Fava, Sergio Cogliati, Umberto Morra di Cella, and Annette Menzel (2014). “Using Digital Camera Images

to Analyse Snowmelt and Phenology of a Subalpine Grassland". *Agricultural and Forest Meteorology* 198–199, pp. 116–125. DOI: 10.1016/j.agrformet.2014.08.007.

Keenan, T. F., B. Darby, E. Felts, O. Sonnentag, M. A. Friedl, K. Hufkens, J. O'Keefe, S. Klosterman, J. W. Munger, M. Toomey, and A. D. Richardson (2014). "Tracking Forest Phenology and Seasonal Physiology Using Digital Repeat Photography: A Critical Assessment". *Ecological Applications* 24.6, pp. 1478–1489. DOI: 10.1890/13-0652.1.

Klosterman, S. T., K. Hufkens, J. M. Gray, E. Melaas, O. Sonnentag, I. Lavine, L. Mitchell, R. Norman, M. A. Friedl, and A. D. Richardson (2014). "Evaluating Remote Sensing of Deciduous Forest Phenology at Multiple Spatial Scales Using PhenoCam Imagery". *Biogeosciences* 11.16, pp. 4305–4320. DOI: 10.5194/bg-11-4305-2014.

Koenker, Roger (2005). *Quantile Regression*. Econometric Society monographs 38. Cambridge, UK: Cambridge University Press.

Koenker, Roger and Gilbert Bassett Jr. (1978). "Regression Quantiles". *Econometrica* 46.1, pp. 33–50. DOI: 10.2307/1913643.

Koenker, Roger and Kevin Hallock (2001). "Quantile Regression". *Journal of Economic Perspectives* 15.4, pp. 143–156.

Lal, M, K. K Singh, G Srinivasan, L. S Rathore, D Naidu, and C. N Tripathi (1999). "Growth and Yield Responses of Soybean in Madhya Pradesh, India to Climate Variability and Change". *Agricultural and Forest Meteorology* 93.1, pp. 53–70. DOI: 10.1016/S0168-1923(98)00105-1.

Lee, Kyoungmi, Hee-Jeong Baek, and ChunHo Cho (2013). "Analysis of Changes in Extreme Temperatures Using Quantile Regression". *Asia-Pacific Journal of Atmospheric Sciences* 49.3, pp. 313–323. DOI: 10.1007/s13143-013-0030-1.

Leng, Guoyong, Xuesong Zhang, Maoyi Huang, Ghassem R. Asrar, and L. Ruby Leung (2016). "The Role of Climate Covariability on Crop Yields in the Conterminous United States". *Scientific Reports* 6, p. 33160. DOI: 10.1038/srep33160.

Lenth, Russell (2017). *Lsmeans: Least-Squares Means*. R-package.

Licker, Rachel, Christopher J. Kucharik, Thierry Doré, Mark J. Lindeman, and David Makowski (2013). "Climatic Impacts on Winter Wheat Yields in Picardy, France and Rostov, Russia: 1973–2010". *Agricultural and Forest Meteorology* 176, pp. 25–37. DOI: 10.1016/j.agrformet.2013.02.010.

Llano, María Paula and Walter Vargas (2016). "Climate Characteristics and Their Relationship with Soybean and Maize Yields in Argentina, Brazil and the United States". *International Journal of Climatology* 36.3, pp. 1471–1483. DOI: 10.1002/joc.4439.

Lobell, David B. and Christopher B. Field (2007). “Global Scale Climate–crop Yield Relationships and the Impacts of Recent Warming”. *Environmental Research Letters* 2.1, p. 014002. DOI: 10.1088/1748-9326/2/1/014002.

Lobell, David B., Wolfram Schlenker, and Justin Costa-Roberts (2011). “Climate Trends and Global Crop Production Since 1980”. *Science* 333.6042, pp. 616–620. DOI: 10.1126/science.1204531.

Lobell, David B., Adam Sibley, and J. Ivan Ortiz-Monasterio (2012). “Extreme Heat Effects on Wheat Senescence in India”. *Nature Climate Change* 2.3, pp. 186–189. DOI: 10.1038/nclimate1356.

Lobell, David B., Marianne Bänziger, Cosmos Magorokosho, and Bindiganavile Vivek (2011). “Nonlinear Heat Effects on African Maize as Evidenced by Historical Yield Trials”. *Nature Climate Change* 1.1, pp. 42–45. DOI: 10.1038/nclimate1043.

Lobell, David B., Graeme L. Hammer, Greg McLean, Carlos Messina, Michael J. Roberts, and Wolfram Schlenker (2013). “The Critical Role of Extreme Heat for Maize Production in the United States”. *Nature Climate Change* 3.5, pp. 497–501. DOI: 10.1038/nclimate1832.

Lobell, David B., Michael J. Roberts, Wolfram Schlenker, Noah Braun, Bertis B. Little, Roderick M. Rejesus, and Graeme L. Hammer (2014). “Greater Sensitivity to Drought Accompanies Maize Yield Increase in the U.S. Midwest”. *Science* 344.6183, pp. 516–519. DOI: 10.1126/science.1251423.

Lybbert, Travis J., Aaron Smith, and Daniel A. Sumner (2014). “Weather Shocks and Inter-Hemispheric Supply Responses: Implications for Climate Change Effects on Global Food Markets”. *Climate Change Economics* 05.04, p. 1450010. DOI: 10.1142/S2010007814500109.

Maes, W. H. and K. Steppe (2012). “Estimating Evapotranspiration and Drought Stress with Ground-Based Thermal Remote Sensing in Agriculture: A Review”. *Journal of Experimental Botany* 63.13, pp. 4671–4712. DOI: 10.1093/jxb/ers165.

Maltais-Landry, Gabriel and David B. Lobell (2012). “Evaluating the Contribution of Weather to Maize and Wheat Yield Trends in 12 U.S. Counties”. *Agronomy Journal* 104.2, p. 301. DOI: 10.2134/agronj2011.0220.

Matiu, Michael, Donna P. Ankerst, and Annette Menzel (2016). “Asymmetric Trends in Seasonal Temperature Variability in Instrumental Records from Ten Stations in Switzerland, Germany and the UK from 1864 to 2012”. *International Journal of Climatology* 36.1, pp. 13–27. DOI: 10.1002/joc.4326.

– (2017). “Interactions between Temperature and Drought in Global and Regional Crop Yield Variability during 1961-2014”. *PLOS ONE* 12.5, e0178339. DOI: 10.1371/journal.pone.0178339.

Matiu, Michael, Ludwig Bothmann, Rainer Steinbrecher, and Annette Menzel (2017). “Monitoring Succession after a Non-Cleared Windthrow in a Norway Spruce Moun-

tain Forest Using Webcam, Satellite Vegetation Indices and Turbulent CO2 Exchange". *Agricultural and Forest Meteorology* 244–245, pp. 72–81. DOI: 10.1016/j.agrformet.2017.05.020.

Matthews, Robin B, Martin J Kropff, Dominique Bachelet, and HH van Laar, eds. (1995). *Modeling the Impact of Climate Change on Rice Production in Asia*. Wallingford: CAB International in association with the International Rice Research Institute.

Menzel, Annette, Raimund Helm, and Christian Zang (2015). "Patterns of Late Spring Frost Leaf Damage and Recovery in a European Beech (Fagus Sylvatica L.) Stand in South-Eastern Germany Based on Repeated Digital Photographs". *Frontiers in Plant Science* 6, p. 110. DOI: 10.3389/fpls.2015.00110.

Menzel, Annette, Tim H. Sparks, Nicole Estrella, Elisabeth Koch, Anto Aasa, Rein Ahas, Kerstin Alm-Kübler, Peter Bissolli, Ol'ga Braslavská, Agrita Briede, Frank M. Chmielewski, Zalika Crepinsek, Yannick Curnel, Åslög Dahl, Claudio Defila, Alison Donnelly, Yolanda Filella, Katarzyna Jatczak, Finn Måge, Antonio Mestre, Øyvind Nordli, Josep Peñuelas, Pentti Pirinen, Viera Remišová, Helfried Scheifinger, Martin Striz, Andreja Susnik, Arnold J. H. Van Vliet, Frans-Emil Wielgolaski, Susanne Zach, and Ana Zust (2006). "European Phenological Response to Climate Change Matches the Warming Pattern". *Global Change Biology* 12.10, pp. 1969–1976. DOI: 10.1111/j.1365-2486.2006.01193.x.

Mishra, Ashok K. and Vijay P. Singh (2010). "A Review of Drought Concepts". *Journal of Hydrology* 391.1–2, pp. 202–216. DOI: 10.1016/j.jhydrol.2010.07.012.

Murphy, Katelyn (2012). *Secondary Succession*. https://commons.wikimedia.org/wiki/File:Secondary_Succession.png. Wikimedia Commons, accessed 19th June 2017.

Nemani, Ramakrishna R., Charles D. Keeling, Hirofumi Hashimoto, William M. Jolly, Stephen C. Piper, Compton J. Tucker, Ranga B. Myneni, and Steven W. Running (2003). "Climate-Driven Increases in Global Terrestrial Net Primary Production from 1982 to 1999". *Science* 300.5625, pp. 1560–1563. DOI: 10.1126/science.1082750.

Nielsen, David C., Merle F. Vigil, and Joseph G. Benjamin (2009). "The Variable Response of Dryland Corn Yield to Soil Water Content at Planting". *Agricultural Water Management* 96.2, pp. 330–336. DOI: 10.1016/j.agwat.2008.08.011.

O'Neill, Marie S and Kristie L Ebi (2009). "Temperature Extremes and Health: Impacts of Climate Variability and Change in the United States". *Journal of occupational and environmental medicine / American College of Occupational and Environmental Medicine* 51.1, pp. 13–25. DOI: 10.1097/JOM.0b013e318173e122.

Olesen, J. E. and M. Bindi (2002). “Consequences of Climate Change for European Agricultural Productivity, Land Use and Policy”. *European Journal of Agronomy* 16.4, pp. 239–262. DOI: 10.1016/S1161-0301(02)00004-7.

Parker, D. E., P. D. Jones, C. K. Folland, and A. Bevan (1994). “Interdecadal Changes of Surface Temperature since the Late Nineteenth Century”. *Journal of Geophysical Research: Atmospheres* 99.D7, pp. 14373–14399. DOI: 10.1029/94JD00548.

Patz, Jonathan A., Diarmid Campbell-Lendrum, Tracey Holloway, and Jonathan A. Foley (2005). “Impact of Regional Climate Change on Human Health”. *Nature* 438.7066, pp. 310–317. DOI: 10.1038/nature04188.

Pau, Grégoire, Florian Fuchs, Oleg Sklyar, Michael Boutros, and Wolfgang Huber (2010). “EBImage—an R Package for Image Processing with Applications to Cellular Phenotypes”. *Bioinformatics* 26.7, pp. 979–981. DOI: 10.1093/bioinformatics/btq046.

Pebesma, Edzer, Roger Bivand, Barry Rowlingson, Virgilio Gomez-Rubio, Robert Hijmans, Michael Sumner, Don MacQueen, Jim Lemon, and Josh O’Brien (2016). *Sp: Classes and Methods for Spatial Data*. R-package.

Penalba, Olga C., M. Laura Bettolli, and Walter M. Vargas (2007). “The Impact of Climate Variability on Soybean Yields in Argentina. Multivariate Regression”. *Meteorological Applications* 14.1, pp. 3–14. DOI: 10.1002/met.1.

Piesse, Jenifer and Colin Thirtle (2009). “Three Bubbles and a Panic: An Explanatory Review of Recent Food Commodity Price Events”. *Food Policy* 34.2, pp. 119–129. DOI: 10.1016/j.foodpol.2009.01.001.

Pinheiro, José C. and Douglas M. Bates (2000). *Mixed-Effects Models in S and S-PLUS*. Statistics and computing. New York: Springer.

Pinheiro, José, Douglas Bates, Saikat DebRoy, Deepayan Sarkar, EISPACK authors, Siem Heisterkamp, Bert Van Willigen, and R-core (2017). *Nlme: Linear and Nonlinear Mixed Effects Models*. R-package.

Porter, J.R., L. Xie, A.J. Challinor, K. Cochrane, S.M. Howden, M.M. Iqbal, D.B. Lobell, and M.I. Travasso (2014). “Food Security and Food Production Systems”. *Climate Change 2014: Impacts, Adaptation, and Vulnerability. Part A: Global and Sectoral Aspects. Contribution of Working Group II to the Fifth Assessment Report of the Intergovernmental Panel on Climate Change*. Ed. by C.B. Field, V.R. Barros, D.J. Dokken, K.J. Mach, M.D. Mastrandrea, T.E. Bilir, M. Chatterjee, K.L. Ebi, Y.O. Estrada, R.C. Genova, B. Girma, E.S. Kissel, A.N. Levy, S. MacCracken, P.R. Mastrandrea, and L.L. White. Cambridge, United Kingdom and New York, NY, USA: Cambridge University Press, pp. 485–533.

Pradhan, Prajal, Günther Fischer, Harrij van Velthuizen, Dominik E. Reusser, and Juergen P. Kropp (2015). “Closing Yield Gaps: How Sustainable Can We Be?” *PLOS ONE* 10.6, e0129487. DOI: 10.1371/journal.pone.0129487.

Qin, Wei, Chunsheng Hu, and Oene Oenema (2015). “Soil Mulching Significantly Enhances Yields and Water and Nitrogen Use Efficiencies of Maize and Wheat: A Meta-Analysis”. *Scientific Reports* 5, p. 16210. DOI: 10.1038/srep16210.

Rao, B. Bapuji, P. Santhibhushan Chowdary, V. M. Sandeep, V. P. Pramod, and V. U. M. Rao (2015). “Spatial Analysis of the Sensitivity of Wheat Yields to Temperature in India”. *Agricultural and Forest Meteorology* 200, pp. 192–202. DOI: 10.1016/j.agrformet.2014.09.023.

Ray, Deepak K., James S. Gerber, Graham K. MacDonald, and Paul C. West (2015). “Climate Variation Explains a Third of Global Crop Yield Variability”. *Nature Communications* 6. DOI: 10.1038/ncomms6989.

Reich, Brian J. (2012). “Spatiotemporal Quantile Regression for Detecting Distributional Changes in Environmental Processes”. *Journal of the Royal Statistical Society: Series C (Applied Statistics)* 61.4, pp. 535–553. DOI: 10.1111/j.1467-9876.2011.01025.x.

Reidsma, Pytrik, Frank Ewert, Alfons Oude Lansink, and Rik Leemans (2010). “Adaptation to Climate Change and Climate Variability in European Agriculture: The Importance of Farm Level Responses”. *European Journal of Agronomy*. Cropping Systems Design: new methods for new challenges 32.1, pp. 91–102. DOI: 10.1016/j.eja.2009.06.003.

Reyer, Christopher P.O., Sebastian Leuzinger, Anja Rammig, Annett Wolf, Ruud P. Bartholomeus, Antonello Bonfante, Francesca de Lorenzi, Marie Dury, Philipp Gloning, Renée Abou Jaoudé, Tamir Klein, Thomas M. Kuster, Monica Martins, Georg Niedrist, Maria Riccardi, Georg Wohlfahrt, Paolo de Angelis, Giovanbattista de Dato, Louis François, Annette Menzel, and Marízia Pereira (2013). “A Plant’s Perspective of Extremes: Terrestrial Plant Responses to Changing Climatic Variability”. *Global Change Biology* 19.1, pp. 75–89. DOI: 10.1111/gcb.12023.

Rhines, Andrew, Karen A. McKinnon, Martin P. Tingley, and Peter Huybers (2016). “Seasonally Resolved Distributional Trends of North American Temperatures Show Contraction of Winter Variability”. *Journal of Climate* 30.3, pp. 1139–1157. DOI: 10.1175/JCLI-D-16-0363.1.

Richardson, Andrew D., Julian P. Jenkins, Bobby H. Braswell, David Y. Hollinger, Scott V. Ollinger, and Marie-Louise Smith (2007). “Use of Digital Webcam Images to Track Spring Green-up in a Deciduous Broadleaf Forest”. *Oecologia* 152.2, pp. 323–334. DOI: 10.1007/s00442-006-0657-z.

Roberts, Michael J and Wolfram Schlenker (2013). “Identifying Supply and Demand Elasticities of Agricultural Commodities: Implications for the US Ethanol Mandate”. *American Economic Review* 103.6, pp. 2265–2295. DOI: 10.1257/aer.103.6.2265.

Roland, Jens and Stephen F. Matter (2012). “Variability in Winter Climate and Winter Extremes Reduces Population Growth of an Alpine Butterfly”. *Ecology* 94.1, pp. 190–199. DOI: 10.1890/12-0611.1.

Rusticucci, Matilde and Mariana Barrucand (2004). “Observed Trends and Changes in Temperature Extremes over Argentina.” *Journal of Climate* 17, pp. 4099–4107. DOI: 10.1175/1520-0442(2004)017<4099:OTACIT>2.0.CO;2.

Scherrer, Simon C., Christof Appenzeller, Mark A. Liniger, and Christoph Schär (2005). “European Temperature Distribution Changes in Observations and Climate Change Scenarios”. *Geophysical Research Letters* 32.19, p. L19705. DOI: 10.1029/2005GL024108.

Schlenker, Wolfram and Michael J. Roberts (2009). “Nonlinear Temperature Effects Indicate Severe Damages to U.S. Crop Yields under Climate Change”. *Proceedings of the National Academy of Sciences* 106.37, pp. 15594–15598. DOI: 10.1073/pnas.0906865106.

Seidel, Hannes, Christian Schunk, Michael Matiu, and Annette Menzel (2016). “Diverging Drought Resistance of Scots Pine Provenances Revealed by Infrared Thermography”. *Frontiers in Plant Science*, p. 1247. DOI: 10.3389/fpls.2016.01247.

Seidl, Rupert, Mart-Jan Schelhaas, and Manfred J. Lexer (2011). “Unraveling the Drivers of Intensifying Forest Disturbance Regimes in Europe”. *Global Change Biology* 17.9, pp. 2842–2852. DOI: 10.1111/j.1365-2486.2011.02452.x.

Seidl, Rupert, Mart-Jan Schelhaas, Werner Rammer, and Pieter Johannes Verkerk (2014). “Increasing Forest Disturbances in Europe and Their Impact on Carbon Storage”. *Nature Climate Change* 4.9, pp. 806–810. DOI: 10.1038/nclimate2318.

Seneviratne, S.I., N. Nicholls, C.M. Goodess, S. Kanae, J. Kossin, Y. Luo, J. Marengo, K. McInnes, M. Rahimi, M. Reichstein, A. Sorteberg, C. Vera, and X. Zhang (2012). “Changes in Climate Extremes and Their Impacts on the Natural Physical Environment”. *Managing the Risks of Extreme Events and Disasters to Advance Climate Change Adaptation*. Ed. by C.B. Field, V. Barros, T.F. Stocker, D. Qin, D.J. Dokken, K.L. Ebi, M.D. Mastrandrea, K.J. Mach, G-K. Plattner, S.K. Allen, M. Tignor, and P.M. Midgley. A Special Report of Working Groups I and II of the Intergovernmental Panel on Climate Change (IPCC). Cambridge, UK, and New York, NY, USA: Cambridge University Press, pp. 109–230.

Sentelhas, P. C., R. Battisti, G. M. S. Câmara, J. R. B. Farias, A. C. Hampf, and C. Nendel (2015). “The Soybean Yield Gap in Brazil – Magnitude, Causes and Possible Solutions for Sustainable Production”. *The Journal of Agricultural Science* 153.8, pp. 1394–1411. DOI: 10.1017/S0021859615000313.

Song, Ci, Tao Pei, and Chenghu Zhou (2014). “The Role of Changing Multiscale Temperature Variability in Extreme Temperature Events on the Eastern and Central Tibetan Plateau during 1960–2008”. *International Journal of Climatology*. DOI: 10.1002/joc.3935.

Sonnentag, Oliver, Koen Hufkens, Cory Teshera-Sterne, Adam M. Young, Mark Friedl, Bobby H. Braswell, Thomas Milliman, John O'Keefe, and Andrew D. Richardson (2012). "Digital Repeat Photography for Phenological Research in Forest Ecosystems". *Agricultural and Forest Meteorology* 152, pp. 159–177. DOI: 10.1016/j.agrformet.2011.09.009.

Swinnen, Johan and Pasquamaria Squicciarini (2012). "Mixed Messages on Prices and Food Security". *Science* 335.6067, pp. 405–406. DOI: 10.1126/science.1210806.

Thompson, Ross M, John Beardall, Jason Beringer, Mike Grace, and Paula Sardina (2013). "Means and Extremes: Building Variability into Community-Level Climate Change Experiments". *Ecology Letters* 16.6, pp. 799–806. DOI: 10.1111/ele.12095.

Toomey, Michael, Mark A. Friedl, Steve Frolking, Koen Hufkens, Stephen Klosterman, Oliver Sonnentag, Dennis D. Baldocchi, Carl J. Bernacchi, Sebastien C. Biraud, Gil Bohrer, Edward Brzostek, Sean P. Burns, Carole Coursolle, David Y. Hollinger, Hank A. Margolis, Harry McCaughey, Russell K. Monson, J. William Munger, Stephen Pallardy, Richard P. Phillips, Margaret S. Torn, Sonia Wharton, Marcelo Zeri, and Andrew D. Richardson (2015). "Greenness Indices from Digital Cameras Predict the Timing and Seasonal Dynamics of Canopy-Scale Photosynthesis". *Ecological Applications* 25.1, pp. 99–115. DOI: 10.1890/14-0005.1.

Trenberth, KE, PD Jones, PG Ambenje, R Bojariu, DR Easterling, TG Klein, DE Parker, JA Renwick, M Rusticucci, B Soden, and P Zhai (2007). "Observations: Surface and Atmospheric Climate Change". *Climate Change 2007: The Physical Science Basis. Contribution of Working Group I to the Fourth Assessment Report of the Intergovernmental Panel on Climate Change*. Ed. by S Solomon, D Qin, M Manning, Z Chen, M Marquis, KB Averyt, M Tignor, and HL Miller. Cambridge, United Kingdom and New York, NY, USA: Cambridge University Press, pp. 235–336.

Troy, T. J., C. Kipgen, and I. Pal (2015). "The Impact of Climate Extremes and Irrigation on US Crop Yields". *Environmental Research Letters* 10.5, p. 054013. DOI: 10.1088/1748-9326/10/5/054013.

Urban, Daniel W., Justin Sheffield, and David B. Lobell (2015). "The Impacts of Future Climate and Carbon Dioxide Changes on the Average and Variability of US Maize Yields under Two Emission Scenarios". *Environmental Research Letters* 10.4, p. 045003. DOI: 10.1088/1748-9326/10/4/045003.

Verma, M., M. A. Friedl, A. D. Richardson, G. Kiely, A. Cescatti, B. E. Law, G. Wohlfahrt, B. Gielen, O. Roupsard, E. J. Moors, P. Toscano, F. P. Vaccari, D. Gianelle, G. Bohrer, A. Varlagin, N. Buchmann, E. van Gorsel, L. Montagnani, and P. Propastin (2014). "Remote Sensing of Annual Terrestrial Gross Primary Pro-

ductivity from MODIS: An Assessment Using the FLUXNET La Thuile Data Set". *Biogeosciences* 11.8, pp. 2185–2200. DOI: 10.5194/bg-11-2185-2014.

Welch, Jarrod R., Jeffrey R. Vincent, Maximilian Auffhammer, Piedad F. Moya, Achim Dobermann, and David Dawe (2010). "Rice Yields in Tropical/Subtropical Asia Exhibit Large but Opposing Sensitivities to Minimum and Maximum Temperatures". *Proceedings of the National Academy of Sciences* 107.33, pp. 14562–14567. DOI: 10.1073/pnas.1001222107.

White, Michael A., Peter E. Thornton, and Steven W. Running (1997). "A Continental Phenology Model for Monitoring Vegetation Responses to Interannual Climatic Variability". *Global Biogeochemical Cycles* 11.2, pp. 217–234. DOI: 10.1029/97GB00330.

Wickham, Hadley, Winston Chang, and RStudio (2016). *Ggplot2: Create Elegant Data Visualisations Using the Grammar of Graphics*. R-package.

Wingate, L., J. Ogée, E. Cremonese, G. Filippa, T. Mizunuma, M. Migliavacca, C. Moisy, M. Wilkinson, C. Moureaux, G. Wohlfahrt, A. Hammerle, L. Hörtnagl, C. Gimeno, A. Porcar-Castell, M. Galvagno, T. Nakaji, J. Morison, O. Kolle, A. Knohl, W. Kutsch, P. Kolari, E. Nikinmaa, A. Ibrom, B. Gielen, W. Eugster, M. Balzarolo, D. Papale, K. Klumpp, B. Köstner, T. Grünwald, R. Joffre, J.-M. Ourcival, M. Hellstrom, A. Lindroth, C. George, B. Longdoz, B. Genty, J. Levula, B. Heinesch, M. Sprintsin, D. Yakir, T. Manise, D. Guyon, H. Ahrends, A. Plaza-Aguilar, J. H. Guan, and J. Grace (2015). "Interpreting Canopy Development and Physiology Using a European Phenology Camera Network at Flux Sites". *Biogeosciences* 12.20, pp. 5995–6015. DOI: 10.5194/bg-12-5995-2015.

Wood, Simon (2006). *Generalized Additive Models: An Introduction with R*. Texts in statistical science 67. Boca Raton: CRC Press.

Wright, Brian D. (2011). "The Economics of Grain Price Volatility". *Applied Economic Perspectives and Policy* 33.1, pp. 32–58. DOI: 10.1093/aepp/ppq033.

Wright, Brian (2014). "Global Biofuels: Key to the Puzzle of Grain Market Behavior". *Journal of Economic Perspectives* 28.1, pp. 73–98. DOI: 10.1257/jep.28.1.73.

Wu, Felicia and Hasan Guclu (2013). "Global Maize Trade and Food Security: Implications from a Social Network Model". *Risk Analysis* 33.12, pp. 2168–2178. DOI: 10.1111/risa.12064.

Yin, X. G., J. E. Olesen, M. Wang, I. Öztürk, and F. Chen (2016). "Climate Effects on Crop Yields in the Northeast Farming Region of China during 1961–2010". *The Journal of Agricultural Science* 154.7, pp. 1190–1208. DOI: 10.1017/S0021859616000149.

Zang, C., R. Helm, T. H. Sparks, and A. Menzel (2015). "Forecasting Bark Beetle Early Flight Activity with Plant Phenology". *Climate Research* 66.2, pp. 161–170. DOI: 10.3354/cr01346.

Zanon, Alencar Junior, Nereu Augusto Streck, and Patricio Grassini (2016). “Climate and Management Factors Influence Soybean Yield Potential in a Subtropical Environment”. *Agronomy Journal* 108.4, p. 1447. DOI: 10.2134/agronj2015.0535.

Zhang, Zhao, Xiao Song, Fulu Tao, Shuai Zhang, and Wenjiao Shi (2015). “Climate Trends and Crop Production in China at County Scale, 1980 to 2008”. *Theoretical and Applied Climatology* 123.1-2, pp. 291–302. DOI: 10.1007/s00704-014-1343-4.

List of Figures

List of Tables

Acronyms

E

EOS - End of Season 24
EVI - Enhanced Vegetation Index 24, 32

F

FAO - Food and Agriculture Organization of the United Nations 6, 29

G

GCC - Green Chromatic Coordinate 17, 24, 32
GPP - Gross Primary Production 24, 31, 32

I

IPCC - Intergovernmental Panel on Climate Change 2, 4

N

NDVI - Normalized Difference Vegetation Index 16, 24, 32
NEE - Net Ecosystem Exchange 24

P

PPI - Plant Phenology Index 24, 32

R

ROI - Region of Interest 17–19, 24, 31

S

SD - Standard Deviation 4, 22, 26
SOS - Start of Season 24
SPEI - Standardized Precipitation Evapotranspiration Index 23, 27
SREX - Special Report on Extreme Events 2

Acknowledgements

The best thing about being a statistician is that you get to play in everyone's backyard.
— John W. Tukey

My beginning at the chair was sweetened by my office-mates, Isabel and Christian, which made me very welcome. We had a nice time together, during and outside office hours and I will always keep you in fond memories. With some other colleagues I had the pleasure to spend some time, for example, Upsee, whom I will always remember for her never-ending positivity, Gourav, who always knows a funny story, Hannes, with his abundant relaxing attitude, Schunki, always helping and nice to everyone, Eli, with her kind and funny way, Nicole, whom you can always trust to speak straight and sincere, Tim, the Englishman in Bavaria, Ricardo, the musical mathematician, Marvin and Julia, always a good reason to climb some stairs. Besides, paths also crossed with Nils, Allan, Renee, Anna, Stefan, Ye, Wael, and more. I am fond of collaborating with people outside of the chair, with some more, with some less, but especially, Claus, Julia, David, Tobias, Rainer, Eva, and Sarah.

Not to forget the good hearts that work underneath the surface, but without whom none would be possible, Brigitte, Nik and Toni, that keep organization and technical infrastructure going, and remind of the Bavarian origins in the otherwise very international team.

I want to thank my supervisor, Annette Menzel, who guided me through the PhD, offered me so many opportunities to learn, and allowed me the flexibility to work independently. Special thanks go also my mentor, Donna Ankerst, who not only supported the methodological parts of my PhD, but also guided me through the metaphysics behind a doctorate and the importance beyond the current research. This one's for you, Donna:

I think it was a disastrous mistake to categorize statistics as a branch of mathematics. Certainly it uses mathematics, but so, for example, do chemistry, physics and genetics. It is much more than this. It is a science concerned with the problem of how new knowledge can be generated most efficiently.
— George E. P. Box

Professional work and personal life are so intertwined that they cannot be fully sep-

arated. What happens at work will influence your personality, and what happens in your personal life will be mirrored in your work. During this PhD-time I was allowed to observe the birth of two new earthlings, which changed my perspective on life in ways I could not have imagined. And finally, thank you, my princess, for joining my path in life, supporting me personally and professionally, bringing us so many wonderful experiences, and celebrating life together.

And now here is my secret, a very simple secret: It is only with the heart that one can see rightly; what is essential is invisible to the eye.
— Antoine de Saint-Exupéry, *The little prince*

A. Mathematical background

In the following a formal mathematical derivation of regression quantiles, which were introduced in Section 2.1.1, will be provided.

Regression Quantiles

Given a random variable Y with arbitrary distribution function f_Y, the τ-th quantile is defined as the inverse of the cumulative distribution function F_Y

$$Q_Y(\tau) = F_Y^{-1}(\tau) \qquad \text{for } \tau \in (0,1).$$

If we have a sample of observations $(y_1, \ldots, y_n)$, the sample quantiles divide the observations in proportions. The 0.25-th quantile, for example, is the value y_i, for which one quarter of observations lie below, and three quarters lie above. The most commonly used quantile, the 0.5-th (also called median), then divides the observations into two subsets of equal proportion, half below and half above the median. The obvious way to determine the sample quantile thus seems to rely on sorting and ordering of the observations. Specifically, let $Y = (y_1, \ldots, y_n)^T$ denote a vector of observations and let F_Y be the empirical cumulative distribution function. Then the τ-th quantile is

$$Q_Y(\tau) = F_Y^{-1}(\tau) = \inf_{y_i} \{F_Y(y_i) \geq \tau\} \qquad i = 1, \ldots, n.$$

The sample mean may, next to the obvious way, also be determined via minimizing the residual sum of squares

$$\min_{\mu \in \mathbb{R}} \sum_{i=1}^{n} (y_i - \mu)^2.$$

The same is possible for quantiles. A extended summary, following Koenker and Hallock (2001), will be given here. The median is the solution to minimizing the sum of absolute residuals

$$\min_{\xi \in \mathbb{R}} \sum_{i=1}^{n} |y_i - \xi|,$$

which yields from the symmetry of the absolute value function. This can be generalized to all quantiles by using asymmetrically weighted absolute residuals. The tilted

absolute value function, from now on called check or loss function, is

$$\rho_\tau(x) := x\left(\tau\, \mathbb{I}_{\{x\geq 0\}} - (1-\tau)\, \mathbb{I}_{\{x<0\}}\right) = x(\tau - \mathbb{I}_{\{x<0\}}).$$

Then minimizing

$$r(\xi) := \sum_i \rho_\tau(y_i - \xi)$$

over $\xi \in \mathbb{R}$ yields as solution the τ-th quantile. This can be seen by taking directional derivatives w.r.t. ξ, which exist although $\rho_\tau(\cdot)$ is not differentiable. The right derivative is

$$\begin{aligned}
r'_+(\xi) &:= \lim_{h\searrow 0} \frac{r(\xi+h) - r(\xi)}{h} = \lim_{h\searrow 0} \sum_{i=1}^n \frac{\rho_\tau\left(y_i - (\xi+h)\right) - \rho_\tau(y_i - \xi)}{h} \\
&= \sum_{i=1}^n \lim_{h\searrow 0} \frac{1}{h}\left[(y_i - \xi - h)\left(\tau - \mathbb{I}_{\{y_i-\xi-h<0\}}\right) - (y_i-\xi)\left(\tau - \mathbb{I}_{\{y_i-\xi<0\}}\right)\right] \\
&= \sum_{i=1}^n \lim_{h\searrow 0} \frac{1}{h}\left[-h\left(\tau - \mathbb{I}_{\{y_i-\xi-h<0\}}\right) + (y_i-\xi)\left(\tau - \mathbb{I}_{\{y_i-\xi-h<0\}}\right) - (y_i-\xi)\left(\tau - \mathbb{I}_{\{y_i-\xi<0\}}\right)\right] \\
&= \sum_{i=1}^n \left[\mathbb{I}_{\{y_i\leq\xi\}} - \tau\right] \quad = \quad \sum_{i=1}^n \mathbb{I}_{\{y_i\leq\xi\}} - n\tau.
\end{aligned}$$

The last sum can be interpreted as the difference between the number of y_i's below ξ and the proportion of observations that should be below the τ-th quantile. Similarly, the left derivative is

$$\begin{aligned}
r'_-(\xi) &= \lim_{h\searrow 0} \frac{r(\xi-h) - r(\xi)}{h} = \lim_{h\searrow 0} \sum_{i=1}^n \frac{\rho_\tau\left(y_i - (\xi-h)\right) - \rho_\tau(y_i - \xi)}{h} \\
&= \sum_{i=1}^n \left[\tau - \mathbb{I}_{\{y_i<\xi\}}\right] \quad = \quad n\tau - \sum_{i=1}^n \mathbb{I}_{\{y_i<\xi\}}.
\end{aligned}$$

So, depending on ξ, we have $r'_+(\xi) = -r'_-(\xi)$ or $r'_+(\xi) - 1 = -r'_-(\xi)$. If we put that into one equation, we get $r'_+(\xi) \geq -r'_-(\xi)$, which implies that r'_+ and r'_- can never be < 0 at the same time, but they can both be ≥ 0. When both directional derivatives are positive, we have a local minimum, and because $r(\xi)$ is the sum of convex functions, that minimum is global. It is obvious that ξ must be the τ-th quantile such that $r'_+(\xi) \geq 0 \leq r'_-(\xi)$.

Further let $\tilde{x}_i$ be a vector with dimension p of known covariates for each observation $i = 1, \ldots, n$ and $x_i = (1, \tilde{x}_i^T)^T$. Then the design matrix X of all x_i includes the intercept and has dimension $n \times (p+1)$. The conditional quantile is then defined

as

$$Q_Y(\tau|X) = X\beta(\tau)$$

where $\beta(\tau)$ is a vector of coefficients that depends on τ. By generalizing the aforementioned, the solution to

$$\min_{\beta(\tau) \in \mathbb{R}^{p+1}} \sum_i \rho_\tau(y_i - x_i^T \beta(\tau))$$

is known as regression quantiles, for which Koenker and Bassett (1978) derived efficient solving algorithms and asymptotic theory.

B. Academic CV

Michael Matiu

CV

Birthday	09. April 1987 in Baia Mare (Romania)
Civil status	commited relationship, 1 son (b. 2013), 1 daughter (b. 2015)
Nationality	German, Romanian

Academic career

Education

2013 – 2017 **Ph.D**, *Professorship of Ecoclimatology, Technical University of Munich, Germany*, Thesis title: Climate extremes and variability, and their ecological impacts; supervised by Prof. Dr. Annette Menzel and Prof. Ph.D. Donna Ankerst.

2010 – 2013 **M.Sc. Mathematics in Bioscience**, *Technical University of Munich, Germany*, Thesis title: Incorporating Single Nucleotide Polymorphisms into Prostate Cancer Risk Prediction Models; supervised by Prof. Ph.D. Donna Ankerst, final grade 1.9.

2006 – 2009 **B.Sc. Wirtschaftsmathematik**, *Universität Hamburg, Germany*, Thesis title: Flexible Fertigungssysteme; supervised by Prof. Dr. Wolfgang Brüggemann and Prof. Dr. Hartmut Stadtler, final grade 1.86.

Experience

2017 **Researcher**, *Institute for Earth Observation, EURAC, Bolzano, Italy*. Short term project: Data analysis for the next Klimareport Südtirol.

2016 **Visiting Scientist**, *Institute for Earth Observation, EURAC, Bolzano, Italy*. Three month research stay in course of the Ph.D.

2013 – 2016 **Research Assistant**, *Professorship of Ecoclimatology, Technical University of Munich, Germany*. Statistical data analysis and consulting.

2011 – 2013 **Tutor for Undergraduate students**, *Technical University of Munich, Germany*. Introductory courses in Mathematics.

2011 **Working student in Quantitative Modeling**, *E.ON Vertrieb, Munich, Germany*. Programming assistance.

2008 – 2009 **Tutor for Undergraduate students**, *Universität Hamburg, Germany*. Introductory courses in Mathematics.

Eggen Dorf 19 – 39050 Deutschnofen – Italy
+39 327 0627932 / +49 176 61667606 • michaelmatiu@gmail.com

Publications

2017 Matiu M, Ankerst, DP, Menzel A. Interactions between temperature and drought in global and regional crop yield variability during 1961-2014. *PLOS One* 12(5): e0178339. DOI: 10.1371/journal.pone.0178339.

2017 Matiu M, Bothmann L, Steinbrecher R, Menzel A. Monitoring succession after a non-cleared windthrow in a Norway spruce mountain forest using webcam, MODIS NDVI and turbulent CO2 exchange. *Agricultural and Forest Meteorology* 244–245: 72–81. DOI: 10.1016/j.agrformet.2017.05.020.

2017 Kolářová E, Matiu M, Menzel A, Nekovář J, Lumpe P, Adamík P. 2017. Changes in spring arrival dates and temperature sensitivity of migratory birds over two centuries. *International Journal of Biometeorology* 1–11. DOI: 10.1007/s00484-017-1305-5.

2017 Sauter G, Clauditz T, Steurer S, Wittmer C, Büscheck F, Krech T, Lutz F, Lennartz M, Harms L, Lawrenz L, Möller-Koop C, Simon R, Jacobsen F, Wilczak W, Minner S, Tsourlakis MC, Chirico V, Weidemann S, Haese A, Steuber T, Salomon G, Matiu M, Vettorazzi E, Michl U, Budäus L, Tilki D, Thederan I, Pehrke D, Beyer B, Fraune C, Göbel C, Heinrich M, Juhnke M, Möller K, Bawahab AAA, Uhlig R, Huland H, Heinzer H, Graefen M, Schlomm T. 2017. Integrating Tertiary Gleason 5 Patterns into Quantitative Gleason Grading in Prostate Biopsies and Prostatectomy Specimens. *European Urology*. DOI: 10.1016/j.eururo.2017.01.015.

2017 Menzel A, Matiu M, Michaelis R, Jochner S. Indoor birch pollen concentrations differ with ventilation scheme, room location, and meteorological factors. *Indoor Air* 27(3): 539–550. DOI: 10.1111/ina.12351.

2016 Seidel H, Schunk C, Matiu M, Menzel A. Diverging Drought Resistance of Scots Pine Provenances Revealed by Infrared Thermography. *Frontiers in Plant Science* 1247. DOI: 10.3389/fpls.2016.01247.

2016 Matiu M, Ankerst DP, Menzel A. Asymmetric trends in seasonal temperature variability in instrumental records from ten stations in Switzerland, Germany and the UK from 1864 to 2012. *International Journal of Climatology* 36: 13–27. DOI: 10.1002/joc.4326.

2014 Menzel A, Matiu M, Sparks TH. Twenty years of successful papers in Global Change Biology. *Global Change Biology* 20(12): 3587–3590. DOI: 10.1111/gcb.12630.

Conferences

2016 Data Analysis and Modeling in Earth Sciences (DAMES), Hamburg, Germany. Poster: Spatiotemporal variations of climate, snow and vegetation in an Alpine region

2015 Virtual Alpine Observatory (VAO) Symposium, Salzburg, Austria. Talk: Asymmetric Trends in Seasonal Temperature Variability in Instrumental Records from 1973 to 2012

Training

2015 **Writing scientific proposals**, *Instructor: Prof. Dr. Ulrike Müller*, Graduate School of the Technical University of Munich.

2014 **High Impact Paper Writing for Doctoral candidates and Postdocs**, *Instructor: Prof. Dr. Ulrike Müller*, Graduate School of the Technical University of Munich.

Eggen Dorf 19 – 39050 Deutschnofen – Italy
+39 327 0627932 / +49 176 61667606 • michaelmatiu@gmail.com

2014 **Rhetorik extrem - Frei reden im Freien**, *Instructor: Manuela Richter-Meyer*, Graduate School of the Technical University of Munich.

Languages

Fluent German, English, Romanian

Basics French, Italian

Programming skills

Expert R, LaTeX

Basics Java, Python, XML

Other

2013 – 2014 **Ph.D student speaker**, *Focus Area Water - IGSSE*, Technical University of Munich, Germany.

2011 – 2012 **Student representative**, *Biedersteiner Wohnheim*, Munich, Germany.

2010 – 2012 **Theater projects**, *Qualifikationsspiel, Adam und Esra, Der gewissenlose Mörder Hasse Karlsson, Herz aus Gift*, Munich, Germany.

2009 – 2010 **Work & Travel**, Australia.

2005 – 2006 **Community Service**, *Internationaler Bund für Sozialarbeit*, Rastatt, Germany.

Eggen Dorf 19 – 39050 Deutschnofen – Italy
+39 327 0627932 / +49 176 61667606 • michaelmatiu@gmail.com

C. Publication reprints

The next pages show reprints of the publications used in this thesis (see Section 3). They can be found at page:

(i) 59
(ii) 74
(iii) 97

No restrictions to reprint apply, since:

(i) Open access.
(ii) Open access.
(iii) The publisher (Elsevier) grants access to use in dissertations, without further permission seeking. See subpoint “Can I include/use my article in my thesis/dissertation?” under `https://www.elsevier.com/about/our-business/policies/copyright/permissions` (accessed 2nd June 2017) and author user rights under `https://www.elsevier.com/__data/assets/pdf_file/0007/55654/AuthorUserRights.pdf` (accessed 2nd June 2017).

INTERNATIONAL JOURNAL OF CLIMATOLOGY
Int. J. Climatol. **36**: 13–27 (2016)
Published online 2 April 2015 in Wiley Online Library
(wileyonlinelibrary.com) DOI: 10.1002/joc.4326

RMetS
Royal Meteorological Society

Asymmetric trends in seasonal temperature variability in instrumental records from ten stations in Switzerland, Germany and the UK from 1864 to 2012

Michael Matiu,[a*] Donna P. Ankerst[b] and Annette Menzel[a,c]
[a] *Fachgebiet Ökoklimatologie, Technische Universität München, Freising, Germany*
[b] *Lehrstuhl für Mathematische Modellierung biologischer Systeme, Technische Universität München, Garching, Germany*
[c] *Institute for Advanced Study, Technische Universität München, Garching, Germany*

ABSTRACT: While the rise in global mean temperature over the past several decades is now widely acknowledged, the issue as to whether and to what extent temperature variability is changing continues to undergo debate. Here, variability refers to the spread of the temperature distribution. Much attention has been given to the effects that changes in mean temperature have on extremes, but these changes are accompanied by changes in variability, and it is actually the two together, in addition to all aspects of a changing climate pattern, that influence extremes. Since extremes have some of the largest impacts on society and ecology, changing temperature variability must be considered in tandem with a gradually increasing temperature mean. Previous studies of trends in temperature variability have produced conflicting results. Here we investigated ten long-term instrumental records in Europe of minimum, mean and maximum temperatures, looking for trends in seasonal, annual and decadal measures of variability (standard deviation and various quantile ranges) as well as asymmetries in the trends of extreme versus mean temperatures via quantile regression. We found consistent and accelerating mean warming during 1864–2012. In the last 40 years (1973–2012) trends for Tmax were higher than for Tmin, reaching up to 0.8 °C per 10a in spring. On the other hand, variability trends were not as uniform: significant changes occurred in opposing directions depending on the season, as well as when comparing 1864–2012 trends to those of 1973–2012. Moreover, if variability changed, then it changed asymmetrically, that is only in the part above or below the median. Consequently, trends in the extreme high and low quantiles differed. Regional differences indicated that in winter, high-alpine stations had increasing variability trends for Tmax especially at the upper tail compared to no changes or decreasing variability at low altitude stations. In contrast, summer variability increased at all stations studied.

KEY WORDS Climate change; quantile regression; Europe; robust measures; long-record observations; temperature extremes; Alpine region

Received 31 July 2014; Revised 27 February 2015; Accepted 4 March 2015

1. Introduction

Evidence of global warming of the climate system has been unequivocal: there have been warmer and/or fewer cold days and additionally warmer and/or more frequent hot days in the recent decades [Intergovernmental Panel on Climate Change (IPCC), 2013]. In addition to mean warming, countries across the world are currently facing an increase in the frequency and intensity of temperature extremes, which is of great concern since extreme events have had and will continue to have the greatest impact on socio-economies (Easterling *et al.*, 2000), human health (e.g. O'Neill and Ebi, 2009), and terrestrial ecosystems (e.g. Trigo *et al.*, 2006; Gloning *et al.*, 2013; Reyer *et al.*, 2013). However, temperature extremes are more sensitive to changes in variability rather than changes in mean conditions (Katz and Brown, 1992) and asymmetry, that is the skewness of the distribution, also plays a crucial role in predicting extremes (Ballester *et al.*, 2010). Previous studies implementing schematic graphs of normally distributed temperatures have illustrated how increases in mean temperature, variance, and both could affect extreme temperatures at the tails of the temperature distribution (Beniston and Goyette, 2007; Figure 2.32 in Folland *et al.*, 2001; Meehl *et al.*, 2000). However, recently, the special report on extreme events (SREX) of the IPCC updated the schematic graph to include the possibility of changes in symmetry (see Figure SPM.3 in IPCC, 2012). But the latest Assessment Report (AR5) of the IPCC, published shortly after the SREX, shows again the older symmetric depiction (Figure 1.8 in Cubasch *et al.*, 2013). Since the beginning of the 'variability issue' many climate-related publications have attributed changes in the frequency and intensity of extreme events to both warming and increased variability. The recent accumulation of high-profile extreme events, such as the European heat waves in 2003 and 2006–2007,

* Correspondence to: M. Matiu, Fachgebiet Ökoklimatologie, Technische Universität München, Freising, Germany.
E-mail: matiu@wzw.tum.de

the Australian summer of 2012–2013, the Northern Hemisphere 2010 heat wave, and the Europe 2009 and Argentina 2007 cold waves, have perpetuated this hypothesis.

The detection-attribution algorithm (Hegerl *et al.*, 2004), previously used to estimate the anthropogenic influence on warming of mean temperatures, was extended to temperature extremes using extreme value theory. A significant human influence was found globally for warming of the warmest night, coldest days and coldest nights (Christidis *et al.*, 2005; Shiogama *et al.*, 2006) as well as for the warmest days (Christidis *et al.*, 2011). Regional extreme temperatures were also significantly influenced by humans (Zwiers *et al.*, 2010; Min *et al.*, 2013; Wen *et al.*, 2013) and land use change was found to be of particular importance for changes in warm extremes (Christidis *et al.*, 2013). By analyzing six temperature reconstructions, Rybski *et al.* (2006) found that part of the recent warming could not be attributed to natural variability.

Notwithstanding an accumulation of observed data on extreme events, the question of whether such events have been caused by shifts in mean temperature alone versus additionally by shifts in variability remains to date unresolved. There is still an ongoing debate concerning whether and how variability has changed on a global scale (Easterling *et al.*, 2000; Hansen *et al.*, 2012; Rhines and Huybers, 2013). Correct assessment of climate variability and extremes is of paramount importance for the tools and methods required for applied climate impact research, including the construction of weather generators, the downscaling of model outputs, risk assessment, and the determination of experimental settings for ecological climate change impact studies (Thompson *et al.*, 2013).

As a first step for ascertaining the role of variability in the rise of extreme temperature events, one needs to understand if and how variability has changed over the past decades. This goal is not trivial for several reasons. First, variability of observations may be described on different time scales, such as daily, monthly, or yearly and over different time spans, such as over a decade or several decades. Simple measures for variability translate to approximate measures of the spread of a probability distribution describing the theoretic behavior of the observations, such as the commonly used normal distribution. They include, but are not limited to, the sample variance (sample standard deviation), which assumes symmetric behavior around the mean, and sample quantile ranges, such as the difference between the 0.975 and 0.025 sample quantiles, which describe the interior 95% portion of the underlying probability distribution. More complicated measures of variability could be characterized by examining full probability densities that are not assumed to be normal, such as flexible mixtures of distributions for bimodal or skewed observations. Once the definition of variability has been established a second complication is that the rate of extreme events may depend in a complicated manner on changes in both the mean and the variability. For example, in their theoretical framework, Rahmstorf and Coumou (2011) concluded that the number of heat waves depended non-linearly on the ratio of the warming trend to the short-term standard deviation. Furthermore, the long-term correlations also have an influence on extreme value statistics (Eichner *et al.*, 2006).

Numerous studies have analyzed changing trends in variability and arrived at different conclusions; a collection of these are listed in Table 1. Based on re-analysis of global data and concentrating on inter-annual fluctuations, Huntingford *et al.* (2013) found varying regional patterns but no overall change in temperature variability over the past 44 years. Similar results were found using gridded station data (Parker *et al.*, 1994; Donat and Alexander, 2012). Focusing only on the June-July-August (JJA) summer season, Hansen *et al.* (2012) demonstrated an increase in variability globally over the past 60 years. Scherrer *et al.* (2005) confirmed an increase in variability during the summer season in Europe, a decrease in winter and spring, and no change in fall. Based on recent historical station data, Klein Tank *et al.* (2005) showed patterns of increasing and decreasing variability of mean temperatures in Europe depending on station and season, while Simolo *et al.* (2012) found that minimum and maximum temperatures showed no change except for summer maximum temperatures in one of three regions. In the case of Australia (Collins *et al.*, 2000) overall decreases were found only for minimum temperatures, while for mean and maximum temperatures, trend signs showed regional heterogeneity. For the East Asia and south Pacific regions (Griffiths *et al.*, 2005), no overall change was found, although some stations showed significant decreases in variability of minimum and maximum temperatures. In a comprehensive station network in the United States, China, former Soviet republic and Australia, mean temperature variability did not change, although it declined for some stations (Karl *et al.*, 1995). For Argentina, Rusticucci and Barrucand (2004) found decreasing variability of minimum and maximum temperatures in summer (DJF) and increasing variability in winter (JJA), although most changes were not significant. For the Tibetan Plateau, overall inter-annual variability of mean temperatures increased, however, some stations also showed no change or decreases (Song *et al.*, 2014). Two stations in Switzerland showed no change in variability of minimum and maximum temperatures over 104 years (Beniston and Goyette, 2007). Based on more than 100 years of station data, Della-Marta *et al.* (2007) observed an increase in variability of maximum temperatures during the summer season in Western Europe.

It is difficult to compare the results of these studies due to the different temperature measures and datasets used. Therefore, using high-quality homogenized temperature records of ten stations in Europe dating back 150 years, this report investigates the effects of different time bases for the variability measures, time frames to detect trends, statistical models and measures of variability for three variables (daily minimum, mean, and maximum temperature) on qualitative and quantitative inferences concerning changes in variability.

Table 1. Overview of the recent literature findings on temperature variability. Data origin indicates whether historical observational records (stations; number thereof in brackets; multiple numbers denote different time frames and/or regional availability) versus a climate data product (gridded or re-analysis; product name in brackets) was used. Abbreviations: CDF (cumulative density function), DJF (season: December, January and February), GEV (generalized extreme value distribution), JJA (season: June, July and August), NA (not applicable), NH/SH (Northern/Southern hemisphere), PDF (probability density function), SD (standard deviation), Qxx (0.xx quantile), Var (Variability).

Article	Data origin (number)	Time frame	Region	Var-measure	Time base for Var-measure	Temperature parameter	Method summary	Results
Beniston and Goyette (2007)	Station (2)	1901–2004	Switzerland	variance	year	min, max	5-point moving average; linear regression	No change.
Collins *et al.* (2000)	Station (88)	1880–1996	Australia	SD	year	min, mean, max	daily anomalies (based on 61–90 for each day); area-weighted average; linear regression	Overall decrease only for Tmin. Majority of stations decreased (most of them significantly); regional heterogeneity of trend sign.
Della-Marta *et al.* (2007)	Station (54)	1880–2005	Western Europe	(F(0.9) - F(0.1))/2, F is CDF of fitted GEV	14 years (only JJA)	max	standardize each station by mean and SD (1906–1990); split in nine 14-year periods; piecewise linear detrending; fit GEV to each station and period; compute Var measures; robust linear model of measures of all stations inside a region	Significant increase.
Donat and Alexander (2012)	Gridded [HadGHCND]	1951–2010	global (land)	variance	30 years (all seasons)	min, max	split in two periods (51–80, 81–10; daily anomalies of each period; empirical PDF of each grid box/spatial aggregation; F-test for change in variance	Spatial heterogeneity (increases and decreases). Mostly non-significant changes.
Griffiths *et al.* (2005)	Station (89)	1961–2003	East Asia, South Pacific	SD	year	min, max	linear regression	Some significant decreases: more for Tmin than Tmax; almost no significant increases. Majority of stations no change.
Hansen *et al.* (2012)	Gridded [GISS-GHCNv2]	1951–2010	global (land and sea)	empirical PDF	10 years (only JJA)	mean	standardize each time series by mean & sd (of 1951–1980); empirical PDF	Increase in variability
Huntingford *et al.* (2013)	Re-analysis [ECMWF ERA-40]	1958–2001	global (land and sea)	empirical PDF	10-13 years	Mean	Mean yearly temp; yearly standardized anomalies (from mean & sd of each 10 yr period); empirical PDF	No global change Regional patterns with increase/decrease
Karl *et al.* (1995)	Station (187/ 223/197/40)	1911–92/ 1935–89/ 1952–89/ 1961–93	USA/China/ Former Soviet Union/Australia	Mean of daily running difference per period	1, 2, 5, 10, 30 days per season per year	min, mean, max	Daily anomalies (from third-order harmonics); running difference per period (not for yearly variability); area-averaged to country	Mostly no change. Some significant decreases.
Klein Tank *et al.* (2005)	Station (185)	1946–99	Europe	(Q90 – Q10)/2	season & year	mean	Running percentiles (5 day window); average over season/year; *t*-test for two periods (before and after 1975)	Significant increases and decreases depending on station and season.
Parker *et al.* (1994)	Gridded [MOHSST5 & CRU data]	1954–93	global (land and sea)	Variance	20 years (for each season)	mean	Variance of period for each grid and season	No overall change

Table 1. Continued.

Article	Data origin (number)	Time frame	Region	Var-measure	Time base for Var-measure	Temperature parameter	Method summary	Results
Reich (2012)	Station (188/343)	1931–2009/ 1980–2009	south-east US	NA	NA	min, mean, max	Hierarchical Bayesian approach; spatiotemporal and simultaneous quantile regression	Locations with increasing and decreasing variability, more spatial variability for Tmin and Tmean, almost none for Tmax.
Rusticucci and Barrucand (2004)	Station (not mentioned)	1959–98	Argentina	SD	Season (JJA and DJF)	min, max	Linear regression	Tmin in summer (DJF) decreasing, partly also Tmax. Tmax in winter (JJA) increasing, partly also Tmin. Mostly non-significant changes.
Scherrer *et al.* (2005)	Gridded [CRUTEM2v]	1961–2004	Europe [all land grid 3°W-27°E and 44-55°N]	SD	30 years (each season)	mean	Piecewise detrending; 30 year running SD; standardize by SD of 1961–90; mean vs SD change by time (bootstrapped confidence)	Significant increase in summer, decrease in winter and spring, no change in fall
Simolo *et al.* (2012)	Station (69)	1961–2007	Europe	Second L-moment	Year, DJF & JJA	min, max	Standardize each series by mean of 1961–90; average into 3 regional series; compute L-moments for every season/year; linear regression	No change except for JJA Tmax in one region
Song *et al.* (2014)	Station (63)	1960–2008	Tibetan Plateau	SD	Year/10 years	mean	Intra-annual: linear regression of SD; inter-annual: linear regression of annual means, SD of running 10 year residuals; regional series: area-weighted mean	Significant decrease/increase in intra-annual/inter-annual variability for the whole region. For individual stations regional patterns with increases, no change and decreases.

Table 2. Summary of station details. Station name is followed by country abbreviation in parentheses (CH = Switzerland, DE = Germany, GB = United Kingdom). The last column shows the number of years of available data for minimum/mean/maximum temperatures. Geographic coordinates of HadCET are an indicator of the series' regional cover. Group abbrevations: High-Alps (High), northern Low-Alps (Low) and Rest comprises Lugano in the southern Alps as well as Central England.

Station ID	Station name	Longitude	Latitude	Altitude[m a.s.l.]	Group	Years of data [min / mean / max]
BAS	Basel / Binningen (CH)	7°35'E	47°32'N	316	Low	115/149/115
BER	Bern / Zollikofen (CH)	7°28'E	46°59'N	552	Low	149/149/149
DAV	Davos (CH)	9°51'E	46°49'N	1594	High	123/137/123
HadCET	Central England (GB)	0°-3°W[a]	51°–54°N[a]	0-200[a]	Rest	135/135/135
Hopei	Hohenpeissenberg (DE)	11°01'E	47°48'N	1000	High	131/131/131
LUG	Lugano (CH)	8°58'E	46°00'N	273	Rest	148/149/148
LUZ	Luzern (CH)	8°18'E	47°02'N	454	Low	127/132/127
NEU	Neuchâtel (CH)	6°57'E	47°00'N	485	Low	148/149/148
SAE	Säntis (CH)	9°21'E	47°15'N	2502	High	121/129/112
SMA	Zürich / Fluntern (CH)	8°34'E	47°23'N	555	Low	131/149/131

[a]Approximate.

2. Data and methods

2.1. Data

Minimum, mean, and maximum daily temperature data were available for eight Swiss stations with long-term records (115–149 years) from the SwissMETEO website (Begert *et al.*, 2005). In addition, data from the Hadley Centre Central England Temperature (HadCET) composite time series (Parker *et al.*, 1992) and the oldest mountain climate station in southern Germany, Hohenpeissenberg (DWD, German Meteorological Service), were available for analysis with 135 and 131 years of data, respectively. The HadCET series is a composite of multiple stations in central England. The region spans a roughly triangular area between London, Bristol and Lancashire; for a complete list of stations see Parker *et al.* (1992). The ten stations were roughly grouped according to altitude and whether they lay North or South to the Alps-ridge into three categories: High-Alps, northern Low-Alps and Rest (Lugano in the Southern Alps and Central England). Table 2 provides summary data for the individual stations and Figure 1, a map. The collective dataset comprised daily temperature readings starting with 1864 and ending with 2012.

Except for minimum temperatures at the Swiss stations, all temperature series were homogenized in order to reduce non-meteorological effects, such as changes in site location, measurement devices, measurement times etc.; the processes are described in detail in the original and subsequent reports (Parker *et al.*, 1992; Begert *et al.*, 2005; Parker and Horton, 2005). No statistical outliers were found and no further data standardization was performed due to the high quality standards of the data. A small amount of the daily data was missing (<0.5% per station and temperature variable, i.e. minimum, mean or maximum temperature), which was filled by single imputation (Rubin, 1978; Baraldi and Enders, 2010). Single rather than multiple imputation was used following the recommendation that the number of necessary imputations be set as the percent of missing information, which in this case was less than 1% (Bodner, 2008; White *et al.*, 2011). To perform the imputation of missing values,

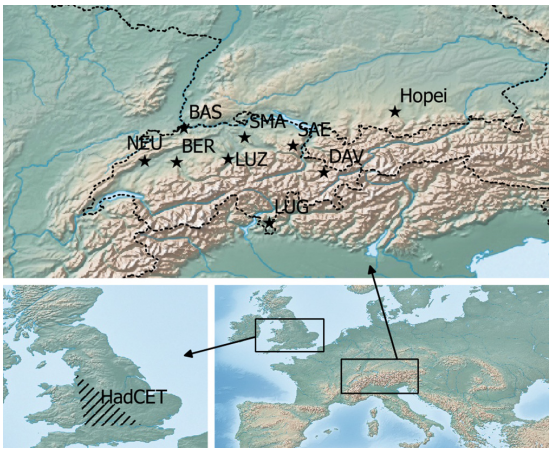

Figure 1. Map of available stations. Top panel shows the eight Swiss stations and Hohenpeissenberg (Hopei), bottom left is a rough representation of the area covered by the Hadley Centre Central England Temperature (HadCET) series. Station names are provided in Table 2.

linear models were fit with the missing temperature variable as outcome, e.g. maximum temperature, and the other temperature variables as predictors, e.g. mean and minimum temperature, within 10 years with no missing outcomes or predictors. Rather than using the mean from the regression, the missing value was replaced with a randomly sampled value from a normal distribution with predicted mean and variance from the imputation regression, corresponding to imputation from the predictive distribution (Brick and Kalton, 1996).

Analyses were done on seasonal, annual and decadal scale. The daily observations were grouped into meteorological seasons: December-January-February (DJF, winter), March-April-May (MAM, spring), June-July-August (JJA, summer) and September-October-November (SON, fall). Incomplete winter seasons (at the start and end of the series) were removed. The most recent decade was 2003–2012 preceded by 10-year periods (1993–2002, and so forth). An incomplete decade at the beginning of the series was removed from the decadal analysis. Increasing

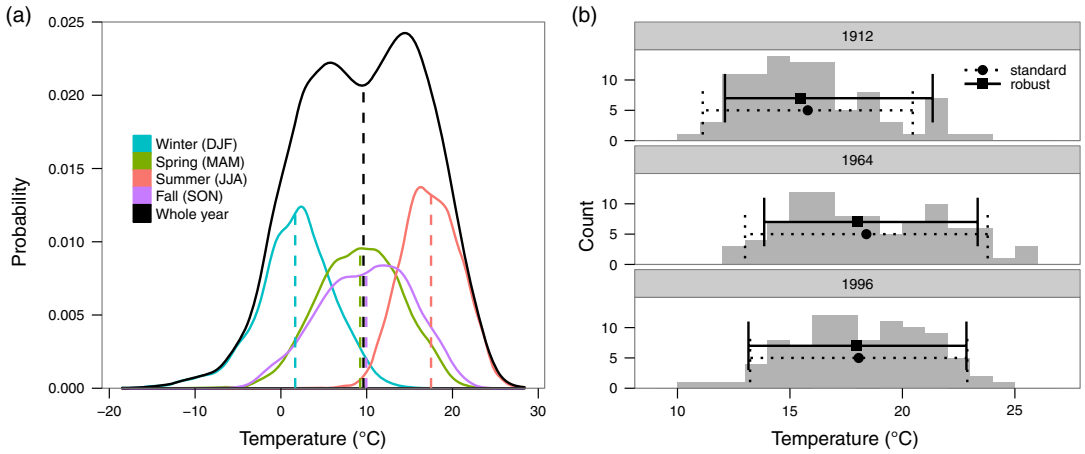

Figure 2. (a) Densities of daily mean temperatures from 1961 to 1990 at the Basel station according to season and for the whole year. Vertical dashed lines denote the mean of the distribution. (b) Histograms of daily mean temperatures in summer (JJA) for the Basel station for 3 distinct years. Superimposed are range bars: Standard implies the mean as center point and 1.64 times the standard deviation as a 90% confidence interval as would be estimated assuming a normal distribution. Robust has the median as its center point and the span between the 0.05th and the 0.95th quantiles as the interval limits (i.e. empirical 90%).

temperature within a decade might inflate the decadal variability measures. We also calculated the decadal variability measures after de-trending each year with its annual mean, but found results to be identical to the original measures, and thus used the raw values for the analysis.

2.2. Methods

In the following, measures for temperature variability are defined. We first motivate the distinction between seasonal and annual measures of variability. Then robust quantile-based variability measures are compared to the symmetric standard deviation. Afterwards we describe the structure of the linear mixed effects model used to detect changes in variability over time. In order to study how changes in variability and mean relate to changes in extremes, we use quantile regression, as described further below.

2.2.1. Seasonal vs. annual variability

Changes in seasonal variability of temperatures may not correspond to similar changes in annual variability. Consequently, it is critical to compare the same type (seasonal versus annual) when discussing results in the context of other studies. To illustrate, Figure 2(a) shows the daily mean temperature distribution of Basel from 1961 to 1990. The mean of the annual temperature distribution is approximately equal to the average over the four means of the seasonal temperature distributions. This fact is supported by principles in statistics, that the grand mean (in this case over the annual temperatures) is equal to the mean of the sub-means (in this case over the component seasons), if the sub-means are of equal size. However, the same general principle does not hold statistically for the variance by the law of total variance, also known as Eve's law. Specifically, the variance of temperatures on the annual scale depends on both the seasonal variances as well as the seasonal means. To see this, picture in Figure 2(a) shifting either the individual season means or increasing or decreasing the individual season variances: both will affect the overall spread of the annual distribution in any multitude of ways. Thus we used seasonal as well as annual measures of variability in all our analyses.

2.2.2. Normal-based vs. asymmetric and robust approaches to variability

In addition to or in lieu of the commonly used standard deviation (SD), there are more robust measures to quantify variability that can also handle asymmetrical distributions. These do not assume a symmetric normal distribution where variability for temperatures above the mean is assumed to be the same as that for temperatures below the mean, so that a single measure, the SD, applies to both. Rather, they rely on sample quantiles of the observed temperatures, say the difference between the 2.5th and 97.5th largest temperatures in the observed dataset (all observed temperatures are ordered from smallest to largest to make this ranking). We term these approaches as robust because they yield the same results as SD-based symmetric confidence intervals (CIs), such as 95% CIs (mean $\pm 2 \times$ SD), when the distribution of temperatures does indeed follow a normal distribution, but also yield accurate results when the true distribution of temperatures does not follow a normal distribution, and in fact under whatever the true underlying distribution of temperatures happens to be (see Stigler (2010) for a history of robust statistics). These approaches are also robust to outliers, which are individual temperature values that are extremely high or low. The 0.025 quantile of the dataset (that temperature below which 2.5% of the observations fall below it) is not affected whether the lowest temperature in the dataset was its observed value or an extreme event with 10° below

it. Figure 2(b) shows specific examples of how robust asymmetric interval ranges can differ from symmetric CIs. For our analyses we used both, the SD as well as robust and potentially asymmetric quantile ranges.

2.2.3. *Modeling changes in mean temperature and variability over time*

Climate change affects all aspects of the temperature distribution, from central mean or median aspects, to variability, to extremes. In this section we study trends in mean, median, and variability measures, in the next, we look at associations between these changes. We begin with mean trends, using as response variables the seasonal, annual and decadal means calculated from daily minimum, mean and maximum temperature values. We used data from all stations together in one mixed-effects model:

$$Y_{st,t} = \left(\beta_0 + b_{0,st}\right) + \left(\beta_1 + b_{1,st}\right) * t + \varepsilon_{st,t} \ ,$$
$$b_{0,st} \ \sim \ N\left(0, \sigma_0^2\right), \ \ b_{1,st} \ \sim \ N\left(0, \sigma_1^2\right),$$
$$\varepsilon_{st,t} \ \sim \ N\left(0, \sigma_\varepsilon^2\right),$$

where $Y_{st,t}$ is the seasonal/annual/decadal mean at station st at time t, β_0 is the common intercept of all stations, $b_{0,st}$ is the deviation of each station from the common intercept (treated as a random variable in the model), β_1 is the common time trend in Y for all stations, $b_{1,st}$ is the deviation of each station from the common time trend (treated as a random variable in the model), t is the time of Y (for seasonal and annual means it is the year centered at the median year 1945 and divided by ten; for decadal means it is the decade; thus time trends are per decade in all three cases) and $\varepsilon_{st,t}$ is the independent normally distributed within-station error. The deviations of each station from the common intercept and trend ($b_{0,st}$ and $b_{1,st}$, respectively) account for differences among the stations in terms of both the mean and trend with time in Y. We additionally fit the model restricted to the last 80 and 40 years of available data, as the last third of the data (1972–2012) corresponded to a period of strong temperature increase that occurred since the mid-1970s, and the last 80 years (1933–2012) additionally included a previous period of slight cooling. Residual plots were inspected to verify model assumptions. The residuals had significant autocorrelation up to order 3, thus an autoregressive process of order 3 was added to the model residuals, i.e. $\varepsilon_{st,t} = \varphi_1\varepsilon_{st,t-1} + \varphi_2\varepsilon_{st,t-2} + \varphi_3\varepsilon_{st,t-3} + u_{st,t}$ with estimated autoregressive coefficients φ_1, φ_2, φ_3 and independent within-station errors $u_{st,t} \ \sim \ N\left(0, \sigma_\varepsilon^2\right)$.

A more robust estimate of mean conditions is the median, thus we repeated the above process with seasonal, annual and decadal medians of daily temperatures (replace Y in the model above with the median instead of the mean).

The same model structure was used to detect changes in variability. We took the standard deviation (SD) and three different quantile ranges to account for different measures of the variability of the temperature distribution: the central 50% region (difference between the 0.75 and 0.25 quantile, Q75-25), the central 90% region (0.95–0.05 quantile, Q95-05) and the central 95% region (0.975–0.025 quantile, Q975-025). In order to detect possible asymmetries related to changes in the spread or variability of the probability distribution, we further divided the central 90% region into a lower 45% region (0.05–0.50 quantile, Q50-05) measuring the spread of the lowest temperatures and an upper 45% measure (0.50–0.95 quantile, Q95-50) measuring the spread of the highest temperatures to better identify how variability changed, e.g. by a symmetric increase in variability for low and high temperatures, for only high temperatures, and so forth. With all measures of variability, the model residuals were not autocorrelated, thus the models were fit without the autoregressive error structure. Table 3 provides a summary of all measures used as model outcome variables.

Qualitative statements on changes in extremes could be derived by examining trends in mean temperature and variability together. If, for example, mean temperature increased, then there would be more warm and less cold extremes. If additionally variability increased

Table 3. Summary of measures used to detect changes in mean conditions and variability over time. Each of these was calculated out of daily minimum, mean and maximum temperatures on a seasonal, annual and decadal basis. They served as response variable (Y) in the mixed-effects model. Last column shows whether the model residuals had significant autocorrelation and if so, up to what lag.

Measure	Description	Autocorrelation
Mean	sample mean	Yes, up to lag 3
Median	sample median (i.e. the 0.50 quantile)	Yes, up to lag 3
SD	sample standard deviation; for a normal-distributed sample, the interval of ±1 SD around the mean holds approximately 68% of observations	No
Q75-25	difference between the 0.75 and 0.25 quantile; length of the interval that contains the central 50% of observations	No
Q95-05	difference between the 0.95 and 0.05 quantile; length of the interval that contains the central 90% of observations	No
Q975-025	difference between the 0.975 and 0.025 quantile; length of the interval that contains the central 95% of observations	No
Q50-05	difference between the 0.50 and 0.05 quantile; length of the interval that contains 45% of observations below the median, without the lowest 5%	No
Q95-50	difference between the 0.95 and 0.50 quantile; length of the interval that contains 45% of observations above the median, without the highest 5%	No

symmetrically, there would be even more warm extremes, as well as more cold extremes than with merely an increase in mean temperature. This approach has multiple drawbacks. First, only qualitative and not quantitative statements are possible. Secondly, relating trends in mean to variability results in many possibilities, especially if variability changes asymmetrically, such as only in the warmer part. Thus we propose an alternative method: quantile regression.

2.2.4. Joint assessment of changes in mean temperature, variability and extremes via quantile regression

Changes in the distribution of minimum, mean and maximum temperatures were detected by simultaneously examining trends in multiple quantiles thereof. Assuming that the temperature distribution is characterized by the set of 19 equally spaced quantiles (0.05, 0.10, … , 0.95), time trends of these quantiles could identify changes in distribution, for example, if the higher quantiles increased and the lower quantiles decreased, then the spread of the distribution has increased and thus also variability has increased. Also changes in extremes (i.e. the extreme quantiles 0.05 and 0.95) could be related to changes in mean temperature (i.e. the median; 0.50 quantile).

We used quantile regression (Koenker and Bassett, 1978; Koenker, 2005) to estimate linear time trends of the seasonal and annual distribution of minimum, mean and maximum temperatures for each station. To estimate time trends, we used the total amount of data which was available at each station (see Table 2) and in a second step only the last 40 years (1973–2012), in order to distinguish between long- and short-term trends. Trends were estimated simultaneously for 19 quantiles (0.05, 0.10, … , 0.95) with the algorithm specified in Bondell *et al.* (2010) in order to ensure non-crossing of the quantile trend lines. Crossing quantile trend lines would contradict the definition of quantiles, e.g. if the 0.95 quantile trend line crossed the 0.90 quantile trend line at a certain time, then for some years the estimated temperature at the 0.95 quantile would be below the temperature at the 0.90 quantile, which is impossible via definition.

All statistical analyses were performed in R version 3.1.0 (RCoreTeam, 2008). The *quantreg*-package (Koenker, 2008) was used for quantile regression and the *nlme*-package (Pinheiro *et al.*, 2013) for linear mixed effects models. Statistical significance was assumed at the 0.05 level unless otherwise stated.

3. Results

3.1. Overall trends in mean temperature and variability measures

Time trends of mean temperatures, median temperatures and all the measures of variability, such as SD and robust intervals (Q75-25, Q95-05, Q975-025, Q50-05 and Q95-50) across all stations included in the study are shown in Figure 3 for Tmax and Tmin, the temperature variables of interest, and Supplementary Figures S1 for Tmean. We first present mean and median trends followed by trends in variability. We conclude with a few remarks on the individual station level.

3.1.1. Mean/Median trends

Seasonal, annual and decadal mean and median trends of daily Tmax were all significantly positive. For the period 1864–2012 they were between 0.09 and 0.15 °C per 10a (all $p < 0.001$) and for the period 1933–2012 they were between 0.13 and 0.21 °C per 10a (all $p < 0.001$). For the last 40 years (1973–2012) warming was not as uniform over seasonal, annual and decadal measures as compared to the longer periods, however still significantly positive. Trends of annual and decadal means were 0.46 °C per 10a (0.41, 0.50; 95% confidence interval), while trends of annual and decadal medians were higher with 0.67 °C per 10a (0.59, 0.75) and 0.65 °C per 10a (0.58, 0.71), respectively. Seasonal trends differed even more, as for instance mean winter Tmax rose at only 0.14 °C per 10a (0.02, 0.26) compared to mean spring Tmax, which rose at 0.80 °C per 10a (0.73, 0.87). In summary, mean and median trends show consistent and accelerating warming of maximum temperatures from 1864 to 2012 and seasonally diverging trends in the period 1973–2012. Tmin trends exhibited the same patterns in general, however, during 1864–2012 winter and summer Tmin warmed more than Tmax, e.g. the mean winter Tmin trend was 0.16 (0.11, 0.20) compared to 0.10 °C per 10a (0.07, 0.13) for Tmax. In the 1973–2012 period the opposite was true, i.e. Tmin warmed less than Tmax in all seasons, as well as on annual and decadal scale. This effect was most apparent in spring, where the mean Tmin trend [0.46 °C per 10a (0.36, 0.56)] was approximately half of the Tmax trend [0.80 °C per 10a (0.73, 0.87)], and in winter, where mean Tmin did not change at all ($p = 0.95$) compared to small increases in Tmax (0.14 °C per 10a, $p = 0.02$).

3.1.2. Trends in measures of temperature variability

Contrary to mean and median, trends in temperature variability did not point in the same direction for each time base, time frame and temperature variable (Figure 3). For instance, during the period 1864–2012, variability of Tmax did not change for winter, spring, fall, annual and decadal measures ($p > 0.05$), only in summer all variability measures showed a significant increase in variability (all $p < 0.01$). For the period 1973–2012, however, the opposite is true: summer variability did not change (all measures $p > 0.05$), but winter, spring, annual and decadal variability increased and fall variability decreased (all measures except Q75-25; $p < 0.01$). While there were high differences in trends between the four measures of variability for each time base, e.g. annual SD increased at 0.12 °C per 10a (0.06, 0.17) and annual Q95-05 increased at 0.45 °C per 10a (0.26, 0.63), the trends of each of the four measures were of similar magnitude between time bases, i.e. the seasons, year and decade. For instance, SD increased at 0.12 °C per 10a (0.06, 0.18) in winter, 0.09 °C

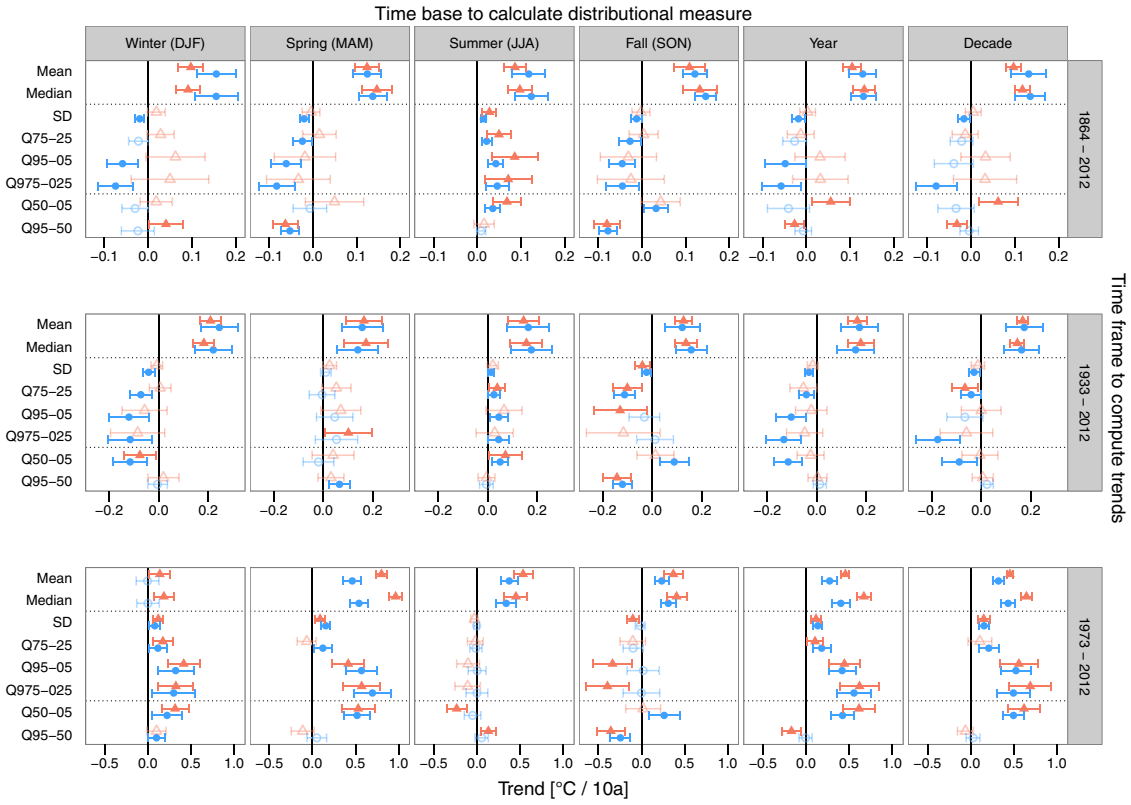

Figure 3. Estimated common time trend coefficients for linear mixed effects models of various distributional measures of maximum temperatures (Tmax; red triangles) and minimum temperatures (Tmin; blue circles) versus time of all stations, depending on the time base used to compute the measures (columns) and the time frame for trend estimation (rows). Error bars show 95% confidence intervals. Trends in solid lines are significant at the 0.05 level, while the transparent ones are not, i.e. zero is within the confidence bounds. SD = Standard deviation, quantile-based measures start with Q, followed by the bounds (e.g. Q95-05 is the range between the 0.95 and the 0.05 quantile).

per 10a (0.03, 0.14) in spring and 0.15 °C per 10a (0.08, 0.22) when calculated on a decadal base; Q95-05 increased at 0.42 °C per 10a (0.23, 0.60) in winter and spring, and 0.56 °C per 10a (0.34, 0.78) when calculated by decade. In summary, there were opposing variability trends for maximum temperatures of the 1864–2012 period compared to those of the recent 1973–2012 period, and seasonal divergence of variability trends in the recent period. Variability trends for Tmin were close to Tmax during the last 40 years (1973–2012), but not so for the 1864–2012 period, where variability of Tmin decreased in winter, spring, fall and on the annual time base (all measures except Q75-25, $p < 0.05$) compared to no changes in Tmax variability.

3.1.3. *Asymmetric changes in temperature variability*

The increase in Tmax summer variability during 1864–2012 was accompanied by an increase in variability of the colder part of temperatures but not in the warmer part, as Q50-05 increased and Q95-50 did not change ($p < 0.001$ and $p = 0.19$). Annual variability during the same period did not change, however, Q50-05 increased at 0.06 °C per 10a (0.01, 0.10) and Q95-50 decreased to −0.03 °C per 10a (−0.05, 0.00), i.e. changes in the variability of the colder and warmer part of Tmax canceled each other out in terms of total variability. This further implies that the distribution of annual temperatures did not become wider as such, but changed shape. Even more asymmetric changes were found for Tmax during the period 1973–2012, where either only one of the two measures (Q50-05 and Q95-50) changed, or both changed but in opposite directions. For instance winter and spring Q95-50 of Tmax showed no change (both $p > 0.05$), only Q50-05 increased at 0.32 (0.16, 0.47) and 0.53 °C per 10a (0.34, 0.72), respectively. In other words, the increased variability [Q95-05 trend of 0.42 °C per 10a (0.23, 0.60)] is only because variability of the colder part of temperatures increased, but not in the warmer part. Based on annual measures of Tmax, variability of the colder part increased much stronger [0.62 °C per 10a (0.43, 0.80)] than variability of the hotter part decreased [−0.17 °C per 10a (−0.28, −0.06)]. This yielded a smaller net increase in total variability Q95-05 [0.45 °C per 10a (0.26, 0.63)], which masked the asymmetric changes.

Q50-05 and Q95-50 trends of Tmin were different than corresponding trends of Tmax in few cases, most notably during the last 40 years (1973–2012). Variability of winter Tmin during 1864–2012 and 1973–2012 changed symmetrically, as variability of the upper and lower part did

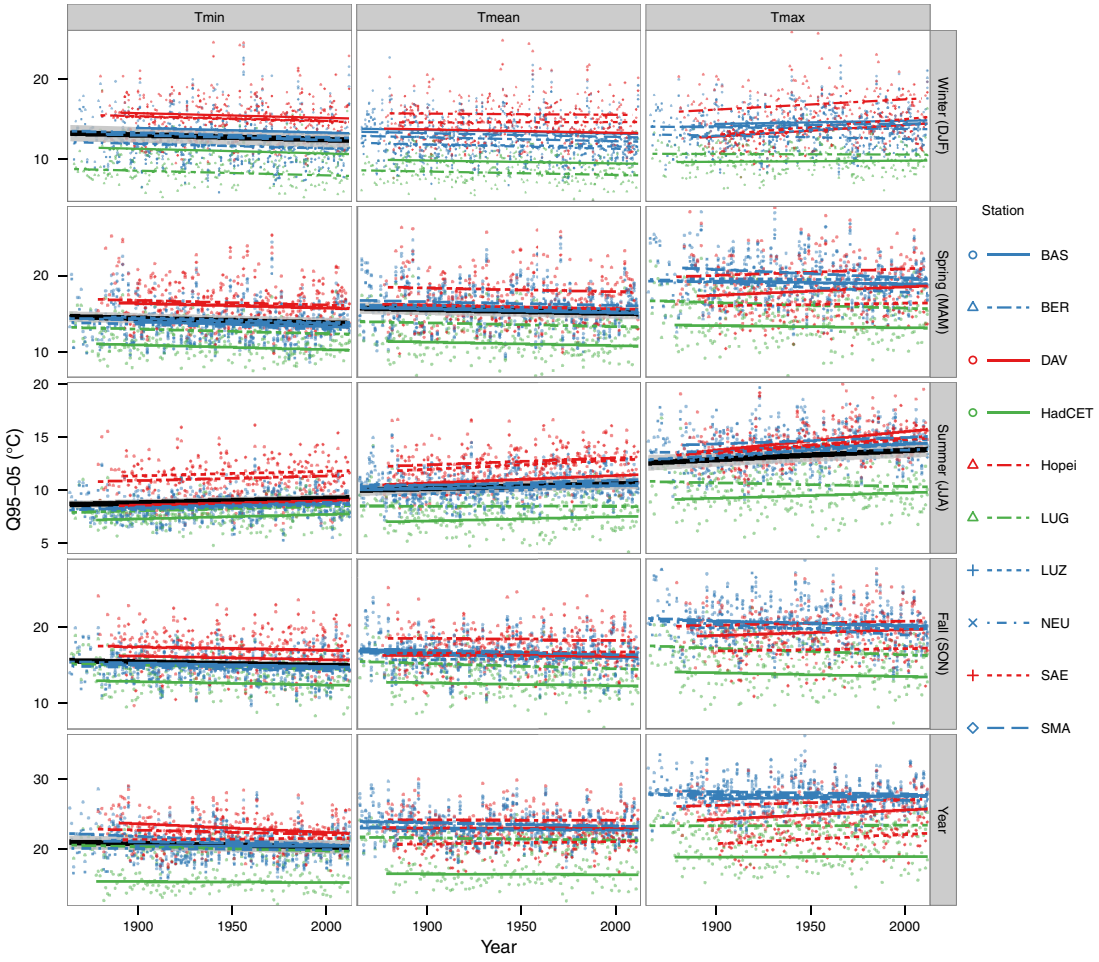

Figure 4. Modelled trends and raw values of Q95-05 (difference between 0.95 and 0.05 quantile) for each station according to time base and temperature variable for all years of data. Stations were grouped into High-Alps (red), northern Low-Alps (blue) and South-Alps/England (green). Overall trends for all stations combined are shown in black (95% confidence bands grey), if they are significant (see also values for Q95-05 in Figure 3 and S1).

not change for the 1864–2012 period (both $p > 0.05$) and increased simultaneously during 1973–2012 (both $p < 0.05$). Additionally, summer Tmin variability as well as asymmetry did not change (all $p > 0.1$), but fall showed the strongest sign of asymmetry, as Q50-05 increased at 0.26 °C per 10a (0.08, 0.44), while Q95-50 decreased to −0.24 °C per 10a (−0.36, −0.13), which lead to no change in the total variability (all four measures had $p > 0.1$). In summary, variability of the upper and lower part of temperatures rarely changed in the same direction, i.e. changes in total variability were driven by changes in either variability of colder or warmer temperatures and in few cases no change in total variability was caused by opposing effects of the upper and lower variability, which canceled each other out.

3.1.4. *Individual stations*

Individual station trajectories in the Q95-05 measure of variability across all years of data and all three temperature variables are shown in Figure 4. For Tmin, variability trends of the individual stations were almost identical to the overall trend, however, baseline Q95-05 was different: high alpine stations had the highest and Central England (HadCET) had the lowest baseline rate of Q95-05 due to the maritime influence, for instance, annual variability (Q95-05) in 1945 was 23.1 °C in Davos (DAV) and 15.3 °C in Central England (HadCET). The same applied to winter, spring and summer Tmean trends. Fall and yearly Tmean and all of Tmax trends revealed more differences among the individual stations as well as a greater magnitude of variation from the overall trend. For winter, spring and fall Tmax, individual stations showed opposing behavior: in High-Alps stations variability increased, while in the other stations it decreased, e.g. spring Q95-05 trend was 0.08 °C per 10a at Hohenpeissenberg (Hopei) and −0.07 °C per 10a at Lugano (LUG).

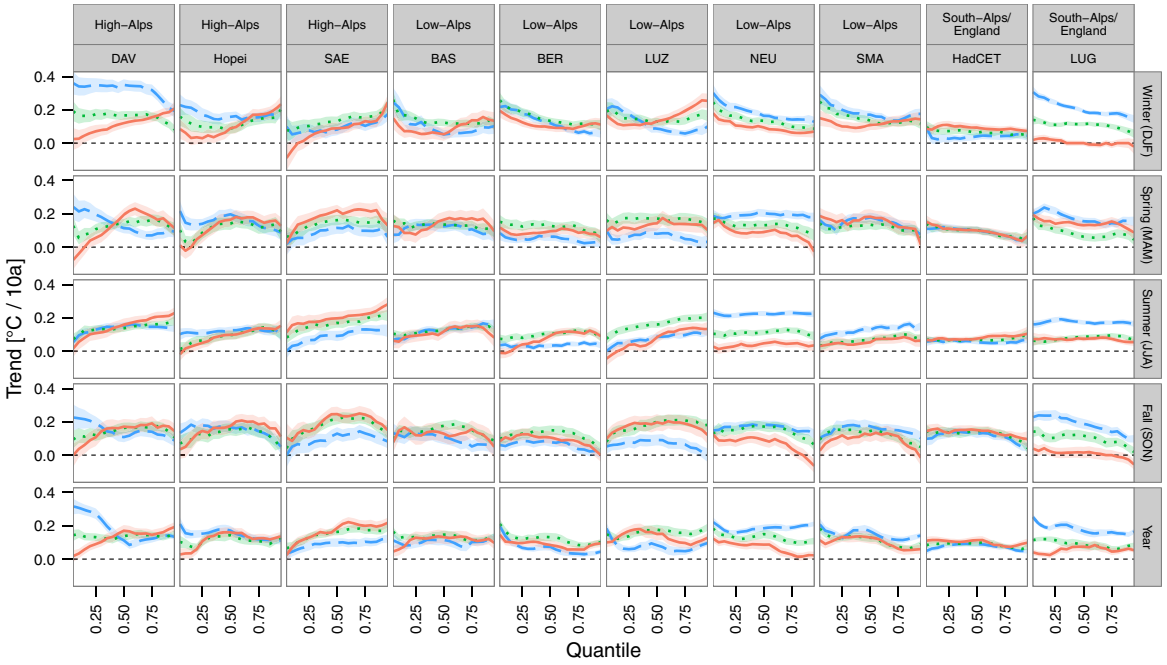

Figure 5. Slope-quantile plots from quantile regression of temperature versus time for the ten stations and different seasons, as well as for the whole year as time base. Time trends were estimated for the 0.05, 0.10, … , 0.95 quantiles. Colors code the different temperature variables (Tmin = blue dashed, Tmean = green dotted, Tmax = red solid). Trends at the specific quantiles are significant at the 0.05 level, if the 95% confidence bands do not cross the dashed zero line, and not significant if they cross it. See Supplementary Figure S2 for an explanation of slope-quantile plots.

3.2. Simultaneous changes in temperature mean and variability and their effect on extremes

We used quantile regression to model changes in the full temperature distribution of each station, characterized by time trends of the 0.05, 0.10, … , 0.95 quantiles of Tmin, Tmean and Tmax, in contrast to the previous section, which dealt with overall trends in ranges of quantiles. Seasonal and annual quantile trends are summarized in terms of slope-quantile plots for each of the ten stations (Figure 5).

The stations at high elevation (DAV, SAE and Hopei) exhibited an increasing variability of the Tmax distribution during 1864–2012, as lower quantiles had smaller trends than high quantiles, i.e. coldest Tmax warmed less than hottest Tmax. For instance coldest summer Tmax, i.e. the 0.05 quantile, at Saentis (SAE) increased at 0.11 °C per 10a (0.07, 0.15), while the hottest temperatures, i.e. the 0.95 quantile, increased at 0.28 °C per 10a (0.24, 0.33). Actually, coldest Tmax did not change for the high-Alpine stations in some seasons and annually, where e.g. 0.05 quantile trends were not significantly different from zero ($p > 0.05$). Thus the increase in variability totally offset the effect of mean warming for coldest Tmax at these high elevation sites. This effect also occurred for Tmin at the highest site (SAE) in all seasons except winter, i.e. coldest Tmin did not warm in spring, summer and fall (all $p > 0.05$).

Sites at lower elevation (BAS, BER, LUZ and NEU) showed an increase in variability mainly for Tmax in summer, which was due to smaller warming trends of the lowest quantiles compared to the median. Higher quantiles had trends similar to the median, thus for these stations the increase in hot Tmax extremes is in accordance to median (or mean) trends. For instance with summer Tmax at BER, the trend of the 0.05 quantile was −0.01 °C per 10a (−0.04, 0.02), which is lower than the median trend of 0.09 °C per 10a (0.07, 0.12), which itself is almost identical to the trend of the 0.95 quantile 0.09 °C per 10a (0.06, 0.12).

For LUG, which is located south of the Alps ridge, trends for Tmin were higher than for Tmax for all quantiles and seasons. Additionally, winter, spring and fall Tmin showed reduced variability, as warming of the coldest temperatures was higher than for hottest temperatures, for example in winter the 0.05 quantile of Tmin increased at 0.31 °C per 10a (0.27, 0.34), while the 0.95 quantile increased less at only 0.14 °C per 10a (0.12, 0.17).

Restricting the analyses to the last 40 years (Figure 6) yielded trends that differed more between quantiles and seasons, thus implying asymmetric changes in the temperature distribution. For instance, in spring lowest temperatures warmed much less than median and higher temperatures, and especially for Tmin, most stations (except BER and LUG) showed no change at all in lowest temperatures (0.05 quantile trends: all $p > 0.05$). Summer trends showed significant warming in all parts of Tmin and Tmax (trends for all quantiles positive, all $p < 0.05$) except for HadCET. Still asymmetries occurred especially for Tmax, as median trends were in most cases lower than trends at the coldest and highest quantiles, e.g. at SMA

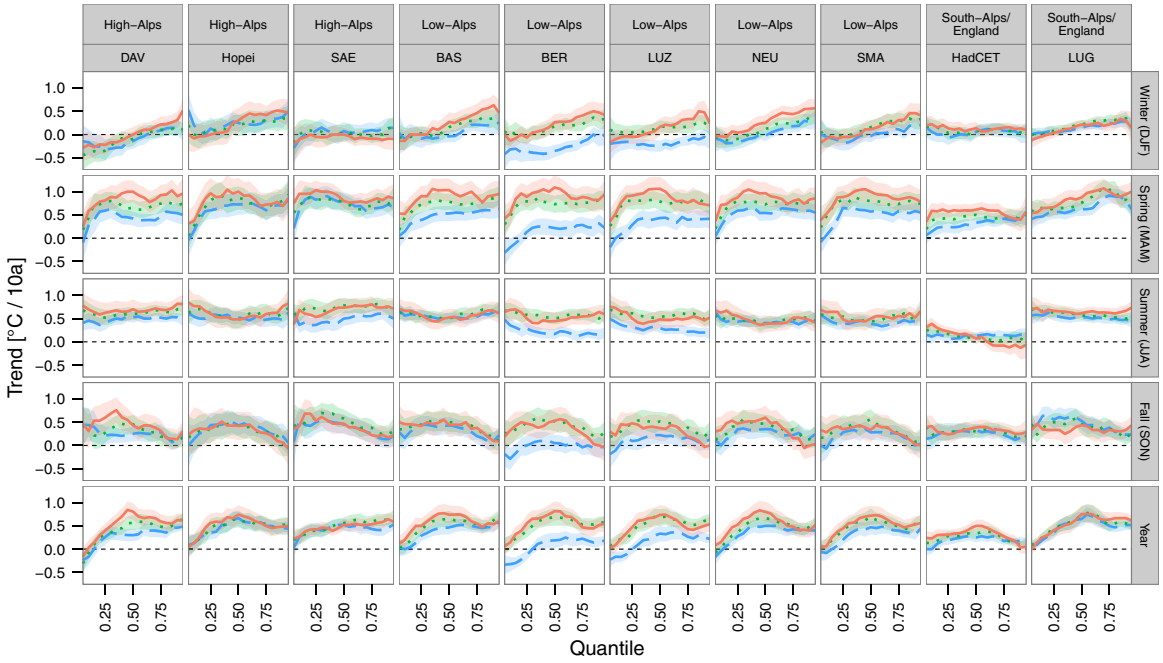

Figure 6. Same as Figure 5, but only for the last 40 years of available data (1973–2012).

the median trend was 0.50 °C per 10a (0.31, 0.69) and trends for the 0.05 and 0.95 quantile were 0.68 (0.44, 0.93) and 0.67 °C per 10a (0.42, 0.9), respectively. Fall trends showed the opposite, i.e. median trends were higher than trends at the lowest and highest quantiles, as e.g. Tmax at NEU had a median trend of 0.60 °C per 10a (0.34, 0.86) compared to 0.30 (0.00, 0.60) and 0.03 °C per 10a (−0.22, 0.28) trends of the 0.05 and 0.95 quantile. In summary, the temperature trends were not the same for the colder and warmer parts of seasonal temperatures, and especially in the last 40 years, extreme temperatures did not change according to median trends.

4. Discussion

Conclusions from this analysis of roughly 150 years of data from ten different stations in Europe were that variability of temperature did change over this period, but not equally in all seasons and that the change in temperature variability was not symmetric in most cases. The asymmetry makes it harder to relate mean temperature trends to variability trends in their compound effect on changes in extreme temperatures. Looking directly at trends in multiple temperature quantiles, changes in mean, variability and extremes and their interdependencies were simultaneously compared.

We used multiple measures of variability and found that time trends for the different measures followed the same direction, however, their magnitude varied (Figure 3). The standard deviation (SD) had the smallest absolute trends out of the four measures and hence the shortest confidence bands, followed by the robust 50% quantile range (Q75-25) with slightly larger trends and confidence intervals. The 90% (Q95-05) and 95% (Q975-025) quantile ranges had the largest absolute trends and confidence intervals. The differences in magnitude and confidence bands of trends tracked the size of the variability measure: SD was the smallest variability measure due to the normality approximation, followed by the quantile ranges, whose length increased with the quantile size. After standardizing the outcome (to zero mean and unit standard deviation), there was no longer a difference between the magnitude of trends (see Supplementary Figure S3).

But the notion of temperature variability has shortcomings since it is a compound measure that combines both the effects in the lower and upper parts of the temperature distribution. Our comprehensive analysis showed that changes in temperature variability can be more precisely characterized by isolating changes in the upper and lower ends of the temperature distribution, i.e. by changes in the coldest temperatures versus changes in the warmest. The observation of no trend in variability could be the result changes in opposite directions at the upper and lower ends that have canceled each other out. The most commonly used measure of SD based on the assumption of an underlying symmetric normal distribution failed in this regard, as e.g. during 1973–2012 summer SD of Tmax showed no change ($p = 0.14$), while the variability of the lower part (Q50-05) decreased and variability of the upper part (Q95-50) increased (both $p < 0.01$; see also Figure 3).

By separating variability into an upper and lower part, we found that asymmetries occurred on different time scales. First, trends in mean and variability were not uniform

across seasons (Figure 3), thus the annual temperature distribution did not have symmetric changes in variability, as the upper and lower variability measures had opposing trends, e.g. during 1864–2012, where variability of the upper part of annual temperatures increased and variability of the lower part decreased (both $p < 0.05$). This is in accordance to previous studies, which found that changes differed by season (see e.g. Caesar *et al.*, 2006 and Scherrer *et al.*, 2005). On the other hand, using an annual or decadal time base to compute variability measures made almost no difference in the estimated trends (Figure 3). Secondly, seasonal variability of the upper and lower parts of the temperature distribution did not change simultaneously and in the same direction (Figure 3), thus changing the shape of the seasonal distribution of minimum and maximum temperatures. Third, Tmax and Tmin had different time trends in mean and variability, especially during the 1973–2012 period, implying that warm and cold temperatures changed at different rates. Similar conclusions were reported by Alexander *et al.* (2006) and Brown *et al.* (2008), who analyzed a global dataset of extreme temperature indices and found higher warming rates for minimum than for maximum temperatures. However, trends of minimum temperatures reported in our study should be taken with caution, especially for the longer periods, as the minimum temperature series from 8 of 10 studied stations were not homogenized. In sum, we draw a similar conclusion to that reported in Seneviratne *et al.* (2012), namely that in addition to mean and variability, multiple aspects of the temperature distribution play an important and regionally varying role toward predicting extreme events in climate.

An appealing alternative to separately reporting temperature changes in terms of mean and variability is the simultaneous quantile regression analysis, which do not assume a symmetric Normal distribution for temperature, but rather analyze trends at multiple quantiles ranging from the lowest temperatures to the highest (Figures 5 and 6). Thus median trends, asymmetric changes in variability and trends in extreme quantiles could be compared directly. This approach could be extended in the future in order to analyze overall trends instead of station-specific trends. Extending the study area to all of Europe and other continents would provide further insight whether asymmetric changes in variability are a special feature of the Alpine region in Europe, or a more general phenomenon.

Acknowledgements

This research has received funding from the European Research Council under the European Union's Seventh Framework Programme (FP7/2007-2013)/ERC grant agreement no [282250]. It was performed with the support of the Technische Universität München – Institute for Advanced Study, funded by the German Excellence Initiative. We thank two anonymous reviewers for their comments and suggestions, which have greatly improved the manuscript.

Supporting Information

The following supporting information is available as part of the online article:

Figure S1. Estimated common time trend coefficients for linear mixed effects models of various distributional measures of mean temperature versus time of all stations, depending on the time base used to compute the measures (columns) and the time frame for trend estimation (rows). Error bars show 95% confidence intervals. Trends in solid lines are significant at the 0.05 level, while the transparent ones are not, i.e. zero is within the confidence bounds. SD = Standard deviation, quantile-based measures start with Q, followed by the bounds (e.g. Q95-05 is the range between the 0.95 and the 0.05 quantile).

Figure S2. Quantile Regression example of slope-quantile plots.

Figure S3. Estimated common time trend coefficients for linear mixed effects models of various distributional measures of minimum and maximum temperature versus time of all stations, depending on the time base used to compute the measures (columns) and the time frame for trend estimation (rows). Error bars show 95% confidence intervals. Trends in solid lines are significant at the 0.05 level, while the transparent ones are not, i.e. zero is within the confidence bounds. SD = Standard deviation, quantile-based measures start with Q, followed by the bounds (e.g. Q95-05 is the range between the 0.95 and the 0.05 quantile), but responses scaled to zero mean and unit standard deviation.

References

Alexander LV, Zhang X, Peterson TC, Caesar J, Gleason B, Klein Tank AMG, Haylock M, Collins D, Trewin B, Rahimzadeh F, Tagipour A, Rupa Kumar K, Revadekar J, Griffiths G, Vincent L, Stephenson DB, Burn J, Aguilar E, Brunet M, Taylor M, New M, Zhai P, Rusticucci M, Vazquez-Aguirre JL. 2006. Global observed changes in daily climate extremes of temperature and precipitation. *J. Geophys. Res.* **111**(D5): D05109, doi: 10.1029/2005JD006290.

Ballester J, Giorgi F, Rodó X. 2010. Changes in European temperature extremes can be predicted from changes in PDF central statistics. *Clim. Change* **98**(1–2): 277–284, doi: 10.1007/s10584-009-9758-0.

Baraldi AN, Enders CK. 2010. An introduction to modern missing data analyses. *J. Sch. Psychol.* **48**(1): 5–37, doi: 10.1016/j.jsp.2009.10.001.

Begert M, Schlegel T, Kirchhofer W. 2005. Homogeneous temperature and precipitation series of Switzerland from 1864 to 2000. *Int. J. Climatol.* **25**(1): 65–80, doi: 10.1002/joc.1118.

Beniston M, Goyette S. 2007. Changes in variability and persistence of climate in Switzerland: exploring 20th century observations and 21st century simulations. *Glob. Planet. Change* **57**(1): 1–15, doi: 10.1002/joc.1118.

Bodner TE. 2008. What improves with increased missing data imputations? *Struct. Equ. Model.* **15**: 651–675, doi: 10.1080/10705510802339072.

Bondell HD, Reich BJ, Wang H. 2010. Noncrossing quantile regression curve estimation. *Biometrika* **97**(4): 825–838, doi: 10.1093/biomet/asq048.

Brick JM, Kalton G. 1996. Handling missing data in survey research. *Stat. Methods Med. Res.* **5**(3): 215–238, doi: 10.1177/096228029600500302.

Brown SJ, Caesar J, Ferro CAT. 2008. Global changes in extreme daily temperature since 1950. *J. Geophys. Res.* **113**(D5): D05115, doi: 10.1029/2006JD008091.

Caesar J, Alexander L, Vose R. 2006. Large-scale changes in observed daily maximum and minimum temperatures: creation and analysis

of a new gridded data set. *J. Geophys. Res.* **111**(D5): D05101, doi: 10.1029/2005JD006280.
Christidis N, Stott PA, Brown S, Hegerl GC, Caesar J. 2005. Detection of changes in temperature extremes during the second half of the 20th century. *Geophys. Res. Lett.* **32**(20): L20716, doi: 10.1029/2005GL023885.
Christidis N, Stott PA, Brown SJ. 2011. The role of human activity in the recent warming of extremely warm daytime temperatures. *J. Clim.* **24**(7): 1922–1930, doi: 10.1175/2011JCLI4150.1.
Christidis N, Stott PA, Hegerl GC, Betts RA. 2013. The role of land use change in the recent warming of daily extreme temperatures. *Geophys. Res. Lett.* **40**(3): 589–594, doi: 10.1002/grl.50159.
Collins D, Della-Marta P, Plummer N, Trewin B. 2000. Trends in annual frequencies of extreme temperature events in Australia. *Aust. Meteorol. Mag.* **49**(4): 277–292.
Cubasch U, Wuebbles U, Chen D, Facchini M, Frame D, Mahowald N, Winther J-G. 2013. Introduction. In *Climate Change 2013: The Physical Science Basis. Contribution of Working Group I to the Fifth Assessment Report of the Intergovernmental Panel on Climate Change*, Stocker T, Qin D, Plattner G-K, Tignor M, Allen S, Boschung J, Nauels A, Xia Y, Bex V, Midgley P (eds). Cambridge University Press: Cambridge, UK and New York, NY.
Della-Marta PM, Haylock MR, Luterbacher J, Wanner H. 2007. Doubled length of western European summer heat waves since 1880. *J. Geophys. Res.* **112**(D15): D15103, doi: 10.1029/2007JD008510.
Donat MG, Alexander LV. 2012. The shifting probability distribution of global daytime and night-time temperatures. *Geophys. Res. Lett.* **39**(14): L14707, doi: 10.1029/2012GL052459.
Easterling DR, Evans JL, Groisman PY, Karl TR, Kunkel KE, Ambenje P. 2000. Observed variability and trends in extreme climate events: a brief review. *Bull. Am. Meteorol. Soc.* **81**(3): 417–425, doi: 10.1175/1520-0477(2000)081<0417:OVATIE>2.3.CO;2.
Eichner JF, Kantelhardt JW, Bunde A, Havlin S. 2006. Extreme value statistics in records with long-term persistence. *Phys. Rev. E* **73**(1): 016130, doi: 10.1103/PhysRevE.73.016130.
Folland CK, Karl T, Christy J, Clarke R, Gruza G, Jouzel J, Mann M, Oerlemans J, Salinger M, Wang S-WT. 2001. Observed climate variability and change. In *Climate Change 2001: The Scientific Basis. Contribution of Working Group I to the Third Assessment Report of the Intergovernmental Panel on Climate Change*, Houghton J, Ding Y, Griggs D, Noguer M, Van der Linden P, Dai X, Maskell K, Johnson C (eds). Cambridge University Press: Cambridge, UK and New York, NY.
Gloning P, Estrella N, Menzel A. 2013. The impacts of climate change on the winter hardiness zones of woody plants in Europe. *Theor. Appl. Climatol.* **113**(3–4): 683–695, doi: 10.1007/s00704-012-0817-5.
Griffiths GM, Chambers LE, Haylock MR, Manton MJ, Nicholls N, Baek H-J, Choi Y, Della-Marta PM, Gosai A, Iga N, Lata R, Laurent V, Maitrepierre L, Nakamigawa H, Ouprasitwong N, Solofa D, Tahani L, Thuy DT, Tibig L, Trewin B, Vediapan K, Zhai P. 2005. Change in mean temperature as a predictor of extreme temperature change in the Asia–Pacific region. *Int. J. Climatol.* **25**(10): 1301–1330, doi: 10.1002/joc.1194.
Hansen J, Sato M, Ruedy R. 2012. Perception of climate change. *Proc. Natl. Acad. Sci. USA* **109**(37): E2415–E2423, doi: 10.1073/pnas.1205276109.
Hegerl GC, Zwiers FW, Stott PA, Kharin VV. 2004. Detectability of anthropogenic changes in annual temperature and precipitation extremes. *J. Clim.* **17**(19): 3683–3700, doi: 10.1175/1520-0442(2004)017<3683:DOACIA>2.0.CO;2.
Huntingford C, Jones PD, Livina VN, Lenton TM, Cox PM. 2013. No increase in global temperature variability despite changing regional patterns. *Nature* **500**(7462): 327–330, doi: 10.1038/nature12310.
IPCC. 2012. Summary for policymakers. In *Managing the Risks of Extreme Events and Disasters to Advance Climate Change Adaptation*, Field CB, Barros V, Stocker TF, Qin D, Dokken DJ, Ebi KL, Mastrandrea MD, Mach KJ, Plattner G-K, Allen SK, Tignor M and Midgley PM (eds). A Special Report of Working Groups I and II of the Intergovernmental Panel on Climate Change (IPCC). Cambridge University Press: Cambridge, UK, and New York, NY, 3–21.
IPCC. 2013. Summary for policymakers. In *Climate Change 2013: The Physical Science Basis. Contribution of Working Group I to the Fifth Assessment Report of the Intergovernmental Panel on Climate Change*, Stocker T, Qin D, Plattner G-K, Tignor M, Allen S, Boschung J, Nauels A, Xia Y, Bex V, Midgley P (eds). Cambridge University Press: Cambridge, UK and New York, NY.
Karl TR, Knight RW, Plummer N. 1995. Trends in high-frequency climate variability in the twentieth century. *Nature* **377**(6546): 217–220, doi: 10.1038/377217a0.
Katz RW, Brown BG. 1992. Extreme events in a changing climate: variability is more important than averages. *Clim. Change* **21**(3): 289–302, doi: 10.1007/BF00139728.
Klein Tank AMG, Können GP, Selten FM. 2005. Signals of anthropogenic influence on European warming as seen in the trend patterns of daily temperature variance. *Int. J. Climatol.* **25**(1): 1–16, doi: 10.1002/joc.1087.
Koenker R. 2005. *Quantile Regression*. Cambridge University Press: Cambridge, UK.
Koenker R. 2008. quantreg: Quantile Regression. R package version 4.98.
Koenker R, Bassett G. 1978. Regression quantiles. *Econometrica* **46**(1): 33–50, doi: 10.2307/1913643.
Meehl GA, Karl T, Easterling DR, Changnon S, Pielke R, Changnon D, Evans J, Groisman PY, Knutson TR, Kunkel KE, Mearns LO, Parmesan C, Pulwarty R, Root T, Sylves RT, Whetton P, Zwiers F. 2000. An introduction to trends in extreme weather and climate events: observations, socioeconomic impacts, terrestrial ecological impacts, and model projections. *Bull. Am. Meteorol. Soc.* **81**(3): 413–416, doi: 10.1175/1520-0477(2000)081<0413:AITTIE>2.3.CO;2.
Min S-K, Zhang X, Zwiers F, Shiogama H, Tung Y-S, Wehner M. 2013. Multimodel detection and attribution of extreme temperature changes. *J. Clim.* **26**(19): 7430–7451, doi: 10.1175/JCLI-D-12-00551.1.
O'Neill MS, Ebi KL. 2009. Temperature extremes and health: impacts of climate variability and change in the United States. *J. Occup. Environ. Med.* **51**(1): 13–25, doi: 10.1097/JOM.0b013e318173e122.
Parker D, Horton B. 2005. Uncertainties in central England temperature 1878–2003 and some improvements to the maximum and minimum series. *Int. J. Climatol.* **25**(9): 1173–1188, doi: 10.1002/joc.1190.
Parker DE, Legg T, Folland CK. 1992. A new daily central England temperature series, 1772–1991. *Int. J. Climatol.* **12**(4): 317–342, doi: 10.1002/joc.3370120402.
Parker DE, Jones PD, Folland CK, Bevan A. 1994. Interdecadal changes of surface temperature since the late nineteenth century. *J. Geophys. Res.* **99**(D7): 14373–14399, doi: 10.1029/94JD00548.
Pinheiro J, Bates D, DebRoy S, Sarkar D, RCoreTeam. 2013. nlme: Linear and Nonlinear Mixed Effects Models. R package version 3.1-109.
Rahmstorf S, Coumou D. 2011. Increase of extreme events in a warming world. *Proc. Natl. Acad. Sci. USA* **108**(44): 17905–17909, doi: 10.1073/pnas.1101766108.
RCoreTeam. 2008. *R: A Language and Environment for Statistical Computing*. R Foundation for Statistical Computing: Vienna, Austria.
Reich BJ. 2012. Spatiotemporal quantile regression for detecting distributional changes in environmental processes. *J. R. Stat. Soc. Ser. C Appl. Stat.* **61**(4): 535–553, doi: 10.1111/j.1467-9876.2011.01025.x.
Reyer CPO, Leuzinger S, Rammig A, Wolf A, Bartholomeus RP, Bonfante A, de Lorenzi F, Dury M, Gloning P, Abou Jaoudé R, Klein T, Kuster TM, Martins M, Niedrist G, Riccardi M, Wohlfahrt G, de Angelis P, de Dato G, François L, Menzel A, Pereira M. 2013. A plant's perspective of extremes: terrestrial plant responses to changing climatic variability. *Glob. Change Biol.* **19**(1): 75–89, doi: 10.1111/gcb.12023.
Rhines A, Huybers P. 2013. Frequent summer temperature extremes reflect changes in the mean, not the variance. *Proc. Natl. Acad. Sci. USA* **110**(7): E546–E546, doi: 10.1073/pnas.1218748110.
Rubin DB. 1978. Multiple imputations in sample surveys-a phenomenological Bayesian approach to nonresponse. *Proceedings of the Section on Survey Research Methods*, 20–28.
Rusticucci M, Barrucand M. 2004. Observed trends and changes in temperature extremes over Argentina. *J. Clim.* **17**: 4099–4107, doi: 10.1175/1520-0442(2004)017<4099:OTACIT>2.0.CO;2.
Rybski D, Bunde A, Havlin S, von Storch H. 2006. Long-term persistence in climate and the detection problem. *Geophys. Res. Lett.* **33**(6): L06718, doi: 10.1029/2005GL025591.
Scherrer SC, Appenzeller C, Liniger MA, Schär C. 2005. European temperature distribution changes in observations and climate change scenarios. *Geophys. Res. Lett.* **32**(19): L19705, doi: 10.1029/2005GL024108.
Seneviratne SI, Nicholls N, Goodess CM, Kanae S, Kossin J, Luo Y, Marengo J, McInnes K, Rahimi M, Reichstein M, Sorteberg A, Vera C, Zhang X. 2012. Changes in climate extremes and their impacts on the natural physical environment. In *Managing the Risks of Extreme Events and Disasters to Advance Climate Change Adaptation*, Field CB, Barros V, Stocker TF, Qin D, Dokken DJ, Ebi KL, Mastrandrea MD, Mach KJ, Plattner G-K, Allen SK, Tignor M, Midgley PM (eds). Cambridge University Press: Cambridge, UK, and New York, NY, 109–230.

Shiogama H, Christidis N, Caesar J, Yokohata T, Nozawa T, Emori S. 2006. Detection of greenhouse gas and aerosol influences on changes in temperature extremes. *SOLA* **2**: 152–155, doi: 10.2151/sola.2006-039.

Simolo C, Brunetti M, Maugeri M, Nanni T. 2012. Increasingly warm summers in the Euro–Mediterranean zone: mean temperatures and extremes. *Reg. Environ. Change* **14**: 1825–1832, doi: 10.1007/s10113-012-0373-7.

Song C, Pei T, Zhou C. 2014. The role of changing multiscale temperature variability in extreme temperature events on the eastern and central Tibetan Plateau during 1960–2008. *Int. J. Climatol.* **34**(14): 3683–3701, doi: 10.1002/joc.3935.

Stigler SM. 2010. The changing history of robustness. *J. Am. Stat. Assoc.* **64**(4): 277–281, doi: 10.1198/tast.2010.10159.

Thompson RM, Beardall J, Beringer J, Grace M, Sardina P. 2013. Means and extremes: building variability into community-level climate change experiments. *Ecol. Lett.* **16**(6): 799–806, doi: 10.1111/ele.12095.

Trigo RM, Pereira JMC, Pereira MG, Mota B, Calado TJ, Dacamara CC, Santo FE. 2006. Atmospheric conditions associated with the exceptional fire season of 2003 in Portugal. *Int. J. Climatol.* **26**(13): 1741–1757, doi: 10.1002/joc.1333.

Wen QH, Zhang X, Xu Y, Wang B. 2013. Detecting human influence on extreme temperatures in China. *Geophys. Res. Lett.* **40**(6): 1171–1176, doi: 10.1002/grl.50285.

White IR, Royston P, Wood AM. 2011. Multiple imputation using chained equations: issues and guidance for practice. *Stat. Med.* **30**(4): 377–399, doi: 10.1002/sim.4067.

Zwiers FW, Zhang X, Feng Y. 2010. Anthropogenic influence on long return period daily temperature extremes at regional scales. *J. Clim.* **24**(3): 881–892, doi: 10.1175/2010JCLI3908.1.

PLOS ONE

RESEARCH ARTICLE

Interactions between temperature and drought in global and regional crop yield variability during 1961-2014

Michael Matiu[1]*, **Donna P. Ankerst**[2], **Annette Menzel**[1,3]

1 Ecoclimatology, Technical University of Munich, Freising, Germany, **2** Department of Mathematics, Technical University of Munich, Garching, Germany, **3** Institute for Advanced Study, Technical University of Munich, Garching, Germany

* matiu@wzw.tum.de

Citation: Matiu M, Ankerst DP, Menzel A (2017) Interactions between temperature and drought in global and regional crop yield variability during 1961-2014. PLoS ONE 12(5): e0178339. https://doi.org/10.1371/journal.pone.0178339

Editor: Jose Luis Gonzalez-Andujar, Instituto Agricultura Sostenible, SPAIN

Received: November 10, 2016

Accepted: May 11, 2017

Published: May 26, 2017

Data Availability Statement: All relevant data are within the paper or are freely accessible online at the URLs indicated in the manuscript.

Funding: This work was supported by the Technische Universität München – Institute for Advanced Study, funded by the German Excellence Initiative and the European Union Seventh Framework Programme under the grant agreements n° 291763 and n° 282250. The funders had no role in study design, data collection and analysis, decision to publish, or preparation of the manuscript.

Abstract

Inter-annual crop yield variation is driven in large parts by climate variability, wherein the climate components of temperature and precipitation often play the biggest role. Nonlinear effects of temperature on yield as well as interactions among the climate variables have to be considered. Links between climate and crop yield variability have been previously studied, both globally and at regional scales, but typically with additive models with no interactions, or when interactions were included, with implications not fully explained. In this study yearly country level yields of maize, rice, soybeans, and wheat of the top producing countries were combined with growing season temperature and SPEI (standardized precipitation evapotranspiration index) to determine interaction and intensification effects of climate variability on crop yield variability during 1961–2014. For maize, soybeans, and wheat, heat and dryness significantly reduced yields globally, while global effects for rice were not significant. But because of interactions, heat was more damaging in dry than in normal conditions for maize and wheat, and temperature effects were not significant in wet conditions for maize, soybeans, and wheat. Country yield responses to climate variability naturally differed between the top producing countries, but an accurate description of interaction effects at the country scale required sub-national data (shown only for the USA). Climate intensification, that is consecutive dry or warm years, reduced yields additionally in some cases, however, this might be linked to spillover effects of multiple growing seasons. Consequently, the effect of temperature on yields might be underestimated in dry conditions: While there were no significant global effects of temperature for maize and soybeans yields for average SPEI, the combined effects of high temperatures and drought significantly decreased yields of maize, soybeans, and wheat by 11.6, 12.4, and 9.2%, respectively.

Introduction

Climate change alters global food production, with impacts dependent upon crop, region, magnitude of warming, changes in precipitation patterns and extreme events, production

Competing interests: The authors have declared that no competing interests exist.

technology, and adaptation measures [1]. Past evidence has shown climate change to more likely incur damage rather than draw benefits for crop yields [2–5], with induced yield losses only able to be partly offset by endogenous economic responses [6].

The intention to mitigate climate change took a significant step forward during the 2015 United Nations Climate Change Conference in Paris. But irrespective of the future success of such efforts, year-to-year climate variability is unlikely to diminish, and hence neither will its impacts on food [7]. Climate variability accounts for up to 60% of yield variability in major parts of the world [8] and is thus an important factor in food stability. Low yield variability is desirable, because it leads to more stable food production and farmer income [7]. However, changes in yield variability have been positively associated with changes in climate variability [9], suggesting that food stability might continue to deteriorate if climate variability continues to increase, for example, as a consequence of failures to mitigate climate change [10].

The most influential climate variables affecting yields on a global scale are temperature and precipitation, with some studies indicating that they act nonlinearly [2,8,11–15]. Interactions between temperature and precipitation might lead to reduced sensitivity to heat if enough water is available [16], and thus higher relative importance of heat [17]. So while the importance of climate interactions is acknowledged [12] and in some cases included in the models [8,17,18], they are rarely described in detail because of their complexity. This study proposes a way to visualize interaction effects, and quantify interacting effects by conditioning one variable on quantiles of the other. Another type of climate interactions are intensification effects from consecutive dry or warm years [19], which can be assessed by interaction terms of climate variables with their lagged values from previous years.

To this end, this study aims to quantify the interaction between temperature and drought variability in crop yield variability for the four most important crops worldwide (maize, rice, soybeans, and wheat) both at the global and country scale, in order to assess the (1) effects of temperature and drought interactions on yield, (2) differences between crops, and (3) differences between the global climate sensitivities and that for major producers.

Materials and methods

Yearly country-level data on crop production (tons from 1961 to 2014) and harvested area (ha from 1961 to 2014) was available from the Food and Agriculture Organization of the United Nations (FAO, available at http://faostat.fao.org/default.aspx). Yield was then defined as the ratio of production and harvested area. Additionally, the FAO provided globally aggregated data on world production of crops (in tons from 1961–2014, FAO), which was used to determine the top producing countries. The focus was on the primary staple crops that constitute large parts of the human diet: maize, rice, soybeans and wheat, and restricted to countries that had at least an average share of 1% to global production during 1961–2014.

FAO data is annually reported separately by each country, with the consequence that data quality might be inhomogeneous. If countries reported exactly the same values of production for two or more consecutive years, only data from the years after or before the last occurrence of identical values were used (Argentina maize until 2011, India soybeans from 1972 onwards, United Kingdom wheat from 1991 onwards). Furthermore, yield time series that showed constant trends over multiple years, were also discarded (Iran wheat, Turkey wheat) and some extremely improbable values were removed (~1/10 production of France maize in 2014 compared to 2013; double or half yields from one year to the next of Paraguay soybeans before 1969). A summary of the FAO data used for the analysis can be found in S1 Table.

Monthly temperature on a 0.5˚ grid was taken from the CRU TS 3.23 data set [20], while 1-month SPEI (Standardized Precipitation Evapotranspiration Index) values on the same

temporal and spatial resolution were obtained from the SPEIbase v.2.4 [21], which is also based on the CRU TS 3.23 data set. The SPEI is calculated by taking the difference between precipitation and potential evapotranspiration and thus including the impact of temperature on water demand. Values are then standardized for each month and location using log-logistic distributions. Using precipitation instead of SPEI produced qualitatively similar results but lower accuracy. Explanations for the latter could be that the SPEI describes wet- and dryness more accurately on a global scale since it accounts for the varying rates of evapotranspiration as well as being standardized. Including both in the modelling induced collinearity, since precipitation and SPEI were highly correlated, thus only SPEI was used.

In order to merge the climate and crop data, the climatic variables were aggregated to match the temporal (yearly) and spatial (country) resolution of the crop yields in a two-step procedure. First, the day-of-year of planting and harvesting from the crop calendar of Sacks *et al*. [22] was used to derive yearly growing season means of temperature and SPEI for each 0.5˚ grid. Averages were calculated using all monthly climate values between the days of planting and harvesting; for example, if planting was March 2 (or 29) and harvesting September 23 (or 5), monthly temperatures and SPEI from March to September inclusive were included in the average. Second, the 0.5˚ grid growing season averages were aggregated to crop-area weighted country means, for which crop area weights were taken from planted area estimates [23]. While there is some evidence of advancing planting dates in the recent decades, for example in the central USA maize is planted two weeks earlier compared to when it was routinely planted in the early 1980s [24], for other regions like central Europe advancements in crop planting dates are less prominent (e.g. only 0.4 days earlier per decade) [25], consequently using monthly climate data adjusted to a fixed cropping season still seemed appropriate.

Maize, rice and wheat are all grown in multiple seasons. For maize only the main season was used, since the second season constituted a non-significant share of total yields. For rice, the second season contributed large shares to total yields in some countries, so yields were averaged over the two growing season climates, with weights as given in [26]. Since the distinction of winter and spring wheat in the crop calendar was somewhat arbitrary, and as wheat is dormant and rather insensitive to climate conditions in winter, the four months before harvest of the main season were used as the growing season [2].

The logarithm was applied to yields, which turns absolute into relative effects, since climate affects yield in relative and not absolute terms. In other words a 1˚C difference in temperature should have the same effect irrespective if yields are 5 ton/ha or 1 ton/ha. Using logged yield is standard practice [2,4,13–15], and also removes the issues of the skewed yield distribution and heteroscedascity (increased yield variance for higher yields).

Since the focus is on climate variability and its effects on yield variability, trends in climate and yield could confound the estimated relationship and induce spurious correlations if concurrent trends existed. Thus yield, temperature and SPEI were detrended using separate models for each crop-country combination. For temperature and SPEI, penalized regression splines (mgcv-package in R) were used, with a maximum basis dimension of 5 (the actual basis dimension is determined by cross-validation) and the possibility to penalize to zero when there is no trend. The length of the yield time-series varied between 23 and 54, so the maximum basis dimension was set to number of years divided by ten, but not below 3. Inspecting residuals, some crop-country yield time series (S2 Table) were poorly fit, so in order to have appropriate models the basis dimension was doubled. This flexible approach was chosen over linear, quadratic or cubic trends, because it could handle multiple types of non-linearity and removed the need for selecting the most appropriate polynomial.

For each crop, detrended time-series data of all countries were included into one mixed model to explain log detrended yields:

$$\log dYield_{c,t} = (\alpha + \alpha_c) + (\beta + \beta_c)Climate_{c,t} + (\gamma + \gamma_c)Climate.Interactions_{c,t} + (\delta + \delta_c)Climate.Intensification_{c,t,t-1} + \epsilon_{c,t}$$

where

- c is a country index and t is for year (1961–2014).
- $dYield_{c,t}$ is the detrended yield in country c and year t.
- $Climate_{c,t}$ consists of detrended temperature ($dTemp$) and SPEI ($dSPEI$), as well as quadratic terms which implied optimal temperatures/SPEI for yield, while permitting negative effects for low and/or high temperatures or SPEI values: $(\beta + \beta_c)Climate_{c,t} = (\beta_1 + \beta_{1,c})dTemp_{c,t} + (\beta_2 + \beta_{2,c})dTemp^2_{c,t} + (\beta_3 + \beta_{3,c})dSPEI_{c,t} + (\beta_4 + \beta_{4,c})dSPEI^2_{c,t}$.
- $Climate.Interactions_{c,t}$ are interaction terms between detrended temperature and SPEI. The interaction terms accommodated different temperature effects depending on SPEI, for example, allowing a 1˚C change in temperature to have a different impact on yield for dry compared to wet conditions: $(\gamma + \gamma_c)Climate.Interactions_{c,t} = (\gamma_1 + \gamma_{1,c})dTemp_{c,t}dSPEI_{c,t} + (\gamma_2 + \gamma_{2,c})dTemp^2_{c,t}dSPEI_{c,t} + (\gamma_3 + \gamma_{3,c})dTemp_{c,t}dSPEI^2_{c,t} + (\gamma_4 + \gamma_{4,c})dTemp^2_{c,t}dSPEI^2_{c,t}$.
- $Climate.Intensification_{c,t,t-1}$ are previous year temperature and SPEI, and their interaction terms with current year values. These allow for intensification effects of consecutive warm, cold, dry, or wet years: $(\delta + \delta_c)Climate.Intensification_{c,t,t-1} = (\delta_1 + \delta_{1,c})dTemp_{c,t-1} + (\delta_2 + \delta_{2,c})dSPEI_{c,t-1} + (\delta_3 + \delta_{3,c})dTemp_{c,t-1}dTemp_{c,t} + (\delta_4 + \delta_{4,c})dSPEI_{c,t-1}dSPEI_{c,t}$.

In the above model, α is the global intercept, and β, γ, and δ are slopes for climate variables, while coefficient vectors with subscript c accommodate different sensitivities for each country using a random effects specification, that is $(\alpha_c,\beta_c,\gamma_c,\delta_c) \sim N(0,\Sigma)$ with $\Sigma = I_{13}(\sigma^2_1, \ldots, \sigma^2_{13})$ and I_{13} identity matrix of dimension 13. Residual variability was not homogenous across countries, thus a different error variance per country was included, that is $Var(\epsilon_{c,t}) = \sigma^2\phi_c$ with estimated variance ratios $\phi_c (c \geq 2)$ relative to the first country with $\phi_1 = 1$. To arrive at a parsimonious description, non-significant variables were removed.

To compare global climate sensitivities to country effects, single country time series were modelled using the same variables as above (without random effects) for the five top producers of each crop (Table 1). For model selection, non-significant variables were excluded until the minimum BIC (Bayesian Information Criterion) was attained.

For each crop, interacting climate effects were evaluated as fitted values holding all other variables constant that were not part of the interaction. For example, to show the effects of temperature and SPEI, the fitted values for temperature were evaluated at three quantiles of the SPEI distribution denoting extreme dry (0.05 quantile), normal (0.50, median), and extreme wet (0.95) conditions. Similarly climate intensification effects were evaluated over current year temperature/SPEI given three quantiles (as above) of previous year temperature/SPEI. The effects (fitted values) on the log scale were exponentiated, so they became ratios, and then one was subtracted so they became relative differences.

Robustness of the models was evaluated by cross validation, specifically by LOOCV (leave-one-out-cross-validation). Additionally LOOCV errors were calculated for models without interaction terms (but where variables could be linear or quadratic), and for models where all variables were included only linearly (thus without interactions).

Table 1. The top five producers by crop as of 2014.

Crop	Country	Production [million ton]	Share in global production [%]
Maize	USA	361	29.2
	China	216	17.4
	Brazil	80	6.5
	Ukraine	28	2.3
	India	24	1.9
Rice	China	208	21.9
	India	157	16.6
	Indonesia	71	7.5
	Bangladesh	52	5.5
	Viet Nam	45	4.7
Soybeans	USA	108	33.7
	Brazil	87	27.1
	Argentina	53	16.7
	China	12	3.8
	India	11	3.3
Wheat	China	126	14.8
	India	94	11.0
	Russia	60	7.0
	USA	55	6.5
	France	39	4.6

https://doi.org/10.1371/journal.pone.0178339.t001

As a sensitivity analysis, state-level data for the USA was used to derive the national sensitivity of yields to climate using the same random effects specification as above for the global sensitivity. State-level yields (bu/acre) for maize, soybeans, and wheat were available from the National Agricultural Statistics Service of the United States Department of Agriculture (Quick Stats, available at: https://www.nass.usda.gov/Quick_Stats/index.php) for the same study period (1961–2014). No data had to be removed using the quality criteria adopted above for the FAO data. To ensure comparability, the same work-flow procedure was adopted: state-level climate was derived using the same data sources (the crop calendar data contains information at the state scale); detrending and modelling as above; although yield units differ (bu/acre vs t/ha), modelling results are on the %-scale, so no conversion was needed. For the yield detrending of the state time series, three crop-state combinations had to have double the basis dimension (Arizona maize, Maryland wheat, and Oregon maize).

State level yields and climate variables of the USA were aggregated to country averages using the production in each state as weights. Then the same models as for country level data from the FAO were run, in order to compare results obtained from sub-country data to results from country averages.

To quantitatively assess the potential impact of measurement error in FAO yield data on statistical significance of higher-order effects in the model, such as interactions, a simulation study was performed. Noise was added to the detrended log yields by calculating the standard deviation (sd) of each crop-country time series and then adding normally distributed random noise with mean 0 and sd ranging from 1, 2, 3 . . . to 50% of the initial sd to ensure the same percent relative error across the different crop by country time series. The original models were then refit to the noisy data. The addition of random noise was repeated 100 times for each %-level of added noise, yielding 100 simulations of p-values corresponding to the significance of the highest order term(s), whether they being interaction, quadratic, or linear terms,

depending on model. The 100 replications of p-values corresponding to a specific percent relative noise were presented in terms of stacked bar charts.

Results

What follows is a description of the interaction effects found globally and for the five top producing countries, discussed in turn for each crop, followed by an assessment of the intensification effects by previous year climate variability. Then a sensitivity analysis of using state-level data is presented for the USA.

If not otherwise stated, effects for high and low temperature and SPEI are for the respective 5 and 5% quantiles. Percent effects on yields are followed by 95% confidence intervals in brackets, or ns if not significant.

Effects of climate variability and interactions on crop yields

Maize. Globally, maize yields decreased by -7.8% (-10.7, -4.9) in dry and increased by 5.2% (1.9, 8.7) in wet conditions for average temperatures (Fig 1B), but temperature was non-significant for average SPEI (Fig 1A). However, considering interactions, higher temperatures were linked to decreased yields under dry conditions of -11.6% (-14.3, -8.9), but not under wet conditions (Fig 1C).

For the USA, the top producer of maize, low and high temperatures were linked to yield changes of 4.7% (0.1, 9.5) and -4.1% (-8.3, 0.2) (Fig 1A), and both dry and wet conditions were associated to yield decreases, however, stronger for dry with -10.4%, (-14.8, -5.9) than wet with -3.5%, (-5.7, -1.3) (Fig 1B).

For China, no significant temperature effect was found, only a modest effect of -3.0% (-5.5, -0.4) of dry and 2.8% (0.2, 5.4) of wet conditions (Fig 1B).

For Brazil, only dry conditions were associated to yield reductions of -9.1% (-12.9, -5.2), while wet conditions and temperature were not significant (Fig 1A and 1B).

For Ukraine, temperature variability was negatively associated to maize yield variability with 9.6% (2.8, 16.8) for cold and -8.6% (-14.1, -2.7) for warm conditions (Fig 1A).

For India, the temperature-SPEI interaction was highly significant. While SPEI had no significant effect at average temperatures (Fig 1A), for high temperatures dry conditions were associated to yield decreases of -12.7% (-17.2, -8.0) and wet conditions to yield increases of 10.6% (0.9, 21.2) (Fig 1C).

Rice. Globally, rice yield variability showed some dependence on temperature and SPEI variability (Fig 2A–2C), however, effects between the 5 and 95% quantile of climate variables were non-significant at $p = 0.05$. However, at the country scale, effects of climate variability were clearer.

For China, temperature variability was not significant (Fig 2A), but dry and wet conditions were associated to yield increases of 2.0% (1.0, 3.0) and 2.2% (1.1, 3.2), respectively (Fig 2B).

For India, high temperatures and dry conditions were associated to yield decreases of -3.9% (-6.5, -1.3; Fig 2A) and -3.4% (-5.8, -1.0; Fig 2B). On the other hand, low temperatures and wet conditions were associated to yields increases of 3.4% (0.9, 5.9; Fig 2A) and 4.0% (1.2, 6.9; Fig 2B).

For Bangladesh, low temperatures and dry conditions were linked to yield decreases of -3.1% (-5.8, -0.4; Fig 2A) and -3.7% (-5.9, -1.4; Fig 2B) for average SPEI and temperature conditions, respectively. Considering interacting effects, extreme wet conditions were linked to yield decreases for both low and high temperatures of -8.3% (-13.0, -3.5) and -4.3% (-7.6, -0.8) but not for average temperatures (Fig 2C).

For Viet Nam, dry and wet conditions were linked to yield changes of -2.8% (-4.6, -0.9) and 3.0% (1.0, 5.2) (Fig 2B), while temperature was non-significant for average SPEI (Fig 2A).

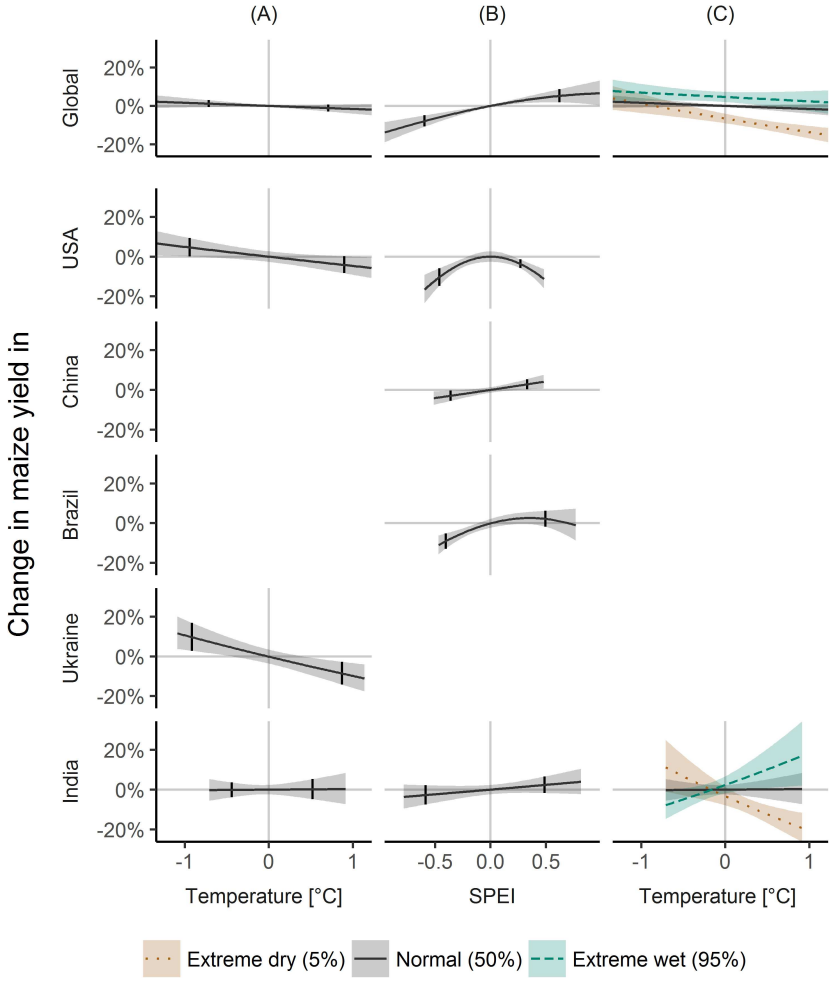

Fig 1. Climate variability effects on maize yield variability. Black lines show the effects of changes in detrended temperature (A, C) and changes in SPEI (standardized precipitation evapotranspiration index, B) on changes in mean maize yield globally and for the five top producing countries. Increasing lines mean that higher temperatures (A, C) or SPEI (B) were associated with greater increases in mean yields, while decreasing lines imply association with decreases in mean yields. Dashed and dotted lines in (C) indicate significant interaction effects. All lines are estimates from the regression models, and the absence of a line indicates non-significance of an association. Shades around the lines indicate pointwise confidence intervals for the mean change in maize yield as estimated from the regression models. Small vertical lines denote the 5 and 95% quantile of detrended temperature (A) and SPEI (B). Countries are ordered according to their total production from the top producer USA downwards.

https://doi.org/10.1371/journal.pone.0178339.g001

However, because of interactions, high temperatures were associated to yield changes of -5.5% (-8.7, -2.1) for dry conditions and 5.6% (1.6, 9.9) for wet conditions (Fig 2C).

Soybeans. Globally, soybeans yield variability was more associated to SPEI variability, with yield effects of 7.1% (3.8, 10.6) and -10.7% (-13.6, -7.7) for wet and dry conditions, respectively (Fig 3B). The effect of temperature was small (Fig 3A), as well as the interaction effect, leading for example to yield decreases of -12.4% (-17.1, -7.4) for hot and dry conditions (Fig 3C).

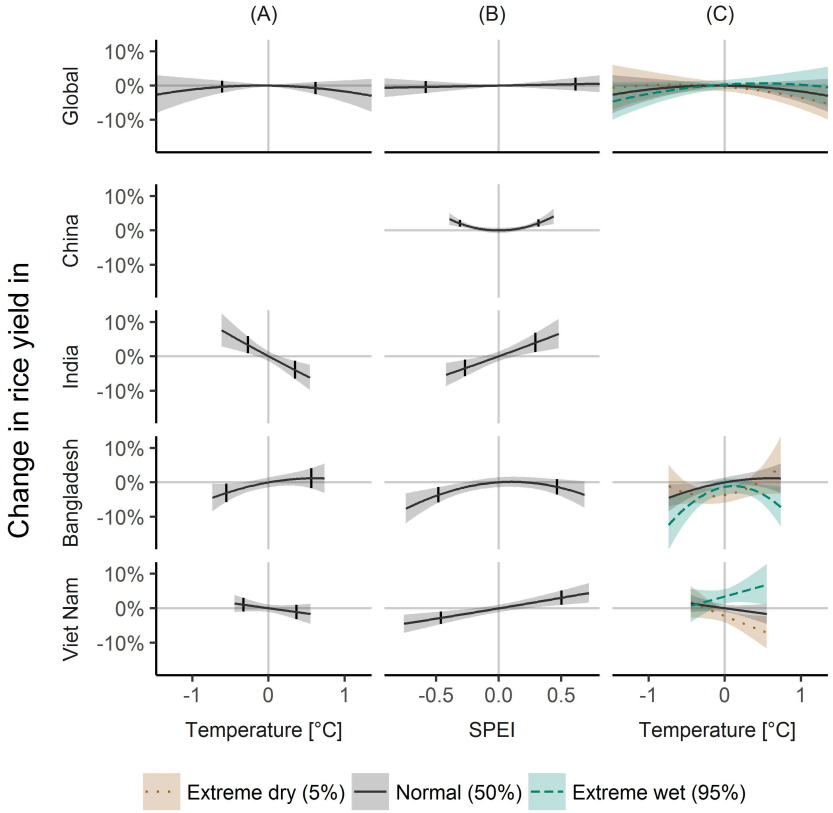

Fig 2. Climate variability effects on rice yield variability. Same as Fig 1, but for rice. Indonesia omitted, because of no significant effects to show.

https://doi.org/10.1371/journal.pone.0178339.g002

For the USA, only SPEI was significant, and yields effects were -5.7% (-9.4, -2.0) for dry conditions and 4.5% (1.2, 7.8) for wet conditions (Fig 3B).

For Brazil, soybean yields were also only affected by dry and wet conditions with -8.1% (-12.5, -3.5) and 8.8% (3.3, 14.4), respectively (Fig 3B).

For Argentina, high temperatures were associated to yield decreases of -14.9% (-20.2, -9.3), while the effect of low temperatures was non-significant (Fig 3A). Dry and wet conditions were linked to -10.7% (-15.9, -5.0) and 8.8% (4.0, 13.9) yield changes (Fig 3B).

For China, only SPEI was significantly linked to soybean yields, with -3.1% (-5.9, -0.1) and 2.8% (0.0, 5.7) changes in yields for dry and wet conditions (Fig 3B).

For India, temperature variability was negatively associated to soybean yields with 16.8% (5.4, 29.3) for cold and -11.8% (-18.4, -4.7) for warm conditions (Fig 3A), and SPEI was positively associated with -12.2% (-21.4, -2.0) for dry and 10.7% (1.2, 21.0) for wet conditions (Fig 3B). However, the combined influence resulted in yield effects of -17.3% (-28.5, -4.4) for hot and dry, and 18.0% (0.6, 38.3) for hot and wet, and non-significant effects for cold and dry, and cold and wet (Fig 3C).

Wheat. Globally, wheat yields were changed by 4.4% (1.7, 7.2) for cold, by -4.2% (-6.8, -1.6) for warm (Fig 4A), by -4.0% (-6.8, -1.1) for dry, and non-significant for wet conditions

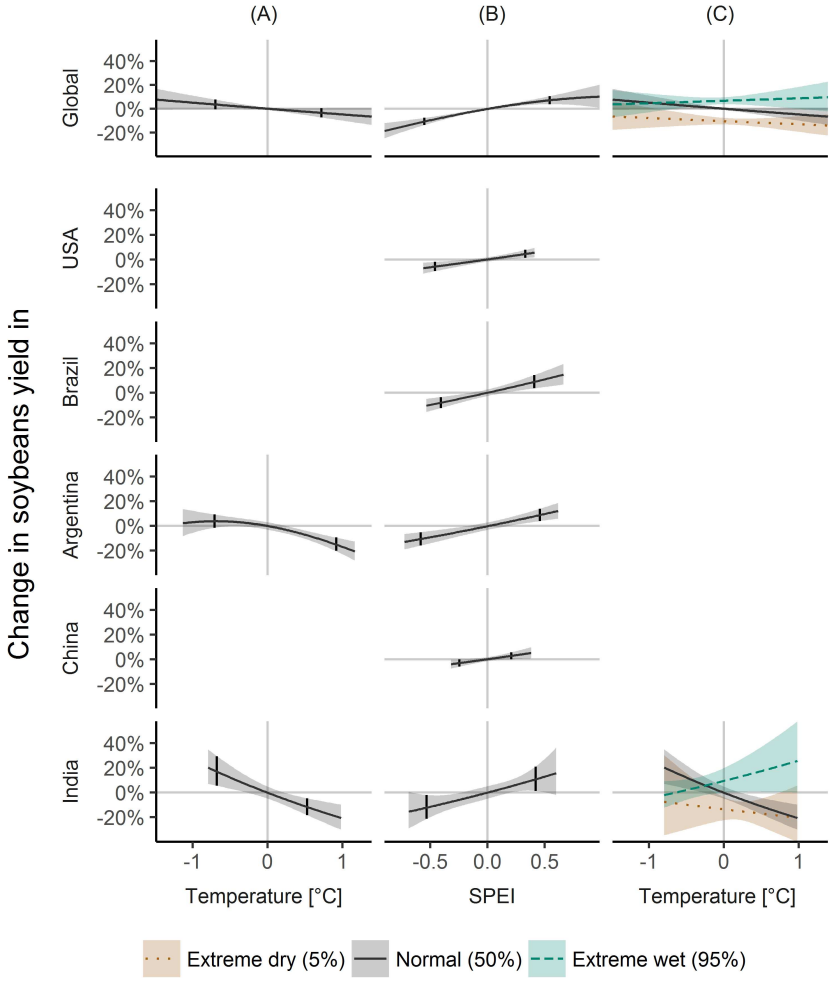

Fig 3. Climate variability effects on soybeans yield variability. Same as Fig 1, but for soybeans.

https://doi.org/10.1371/journal.pone.0178339.g003

(Fig 4B). Interaction effects lead to increased effects of -9.2% (-12.4, -5.9) of high temperature under dry conditions and non-significant temperature effects under wet conditions (Fig 4C).

For China, both low and high temperatures were linked to yield decreases of -4.5% (-7.0, -1.9) and -3.3% (-5.1, -1.4) (Fig 4A).

For India, low and high temperatures were linked to yield changes of 3.2% (0.4, 6.2) and -3.5% (-6.5, -0.5) (Fig 4A).

For Russia, high temperatures were linked to yield decreases of -13.5% (-22.9, -3.1; Fig 4A), while low temperatures and SPEI were non-significant at p = 0.05 (Fig 4A and 4B).

For the USA, dry conditions were associated to yield decreases of -4.5% (-7.7, -1.3), and above average SPEI was non-significant (Fig 4B).

For France, cold temperatures were associated to yield increases of 4.3% (0.7, 7.9; Fig 4A), and wet conditions to yield decreases of -6.0% (-9.3, -2.6; Fig 4B).

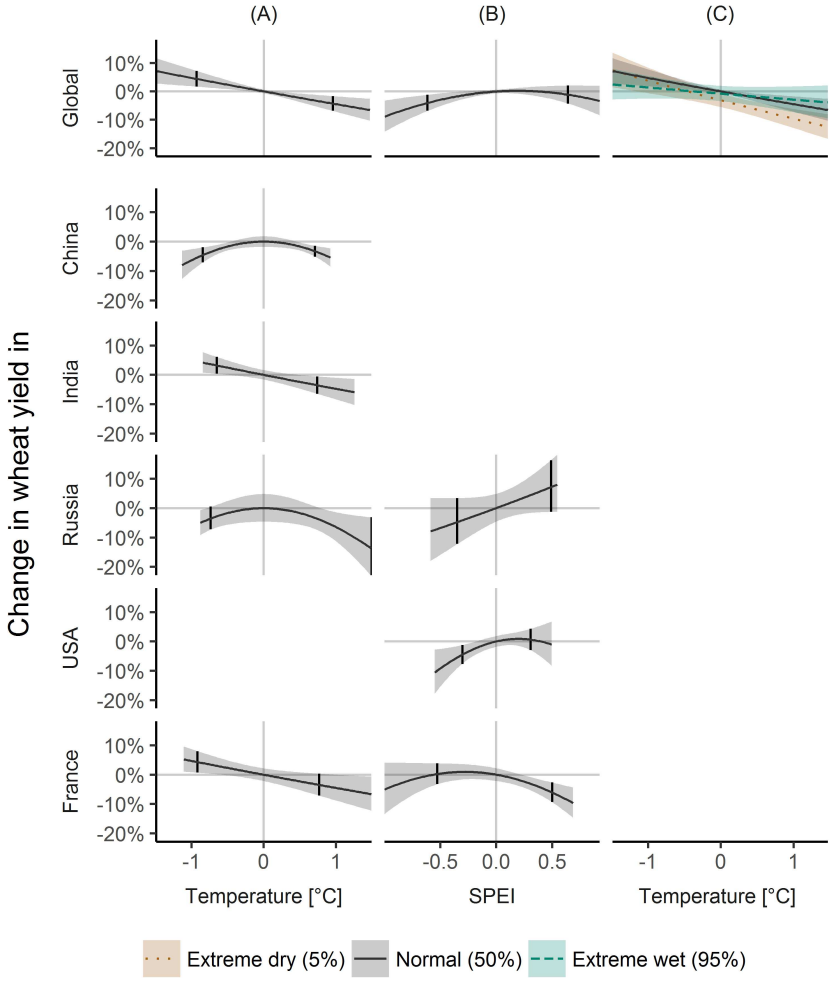

Fig 4. Climate variability effects on wheat yield variability. Same as Fig 1, but for wheat.

https://doi.org/10.1371/journal.pone.0178339.g004

Effects of previous year climate variability

Previous year climate variability was associated globally to rice and soybeans yield variability, and for selected countries to rice, soybeans and wheat yield variability (Fig 5). For rice, previous year temperature was positively associated to yields, such that warm temperatures increased next year yields by 0.9% (0.3, 1.5) globally (Fig 5A), by 0.9% (-0.1, 2.0) for China (Fig 5B), and by 2.4% (0.1, 4.7) for Bangladesh (Fig 5C). Rice yields in Viet Nam were positively associated to previous year SPEI (Fig 5E), and interactions between the previous and current year SPEI resulted in additionally decreased yields for dry conditions if the previous year was also dry with total yield effects of -6.2% (-9.2, -3.1), and no significant effect of current year SPEI, if the previous year was wet (Fig 5H). Soybean yields were linked positively to previous year SPEI with wet conditions followed by yield increases of 2.7% (-0.1, 5.5) globally (Fig 5F) and of 5.6% (0.5, 10.9) for Brazil (Fig 5G). Wheat yields in the USA were negatively associated

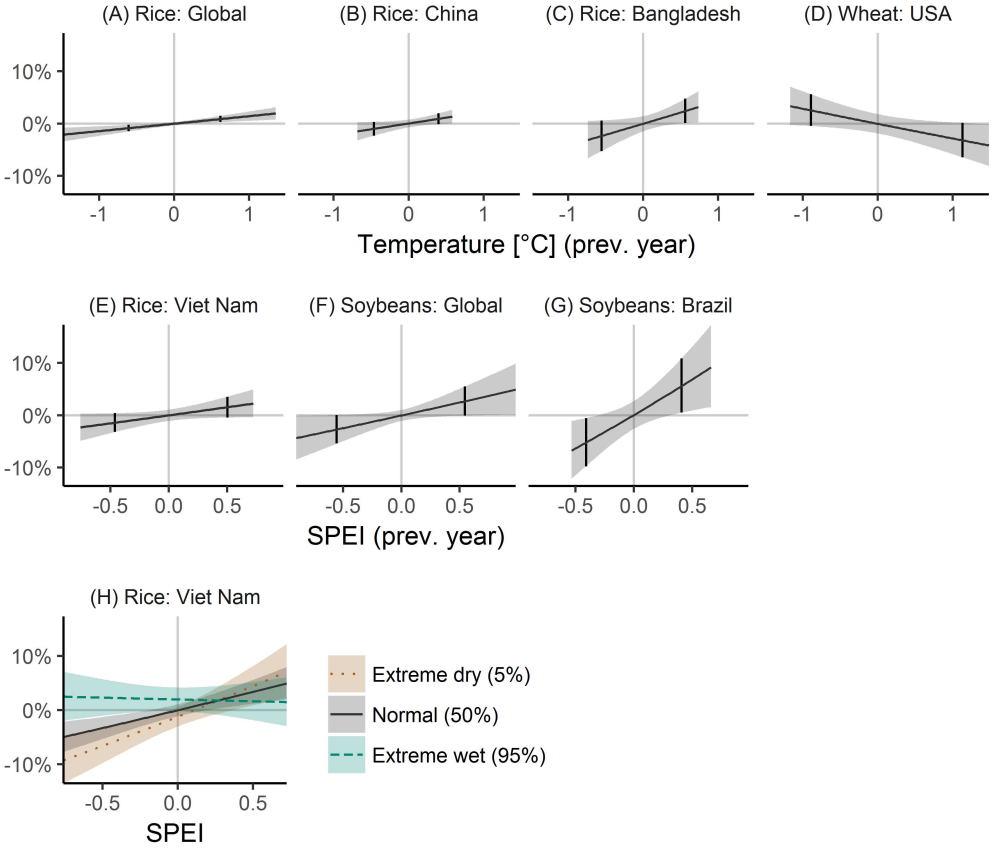

Fig 5. Previous year climate variability effects on crop yield variability. The figure shows how detrended crop yields are affected by previous year (lag) detrended temperature (A-D) and previous year SPEI (standardized precipitation evapotranspiration index, E-G). For rice in Viet Nam also interaction effects with current year climate variability are shown (that is yield effects of current year detrended SPEI given the 5% and 95% quantile of previous year detrended SPEI, H). Small vertical lines denote the 5 and 95% quantile of detrended temperature and SPEI. Crop-country combinations are missing if previous year temperature and SPEI were non-significant. Shaded areas correspond to 95% confidence intervals.

https://doi.org/10.1371/journal.pone.0178339.g005

to previous year temperature, and high temperatures reduced yields in the following year by -3.2% (-6.5, 0.1) (Fig 5D).

Overall, far fewer climate interactions were significant for single country time series than for the global sensitivity. To check, whether this might be related to the low number of observations available to determine single country sensitivities as opposed to pooling the countries using a random effects specification to determine global sensitivities, the analysis was repeated for the USA, but using state-level data.

Sensitivity check USA: Interactions determined from state level yields

As a comparison, instead of using country averages for yields and climate, for the USA, data at the state level were used to estimate the national yield sensitivity to climate variability (Fig 6). Effects of climate variability were naturally more detailed, but also more interactions were observed than with only country averages.

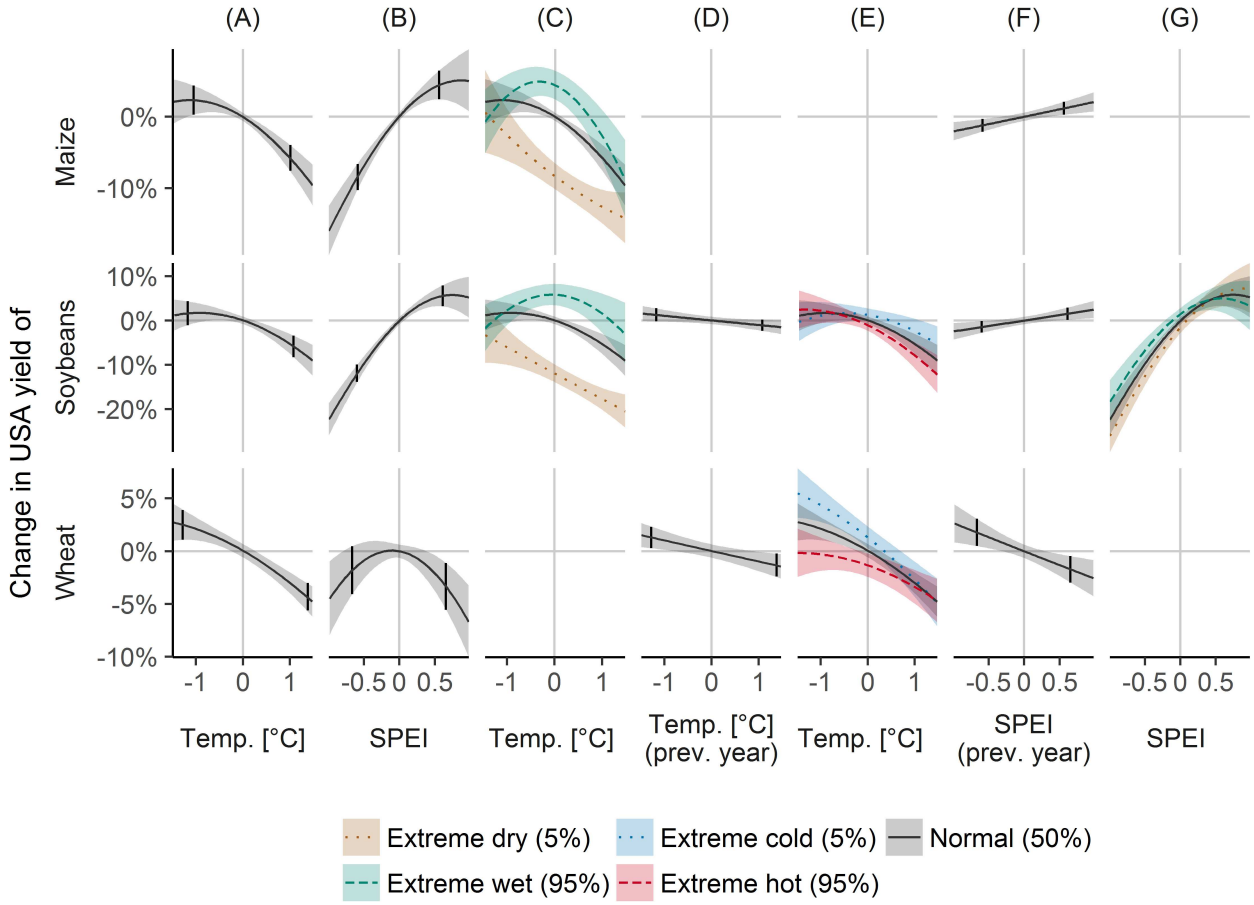

Fig 6. Climate variability effects on crop yield variability for the USA, determined by state level yield statistics. The figure shows how detrended USA yields are affected by detrended temperature (A), SPEI (standardized precipitation evapotranspiration index, B), previous year temperature (D) and previous year SPEI (F) given mean conditions; and how the temperature sensitivity differs by SPEI (for extreme dry and wet conditions denoted by the 5% and 95% quantile of SPEI, C), how the temperature sensitivity differs by previous year temperature (for extreme cold and hot conditions denoted by the 5% and 95% quantiles, E), and how the SPEI sensitivity differs by previous year SPEI (G). Black lines indicate main effects from the regression models, dashed and dotted lines indicate interaction effects, and absence of lines mean absence of significant effects. Small vertical lines denote the 5 and 95% quantile of detrended temperature and SPEI. Shaded areas correspond to 95% confidence intervals.

https://doi.org/10.1371/journal.pone.0178339.g006

For maize, dry conditions and high temperatures reduced yields by -8.5% (-10.3, -6.6; Fig 6B) and -5.8% (-7.6, -3.9; Fig 6A), but lower than average temperature and higher than average SPEI only had small effects on yields that slowly levelled off (Fig 6A and 6B). Regarding interactions, dry conditions reduced yields less at high and low temperatures than at average temperatures, however, yield losses for dry and warm conditions amounted to -12.6% (-14.9, -10.2) (Fig 6C). Wet conditions had positive effects of 4.4% (2.4, 6.4) at average temperatures (Fig 6B), but non-significant effects at low and high temperatures (Fig 6C).

For soybeans, dry conditions and high temperatures were associated to yield decreases of -11.9% (-13.9, -9.9; Fig 6B) and -5.9% (-8.3, -3.4; Fig 6A) for average conditions, and their combined effect amounted to -18.2% (-20.8, -15.5; Fig 6C). Similar to maize, wet conditions were linked to yield increases of 5.5% (3.2, 7.9) only for average temperatures, but not for low and high temperatures (Fig 6C). Previous year temperature had negative effects on yields (Fig

6D) and SPEI positive (Fig 6F), but because of interactions, these effects were only present if the current year was warm or dry, but not if it was cold or wet (Fig 6E and 6G).

For wheat, yield decreases associated with high temperatures were -4.3% (-5.6, -3.0; Fig 6A), with dry conditions -1.8% (-4.1, 0.5) and with wet conditions -3.4% (-5.6, -1.1) (Fig 6B), and yield increases associated with low temperatures were 2.5% (1.1, 3.9; Fig 6A). Previous year temperature and SPEI were negatively associated with wheat yields (Fig 6D and 6F). Because of interactions of current and previous year temperature, the negative effect of previous year temperatures held only if the current year was cold, but not if warm (Fig 6E).

Next, climate variability effects determined by state level data were compared to effects estimated from country averages, which were aggregated from state-level yields and climate (S1 Fig). While they agreed in general, estimating country effects from state-level data was more useful, in that it contained more detailed climate effects. For maize, yield reductions from dry and warm conditions were of similar magnitude if determined from national or state level data, however, the national level data showed negative effects of wet conditions, which were not present for state level data. For soybeans, yield effects of dry and wet conditions agreed between national and state level data, but with national data, effects of temperature, interactions of temperature and SPEI, and previous year temperature were lacking. For wheat, national and state level data agreed for the effect of dry conditions and temperature lag, but disagreed for the effect of wet conditions. Also state level data showed additional effects of temperature, interaction of current and previous year temperatures, and the previous year SPEI.

Model validation and simulation of errors in FAO yield data

To check the accuracy and robustness of the presented model results, cross validation errors were computed for a suite of models (Table 2), that include the original models and models without interactions, as well as models where all terms are included only linearly. For the global models, RMSE (root mean square errors) of the full models were lower than that of the simpler models for maize and wheat, while for rice and soybeans, RMSEs were similar. For the country level models, removing interactions and/or quadratic effects resulted in larger errors across all crops and countries. Using state-level yields for the USA models resulted in similar errors for the full and no interaction models, and higher errors for linear only models.

Errors in yield data would not bias results but induce uncertainty on the estimated effects, thus leading to a loss of significance as measured by higher p-values exceeding 0.05. For this reason, simulation analyses were performed to check for the influence of measurement error in the FAO yield data on the estimated significance of the highest order term (interaction, quadratic, or linear). For the global models, the highest order interaction terms started to lose significance ($p > 0.05$ for maize, rice, wheat, and $p > 0.1$ for soybeans) after adding approximately 15% noise on maize yields, 10% on rice and soybeans yields, and 25% on wheat yields (S2 Fig). After adding 50% of noise, the highest order terms remained still significant in ~ 65% of the models for maize, 40% for rice, 25% for soybeans, and 75% for wheat. For models at the country level, results varied more among countries and crops (S3 Fig). Highest order terms lost significance on average after adding 18% noise, while at 50% noise, ~ 65% of the highest order terms remained significant.

Discussion

According to the FAO, maize, rice and wheat account for more than two thirds of the world's food energy intake, albeit with varying importance across regions. The top five producing countries account for roughly half of the global yield for maize (57%) and rice (56.2%), whereas soybean production is more concentrated (84.6%) and wheat production more

Table 2. Cross validation results. Reported are root mean square error (RMSE) and median absolute error (MAE) of leave-one-out-cross-validation (LOOCV) of each model presented in the study (Full), of models without interaction terms (NoInter), and where additionally all variables enter only linearly (OnlyLin). OnlyLin models are thus nested within NoInter, which are nested within Full. If nested models had the same formula as the more complex model (e.g. no interactions in the full model or only linear terms when interactions were removed), cells were left empty.

Crop	Level	RMSE			MAE		
		Full	NoInter	OnlyLin	Full	NoInter	OnlyLin
Maize	Global	0.118	0.119	0.120	0.048	0.050	0.050
Rice	Global	0.045	0.045	0.045	0.023	0.023	0.024
Soybeans	Global	0.113	0.113	0.113	0.063	0.060	0.063
Wheat	Global	0.108	0.108	0.111	0.051	0.052	0.052
Maize	Brazil	0.069		0.072	0.040		0.049
	China	0.052			0.040		
	India	0.082	0.089		0.058	0.064	
	USA	0.087		0.095	0.059		0.068
	Ukraine	0.086			0.057		
Rice	Bangladesh	0.037	0.039	0.041	0.023	0.021	0.027
	China	0.022		0.023	0.016		0.015
	India	0.053			0.035		
	Viet Nam	0.042	0.046		0.025	0.023	
Soybeans	Argentina	0.094		0.097	0.052		0.051
	Brazil	0.100			0.066		
	China	0.061			0.034		
	India	0.131	0.157	0.154	0.118	0.126	0.120
	USA	0.066			0.028		
Wheat	China	0.052		0.055	0.032		0.031
	France	0.067		0.072	0.055		0.054
	India	0.061			0.040		
	Russia	0.102		0.109	0.065		0.075
	USA	0.063		0.062	0.048		0.048
Maize	USA from state	0.133	0.133	0.135	0.071	0.070	0.071
Soybeans	USA from state	0.130	0.130	0.133	0.076	0.076	0.079
Wheat	USA from state	0.129	0.129	0.130	0.076	0.076	0.075

https://doi.org/10.1371/journal.pone.0178339.t002

distributed (43.9%). Thus impacts of climate variability on these crops in the top producing countries should have sizeable downstream effects on the global population. The two most populated countries, China and India, are among the top 5 producers of all 4 crops studied, the USA for 3 and Brazil for 2.

Yield effects of climate variability

The demonstrated assessment of the nonlinear combined effects of temperature and drought (SPEI) on crop yields focused on climate variability. Thus corresponding estimated percentages of changes reported in this study should be regarded as indicators of sensitivity and ultimately vulnerability. This lies in contrast to the interpretation of reported yield changes in recent decades which depend on perceived climate trends (see e.g. [2]). Consequently, whereas previous studies revealed temperature linked changes in crop yields, this study did not find significant global effects of temperature for maize and soybean yields for average SPEI, but significant effects of drought that were further aggravated in the presence of high temperatures. These combined effects significantly decreased yields of maize, soybeans, and wheat by 11.6, 12.4, and 9.2%, respectively. Among the top producers, maize and soybean yields were

predominantly affected by drought (reductions of maize yields between 3.0 and 10.4%, soybeans 3.1 to 12.2%), whereas for wheat higher temperatures were more important (yield reductions between 3.5 and 13.5%). Rice was least affected by climate variability, both in terms of significant global and regional effects as well as via effect sizes. A more detailed comparison of the single crop results to previous studies underlines the strong variation in sensitivities, both between crops and regions.

Maize yields in the USA have been reported to respond strongly to drought [27,28], and in addition to extreme temperatures [14]. In contrast, this study did not find such a strong temperature link (only -4.1%), probably because SPEI already incorporates evapotranspiration, thus accounting for higher evaporative demand as well as temperature induced soil water depletion, the main source of the yield decreases associated with extreme heat [14]. The negative effect of too wet conditions found in this study may potentially be due to flooding and heavy precipitation events having caused lack of soil aeration or crop damage [29].

It is reported that China maize yield variability depends on temperature and precipitation variability, although there is large spatial variability [30]. Hence, the use of country averages might have obscured variability effects in this study where dry conditions only amounted to a yield reduction of 3.0%. Increased precipitation has been linked to higher yields of maize in Brazil [31,32]. In this study, above average SPEI was not associated with increased yields, but below average SPEI was associated with a 9.1% yield reduction.

The large and highly significant effect of temperature variability on maize in Ukraine might be linked to its continental climate with large temperature variations [33]. However, the effect found in this study was rather large (-8.6%) compared to other regions in Europe as well as in global studies [11,34]. Based on only 23 years of data, the estimates should be taken with caution.

Maize is grown in many parts of India with diverse climates: in the north the yield is mostly temperature dependent and in the rest it is mostly precipitation and only partly temperature dependent [8]. Therefore, country averages need to be interpreted carefully. Nonetheless, findings from this study (-12.7% for dry and hot conditions) match those of [35], where reductions in precipitation were shown to be harmful to maize yields for high temperatures, while increases in precipitation benefitted maize yields.

For rice, previous global studies similarly encountered the large uncertainties and small effect sizes observed here [2,11]. In northern China, temperature variability was linked to rice yields, while in the central and southern parts precipitation was mainly limiting [8]. Also depending on the region, precipitation was correlated positively or negatively to rice yields [30], which could possibly explain, why in this study of country averages, both dry and wet conditions were associated with increased yields.

Rice is planted widely across India. In rainfed areas rice yields have been linked to precipitation variability, and in irrigated areas, to temperature and partly also to precipitation [8]. Increased temperatures were associated with yield decreases [36], similar to the findings of this study. However, the influence of climatic variables differed strongly for winter and monsoon rice [37], suggesting the need for more detailed analyses on the multiple growing seasons.

For Indonesia, no significant effects of climate variability were found in this study, which may be due to data quality issues. Significant associations between temperature and yield variability have recently been reported for sub-country data [8] and significant negative impacts of temperature have been found in the vicinity of Indonesia, for trial farms in the Philippines, for example [38].

Rice in Bangladesh is heavily irrigated, so temperature has been found to be more important [8], and with positive impacts [39]. However, some areas are still prone to drought [40]. The strong decreases in yield for extreme wet conditions found in this study may be due to extreme events, such as cyclones, that are more frequent in these regions of the world [41,42].

For rice in Viet Nam, negative effects of temperature and positive effects of rainfall have been reported in a regional study [43], with impacts also dependent upon the wet- and dry-season [44]. These findings concur with the large effects of high temperature under wet and dry conditions revealed in this study.

In central and eastern parts of the USA, temperature variability has been found to be the main driver of soybean yield variability, while for other parts of the country, precipitation and precipitation combined with temperature have served as the primary drivers [8,12]. This study did not find a temperature effect on country averages, which may be in part because heat induced soil water depletion might be accounted for by the SPEI. However, based on state-level data there is a temperature effect of -5.9% for warm conditions.

The strong effects of SPEI variability on soybeans in Brazil (-8.1%) found in this study are in concordance with water supply being the main limiting factor [45,46]. Regional studies of soybean yields in Argentina showed that high temperatures and precipitation were the major influence on soybean yields [31,47], which matches the significant effects of both temperature and SPEI found in this study. While soybeans growing in the northern parts of China were mostly drought affected [48], in the southern growing regions they also depended on temperature in addition to precipitation [8,49].

Strong effects of heat and rainfall on soybean yields in India (-11.8% and -12.2%) are in concordance to a regional study [50]. However, to our knowledge, the positive effects from interactions of high temperatures under wet conditions found in this study are new.

Wheat is grown in large parts of China. In central China wheat yields have been associated with precipitation variability [8,30]. However, such effects were non-significant and perhaps not detectable at the country level as used in this study.

Extreme heat is a major factor determining wheat yields in India [51,52], also confirmed by this study, and the lack of a significant link to SPEI in this study could be because wheat is almost completely irrigated (96% as of 2013, [53]). Russia's wheat producing area is concentrated in the central and eastern part, which is heavily affected by heat and drought [54,55]. No significant link to SPEI was found in this study, which could be due to the country level analysis as well as the low number of years (22) of data.

According to the literature, wheat growing in the USA was found to depend largely on precipitation [8,56], similar to the findings of this study.

Adverse effects of wet conditions on wheat yields in France, as found in this study, seem counterintuitive at first glance, but could be caused, for example, by negative effects of soil moisture at planting and harvesting, or waterlogging during dormancy [57].

When comparing sensitivities among the major crop producers, it is notable that India appeared to be more vulnerable to drought for growing maize, rice and soybeans than China, whereas the temperature sensitivity of wheat was comparable. India and China are both large countries with similar population size and food consumption habits, however China has less cultivated area, uses less fertilizer and has a higher per area productivity. Most likely, the higher proportion of rainfed agriculture in India (for maize ~80% in India versus ~50% in China, for rice ~43% in India versus virtually none in China, see [53]) results in the lower productivity as well as in the higher vulnerability to drought revealed by this study. A point which can not be clarified in this study is whether short-lived pollutants such as ozone contributed to the yield losses in dry and hot summers, since intensive trophospheric ozone formation is most prone to such weather situations. Such toxic substances directly impact crop growth, for example, black carbon and ozone were identified as major factors for rice and wheat yield losses in India [58].While climate intensification effects, that is interactions between current and previous year climate, have been proposed a few years ago [19], we are unaware of any studies incorporating them. This study found mostly links of previous year climate with rice yields, and some

for soybeans and wheat. It should be noted that, for example, multiple growing seasons might cause spurious effects of previous year climate, so while this study serves as an initial effort to characterize climate intensification, future studies should account for multiple growing seasons more carefully.

Sustainability and food security

The green revolution led to large increases in crop yields worldwide since the 1960s [59], due to the adoption of new varieties, fertilizers, pesticides, and increased mechanization. While anthropogenic input and management played, and still play, a key role in sustaining long-term trends in crop yields [60], year-to-year variation of yields is largely determined by weather [9]. And while crop yields increased globally since the 1960s, crop yield variability did not increase, on the contrary, it primarily decreased [9]. Nevertheless, climate variability causes large fluctuations in crop yields, and with climate change a new player enters the stage of determining long-term crop yields.

Staple crops cover large parts of the human diet, and higher variability in yields leads to less stable production, higher price fluctuations and smaller incomes for food producers. The strong vulnerability of global maize, soybeans and wheat yield to combined effects of heat and drought as revealed in this study will threaten food security in the long run under progressing climate change. For most crops, the significant climate impacts affect all top producers. Consequently, only regionally alternating extreme events may level out the worst consequences. However, even then, regional effects on local prices are still likely, a second factor threatening food security.

Achieving food security is the second of the UN sustainable development goals. The global ecological footprint of agriculture stands in the way of sustainably fulfilling the increasing demand for food. Much research has been devoted to closing yield gaps, that is the difference between the actual yields and the potential yields given same climatic constraints [61–63]. This would eliminate the need for agricultural expansion by managing the existing agricultural areas better, for instance by increasing nutrient and water efficiency [61], or by spatially reallocating crops to where they are economically best profitable [62].

The immense need of water for agriculture, combined with massive groundwater depletion [64], and climate change induced water scarcity [65], calls for additional measures, such as improving crop water productivity or crop water use efficiency [66], which would increase yields, and at the same time provide more water for people and ecological services.

Future climatic variability, which implies more heat and drought, could be coped with by breeding and improving crop varieties such that they have an increased tolerance to heat and drought stress [67] and adapting planting dates [68]. But while these are yet theoretical ideas, practical implementations, such as conservation agriculture, could already be used to deal with these issues.

Conservation agriculture, compromising minimal soil disturbance, permanent soil cover and appropriate rotation, can reduce canopy temperature, increase water efficiency, reduce greenhouse gas emissions, and could also be more profitable from an economic perspective, however, it requires high initial investments in new machinery and high levels of skill and knowledge [69].

Limitations

Some caveats should be noted. Using a mean growing season climate obscures effects of intra-seasonal effects, such as short heat waves or dry periods in critical plant growth stages. Intra-seasonal climate variability was reported to have different impacts depending on the timing of

the events [57]. Since intra-seasonal weather has been averaged over in the calculations of this study, the reported estimates might be seen as indication of the climate variability effects for the whole plant growing period. Similarly, the use of country averages obscures regionally varying impacts. However it allows the assessment of the effects of climate variability on crop yields globally. In order to have at the same time a spatially finer resolved assessment, much more detailed data would be required.

Another limitation of this study is that it did not control for other factors affecting yield variability, such as agricultural management practices, pests, socioeconomic conditions, and conflicts. How much water is available to crops can strongly be influenced by irrigation, which can alleviate the impacts of extreme temperatures [16]. Besides that, water availability is related to soil properties and the management thereof [70–72], however, these could be assumed to be mostly independent of climate variability. The occurence of pests on the other hand is related to climate and climate variability [73,74]. The growing of crops and the socio-economy are closely linked and interdependent [75], especially in areas where agriculture is the main source of livelihood. While climate variability may also directly affect the socio-economic conditions, its main effects are on crop yields. The socio-economic conditions, such as supply chain infrastructure, market availability, labour and health issues, then act on top of the effects of climate variability, and can both enhance or reduce the effects of climate variability [76,77].

Since the focus of this study was on year-to-year climate variability and not climate change, long-term trends in both crop yields and climate were removed, such that time is not a confounding variable anymore. Consequently, impacts of climate change on crop yields [78] or impacts of climate change on climate variability [9] could not be considered.

Conclusion

Using a random effects specification, the multitude of spatial observations on a short time scale were leveraged to determine the interacting climate variability effects on global crop yields from country data, or country yields from sub-country data. In order to estimate detailed interaction effects, sub-country data were necessary to estimate country sensitivities.

Interactions between temperature and SPEI led to a stronger temperature sensitivity of the global maize and wheat yields in dry than normal conditions, and no temperature sensitivity of global soybean yields for wet compared to normal conditions. Using state-level data, USA yields of maize and soybeans were more sensitive to temperature in dry than normal conditions, and soybean yields were less sensitive to temperature in wet than normal conditions. Furthermore, for rice in Viet Nam and soybeans in the USA, consecutive dry years additionally reduced yields, as did consecutive warm years for USA soybeans.

Climate variability accounts for large parts of yield variability, and by not accounting for interactions between temperature and moisture, the effect of temperature on yields might be overestimated in wet conditions and underestimated in dry conditions.

Supporting information

S1 Fig. Climate variability effects on crop yield variability for the USA, determined by national level yield aggregated from state level data. The same as Fig 6, but here effects were estimated from national level yield data as opposed to state level yield data in Fig 6.
(TIFF)

S2 Fig. Significance of highest order term in mixed model of global yields after adding random noise on FAO data. Shown on the y-axis is the percentage of significance levels of the highest order interaction term (listed at the top of each panel) for each crop depending on

noise level added to yields (on the x-axis). Generally speaking, as one adds more noise to the yields (moves to the right of the x-axis) the interaction term becomes less statistically significant, e.g. higher amounts of red indicating p-value > 0.05.
(TIFF)

S3 Fig. Significance of highest order term in linear models of country yields after adding random noise on FAO data. Shown is the percentage of significance levels of the highest order terms (interaction, quadratic, or linear, as listed at the top of each panel) for each crop and country depending on noise level added to yields.
(TIFF)

S1 Table. Time series length of FAO yield data: After (before) quality checks. Maximum number 54 corresponds to full time series length (1961–2014). Quality criteria: if countries reported the identical values in 2 consecutive years, then all years prior or after were excluded; manual visual inspection (see methods for further details).
(DOCX)

S2 Table. Country crop time series that needed higher dimension for yield detrending. See methods for details.
(DOCX)

Acknowledgments

We would like to thank David Wuepper for fruitful discussions. The authors acknowledge funding provided by the European Research Council under the European Union's Seventh Framework Programme (FP7/2007-2013)/ERC grant agreement no [282250] and support of the Technische Universität München–Institute for Advanced Study, funded by the German Excellence Initiative.

Author Contributions

Conceptualization: AM MM.

Data curation: MM.

Formal analysis: MM DPA.

Funding acquisition: AM.

Investigation: MM.

Methodology: MM DPA.

Visualization: MM.

Writing – original draft: MM DPA AM.

Writing – review & editing: MM DPA AM.

References

1. Porter JR, Xie L, Challinor AJ, Cochrane K, Howden SM, Iqbal MM, et al. Food security and food production systems. In: Field CB, Barros VR, Dokken DJ, Mach KJ, Mastrandrea MD, Bilir TE, et al., editors. Climate Change 2014: Impacts, Adaptation, and Vulnerability Part A: Global and Sectoral Aspects Contribution of Working Group II to the Fifth Assessment Report of the Intergovernmental Panel on Climate Change. Cambridge, United Kingdom and New York, NY, USA: Cambridge University Press; 2014. pp. 485–533.

2. Lobell DB, Schlenker W, Costa-Roberts J. Climate Trends and Global Crop Production Since 1980. Science. 2011; 333: 616–620. https://doi.org/10.1126/science.1204531 PMID: 21551030
3. Gourdji SM, Sibley AM, Lobell DB. Global crop exposure to critical high temperatures in the reproductive period: historical trends and future projections. Environ Res Lett. 2013; 8: 024041.
4. Lobell DB, Gourdji SM. The Influence of Climate Change on Global Crop Productivity. Plant Physiol. 2012; 160: 1686–1697. https://doi.org/10.1104/pp.112.208298 PMID: 23054565
5. Rosenzweig C, Parry ML. Potential impact of climate change on world food supply. Nature. 1994; 367: 133–138.
6. Nelson GC, Valin H, Sands RD, Havlík P, Ahammad H, Deryng D, et al. Climate change effects on agriculture: Economic responses to biophysical shocks. Proc Natl Acad Sci. 2014; 111: 3274–3279. https://doi.org/10.1073/pnas.1222465110 PMID: 24344285
7. Reidsma P, Ewert F, Lansink AO, Leemans R. Adaptation to climate change and climate variability in European agriculture: The importance of farm level responses. Eur J Agron. 2010; 32: 91–102.
8. Ray DK, Gerber JS, MacDonald GK, West PC. Climate variation explains a third of global crop yield variability. Nat Commun. 2015; 6.
9. Osborne TM, Wheeler TR. Evidence for a climate signal in trends of global crop yield variability over the past 50 years. Environ Res Lett. 2013; 8: 024001.
10. Scherrer SC, Appenzeller C, Liniger MA, Schär C. European temperature distribution changes in observations and climate change scenarios. Geophys Res Lett. 2005; 32: L19705.
11. Lobell DB, Field CB. Global scale climate–crop yield relationships and the impacts of recent warming. Environ Res Lett. 2007; 2: 014002.
12. Leng G, Zhang X, Huang M, Asrar GR, Leung LR. The Role of Climate Covariability on Crop Yields in the Conterminous United States. Sci Rep. 2016; 6: 33160. https://doi.org/10.1038/srep33160 PMID: 27616326
13. Schlenker W, Roberts MJ. Nonlinear temperature effects indicate severe damages to U.S. crop yields under climate change. Proc Natl Acad Sci. 2009; 106: 15594–15598. https://doi.org/10.1073/pnas.0906865106 PMID: 19717432
14. Lobell DB, Hammer GL, McLean G, Messina C, Roberts MJ, Schlenker W. The critical role of extreme heat for maize production in the United States. Nat Clim Change. 2013; 3: 497–501.
15. Lobell DB, Bänziger M, Magorokosho C, Vivek B. Nonlinear heat effects on African maize as evidenced by historical yield trials. Nat Clim Change. 2011; 1: 42–45.
16. Troy TJ, Kipgen C, Pal I. The impact of climate extremes and irrigation on US crop yields. Environ Res Lett. 2015; 10: 054013.
17. Hawkins E, Fricker TE, Challinor AJ, Ferro CAT, Ho CK, Osborne TM. Increasing influence of heat stress on French maize yields from the 1960s to the 2030s. Glob Change Biol. 2013; 19: 937–947.
18. Urban DW, Sheffield J, Lobell DB. The impacts of future climate and carbon dioxide changes on the average and variability of US maize yields under two emission scenarios. Environ Res Lett. 2015; 10: 045003.
19. Dell M, Jones BF, Olken BA. What Do We Learn from the Weather? The New Climate-Economy Literature. J Econ Lit. 2014; 52: 740–98.
20. Harris I, Jones PD, Osborn TJ, Lister DH. Updated high-resolution grids of monthly climatic observations–the CRU TS3.10 Dataset. Int J Climatol. 2014; 34: 623–642.
21. Beguería S, Vicente-Serrano SM, Reig F, Latorre B. Standardized precipitation evapotranspiration index (SPEI) revisited: parameter fitting, evapotranspiration models, tools, datasets and drought monitoring. Int J Climatol. 2014; 34: 3001–3023.
22. Sacks WJ, Deryng D, Foley JA, Ramankutty N. Crop planting dates: an analysis of global patterns. Glob Ecol Biogeogr. 2010; 19: 607–620.
23. Monfreda C, Ramankutty N, Foley JA. Farming the planet: 2. Geographic distribution of crop areas, yields, physiological types, and net primary production in the year 2000. Glob Biogeochem Cycles. 2008; 22: GB1022.
24. Kucharik CJ. A Multidecadal Trend of Earlier Corn Planting in the Central USA. Agron J. 2006; 98: 1544.
25. Menzel A, Sparks TH, Estrella N, Koch E, Aasa A, Ahas R, et al. European phenological response to climate change matches the warming pattern. Glob Change Biol. 2006; 12: 1969–1976.
26. Robin B Matthews, Martin J Kropff, Dominique Bachelet, HH van Laar, editors. Modeling the impact of climate change on rice production in Asia. Wallingford: CAB International in association with the International Rice Research Institute; 1995.

27. Lobell DB, Roberts MJ, Schlenker W, Braun N, Little BB, Rejesus RM, et al. Greater Sensitivity to Drought Accompanies Maize Yield Increase in the U.S. Midwest. Science. 2014; 344: 516–519. https://doi.org/10.1126/science.1251423 PMID: 24786079
28. Nielsen DC, Vigil MF, Benjamin JG. The variable response of dryland corn yield to soil water content at planting. Agric Water Manag. 2009; 96: 330–336.
29. Rosenzweig C, Tubiello FN, Goldberg R, Mills E, Bloomfield J. Increased crop damage in the US from excess precipitation under climate change. Glob Environ Change. 2002; 12: 197–202.
30. Zhang T, Huang Y. Impacts of climate change and inter-annual variability on cereal crops in China from 1980 to 2008. J Sci Food Agric. 2012; 92: 1643–1652. https://doi.org/10.1002/jsfa.5523 PMID: 22190019
31. Llano MP, Vargas W. Climate characteristics and their relationship with soybean and maize yields in Argentina, Brazil and the United States. Int J Climatol. 2016; 36: 1471–1483.
32. Franchito SH, Brahmananda Rao V, Gan MA, Santo CME. Onset and end of the rainy season and corn yields in São Paulo State, Brazil. Geofísica Int. 2010; 49: 69–76.
33. Maracchi G, Sirotenko O, Bindi M. Impacts of Present and Future Climate Variability on Agriculture and Forestry in the Temperate Regions: Europe. In: Salinger J, Sivakumar MVK, Motha RP, editors. Increasing Climate Variability and Change. Springer Netherlands; 2005. pp. 117–135.
34. Peltonen-Sainio P, Jauhiainen L, Trnka M, Olesen JE, Calanca P, Eckersten H, et al. Coincidence of variation in yield and climate in Europe. Agric Ecosyst Environ. 2010; 139: 483–489.
35. Byjesh K, Kumar SN, Aggarwal PK. Simulating impacts, potential adaptation and vulnerability of maize to climate change in India. Mitig Adapt Strateg Glob Change. 2010; 15: 413–431.
36. Bapuji Rao B, Santhibhushan Chowdary P, Sandeep VM, Rao VUM, Venkateswarlu B. Rising minimum temperature trends over India in recent decades: Implications for agricultural production. Glob Planet Change. 2014; 117: 1–8.
37. Barnwal P, Kotani K. Climatic impacts across agricultural crop yield distributions: An application of quantile regression on rice crops in Andhra Pradesh, India. Ecol Econ. 2013; 87: 95–109.
38. Peng S, Huang J, Sheehy JE, Laza RC, Visperas RM, Zhong X, et al. Rice yields decline with higher night temperature from global warming. Proc Natl Acad Sci. 2004; 101: 9971–9975. https://doi.org/10.1073/pnas.0403720101 PMID: 15226500
39. Sarker MAR, Alam K, Gow J. Exploring the relationship between climate change and rice yield in Bangladesh: An analysis of time series data. Agric Syst. 2012; 112: 11–16.
40. Alam K. Farmers' adaptation to water scarcity in drought-prone environments: A case study of Rajshahi District, Bangladesh. Agric Water Manag. 2015; 148: 196–206.
41. Rabbani MG, Rahman AA, Shoef IJ, Khan ZM. Climate Change and Food Security in Vulnerable Coastal Zones of Bangladesh. In: Habiba U, Hassan AWR, Abedin MA, Shaw R, editors. Food Security and Risk Reduction in Bangladesh. Springer Japan; 2015. pp. 173–185.
42. Mottaleb KA, Mohanty S, Hoang HTK, Rejesus RM. The effects of natural disasters on farm household income and expenditures: A study on rice farmers in Bangladesh. Agric Syst. 2013; 121: 43–52.
43. Chung NT, Jintrawet A, Promburom P. Impacts of Seasonal Climate Variability on Rice Production in the Central Highlands of Vietnam. Agric Agric Sci Procedia. 2015; 5: 83–88.
44. Nhan DK, Trung NH, Sanh NV. The Impact of Weather Variability on Rice and Aquaculture Production in the Mekong Delta. In: Stewart MA, Coclanis PA, editors. Environmental Change and Agricultural Sustainability in the Mekong Delta. Springer Netherlands; 2011. pp. 437–451.
45. Sentelhas PC, Battisti R, Câmara GMS, Farias JRB, Hampf AC, Nendel C. The soybean yield gap in Brazil–magnitude, causes and possible solutions for sustainable production. J Agric Sci. 2015; 153: 1394–1411.
46. Zanon AJ, Streck NA, Grassini P. Climate and Management Factors Influence Soybean Yield Potential in a Subtropical Environment. Agron J. 2016; 108: 1447.
47. Penalba OC, Bettolli ML, Vargas WM. The impact of climate variability on soybean yields in Argentina. Multivariate regression. Meteorol Appl. 2007; 14: 3–14.
48. Yin XG, Olesen JE, Wang M, Öztürk I, Chen F. Climate effects on crop yields in the Northeast Farming Region of China during 1961–2010. J Agric Sci. 2016; 154: 1190–1208.
49. Zhang Z, Song X, Tao F, Zhang S, Shi W. Climate trends and crop production in China at county scale, 1980 to 2008. Theor Appl Climatol. 2015; 123: 291–302.
50. Lal M, Singh KK, Srinivasan G, Rathore LS, Naidu D, Tripathi CN. Growth and yield responses of soybean in Madhya Pradesh, India to climate variability and change. Agric For Meteorol. 1999; 93: 53–70.
51. Lobell DB, Sibley A, Ivan Ortiz-Monasterio J. Extreme heat effects on wheat senescence in India. Nat Clim Change. 2012; 2: 186–189.

52. Rao BB, Chowdary PS, Sandeep VM, Pramod VP, Rao VUM. Spatial analysis of the sensitivity of wheat yields to temperature in India. Agric For Meteorol. 2015; 200: 192–202.
53. FAO. AQUASTAT Main Database [Internet]. 2016 [cited 20 Oct 2016]. Available: http://www.fao.org/nr/water/aquastat/main/index.stm
54. Licker R, Kucharik CJ, Doré T, Lindeman MJ, Makowski D. Climatic impacts on winter wheat yields in Picardy, France and Rostov, Russia: 1973–2010. Agric For Meteorol. 2013; 176: 25–37.
55. Alcamo J, Dronin N, Endejan M, Golubev G, Kirilenko A. A new assessment of climate change impacts on food production shortfalls and water availability in Russia. Glob Environ Change. 2007; 17: 429–444.
56. Maltais-Landry G, Lobell DB. Evaluating the Contribution of Weather to Maize and Wheat Yield Trends in 12 U.S. Counties. Agron J. 2012; 104: 301.
57. Ceglar A, Toreti A, Lecerf R, Van der Velde M, Dentener F. Impact of meteorological drivers on regional inter-annual crop yield variability in France. Agric For Meteorol. 2016; 216: 58–67.
58. Burney J, Ramanathan V. Recent climate and air pollution impacts on Indian agriculture. Proc Natl Acad Sci. 2014; 111: 16319–16324. https://doi.org/10.1073/pnas.1317275111 PMID: 25368149
59. Evenson RE, Gollin D. Assessing the Impact of the Green Revolution, 1960 to 2000. Science. 2003; 300: 758–762. https://doi.org/10.1126/science.1078710 PMID: 12730592
60. Pradhan P, Fischer G, Velthuizen H van, Reusser DE, Kropp JP. Closing Yield Gaps: How Sustainable Can We Be? PLOS ONE. 2015; 10: e0129487. https://doi.org/10.1371/journal.pone.0129487 PMID: 26083456
61. Mueller ND, Gerber JS, Johnston M, Ray DK, Ramankutty N, Foley JA. Closing yield gaps through nutrient and water management. Nature. 2012; 490: 254–257. https://doi.org/10.1038/nature11420 PMID: 22932270
62. Mauser W, Klepper G, Zabel F, Delzeit R, Hank T, Putzenlechner B, et al. Global biomass production potentials exceed expected future demand without the need for cropland expansion. Nat Commun. 2015; 6: 8946. https://doi.org/10.1038/ncomms9946 PMID: 26558436
63. Licker R, Johnston M, Foley JA, Barford C, Kucharik CJ, Monfreda C, et al. Mind the gap: how do climate and agricultural management explain the "yield gap" of croplands around the world? Glob Ecol Biogeogr. 2010; 19: 769–782.
64. McLaughlin D, Kinzelbach W. Food security and sustainable resource management. Water Resour Res. 2015; 51: 4966–4985.
65. Olesen JE, Bindi M. Consequences of climate change for European agricultural productivity, land use and policy. Eur J Agron. 2002; 16: 239–262.
66. Brauman KA, Siebert S, Foley JA. Improvements in crop water productivity increase water sustainability and food security—a global analysis. Environ Res Lett. 2013; 8: 024030.
67. Hellin J, Shiferaw B, Cairns JE, Reynolds M, Ortiz-Monasterio I, Banziger M, et al. Climate change and food security in the developing world: Potential of maize and wheat research to expand options for adaptation and mitigation. J Dev Agric Econ. 2012; 4: 311–321.
68. Deryng D, Sacks WJ, Barford CC, Ramankutty N. Simulating the effects of climate and agricultural management practices on global crop yield. Glob Biogeochem Cycles. 2011; 25: GB2006.
69. Sapkota TB, Jat ML, Aryal JP, Jat RK, Khatri-Chhetri A. Climate change adaptation, greenhouse gas mitigation and economic profitability of conservation agriculture: Some examples from cereal systems of Indo-Gangetic Plains. J Integr Agric. 2015; 14: 1524–1533.
70. Qin W, Hu C, Oenema O. Soil mulching significantly enhances yields and water and nitrogen use efficiencies of maize and wheat: a meta-analysis. Sci Rep. 2015; 5: 16210. https://doi.org/10.1038/srep16210 PMID: 26586114
71. Karlen DL, Kovar JL, Cambardella CA, Colvin TS. Thirty-year tillage effects on crop yield and soil fertility indicators. Soil Tillage Res. 2013; 130: 24–41.
72. Timsina J, Connor DJ. Productivity and management of rice–wheat cropping systems: issues and challenges. Field Crops Res. 2001; 69: 93–132.
73. Bebber DP, Holmes T, Gurr SJ. The global spread of crop pests and pathogens. Glob Ecol Biogeogr. 2014; 23: 1398–1407.
74. Thornton PK, Ericksen PJ, Herrero M, Challinor AJ. Climate variability and vulnerability to climate change: a review. Glob Change Biol. 2014; 20: 3313–3328.
75. VanWey LK, Spera S, de Sa R, Mahr D, Mustard JF. Socioeconomic development and agricultural intensification in Mato Grosso. Philos Trans R Soc Lond B Biol Sci. 2013; 368: 20120168. https://doi.org/10.1098/rstb.2012.0168 PMID: 23610174
76. Gregory PJ, Ingram JSI, Brklacich M. Climate change and food security. Philos Trans R Soc Lond B Biol Sci. 2005; 360: 2139–2148. https://doi.org/10.1098/rstb.2005.1745 PMID: 16433099

77. Brown ME, Funk CC. Food Security Under Climate Change. Science. 2008; 319: 580–581. https://doi.org/10.1126/science.1154102 PMID: 18239116

78. Wheeler T, Braun J von. Climate Change Impacts on Global Food Security. Science. 2013; 341: 508–513. https://doi.org/10.1126/science.1239402 PMID: 23908229

Agricultural and Forest Meteorology 244–245 (2017) 72–81

Contents lists available at ScienceDirect

Agricultural and Forest Meteorology

journal homepage: www.elsevier.com/locate/agrformet

Monitoring succession after a non-cleared windthrow in a Norway spruce mountain forest using webcam, satellite vegetation indices and turbulent CO_2 exchange

Michael Matiu[a,*], Ludwig Bothmann[b], Rainer Steinbrecher[c], Annette Menzel[a,d]

[a] Ecoclimatology, Technical University of Munich, Freising, Germany
[b] Institut für Statistik, Ludwig-Maximilians-Universität, Munich, Germany
[c] Atmospheric Environmental Research, Karlsruhe Institute of Technology (KIT/IMK-IFU), Garmisch-Partenkirchen, Germany
[d] Institute for Advanced Study, Technical University of Munich, Garching, Germany

ARTICLE INFO

Keywords:
Phenocam
Phenology
Climatological growing season index
NDVI

ABSTRACT

Forests cover approximately 30% of the world's land area and are responsible for 75% of terrestrial gross primary production. Disturbances, such as fire, storm or insect outbreaks alter the dynamics and functioning of forest ecosystems with consequences, in terms of species distribution and/or gross primary production, not fully understood. Large forest areas are intensively managed and natural disturbances are yet rare events but expected to increase with climate change. Here, we used digital repeat photography to observe the ecological succession in a windthrow disturbed forest in the Bavarian Forest National Park (Germany) and compared it to satellite-derived vegetation indices (NDVI, EVI, and PPI) as well as turbulent CO_2 exchange. A data-driven clustering of the webcam images identified three regions of interest: spruce, grass and a transition region that showed grass in the beginning and became successively overgrown by spruce. The succession was mirrored in trends of annual maxima of gross primary production (GPP), satellite vegetation indices and derived image greenness (green chromatic coordinate, GCC) in the transition region. These trends were also responsible for a positive link between seasonal GPP and proxies. Start and end of growing season were estimated from GCC, NDVI, EVI, PPI, and GPP, compared to each other, and were linked partly to climatological growing season indices and phenological observations. This study demonstrates the suitability and benefits of a webcam in monitoring forest recovery after a severe windthrow event, thus offering a versatile tool that helps to understand successional and phenological processes after a disturbance.

1. Introduction

Forests play an important role in the global carbon cycle (Dixon et al., 1994; Luyssaert et al., 2010) and intact forests ecosystems act as strong carbon sinks (Grünwald and Bernhofer, 2007). With longer vegetation seasons, caused by anthropogenic climate change, a further increase of productivity is expected (Dragoni et al., 2011). However, climate change induced increases in the frequency of disturbances, such as fire, insect outbreaks, and storms, also negatively impacts forest growth (Seidl et al., 2011). Such disturbances can switch an ecosystem from a carbon sink to a carbon source and have the potential to offset any climate change or forest management induced benefits (Seidl et al., 2014). Observing and understanding consequences of disturbances thus plays a key role in understanding ecosystem functioning under climate change.

Major efforts are underway to observe ecosystem carbon fluxes (see FLUXNET, https://fluxnet.ornl.gov/), and also disturbed forest ecosystems are monitored (Lindauer et al., 2014). However, the recently implemented techniques are cost-intensive, depend on flatness of the terrain, homogeneity of the vegetation cover in the footprint area as well as atmospheric conditions (see e.g. Foken et al., 2012), and are thus not ideally suited for large scale observations. An alternative approach is to exploit the links between canopy carbon uptake (net ecosystem exchange, NEE) and phenology (Richardson et al., 2013; Wingate et al., 2015).

One approach is the use of digital repeat photography to directly track the phenological development (Migliavacca et al., 2011). Digital cameras offer many advantages to traditional phenological research (Sonnentag et al., 2012), and are suited to predict NEE dynamics and total productivity but not yet for all plant functional types (Toomey

* Corresponding author at: Ecoclimatology, Hans-Carl-von-Carlowitz-Platz 2, 85354, Freising, Germany.
E-mail address: matiu@wzw.tum.de (M. Matiu).

http://dx.doi.org/10.1016/j.agrformet.2017.05.020
Received 17 October 2016; Received in revised form 11 May 2017; Accepted 29 May 2017

et al., 2015). Phenocams (digital cameras used to monitor phenology) are a new but promising technology, mirrored in the large amount of recently published research (Henneken et al., 2013; Julitta et al., 2014; Keenan et al., 2014; Klosterman et al., 2014; Menzel et al., 2015; Morris et al., 2013; Nijland et al., 2014; Petach et al., 2014; Toomey et al., 2015; Wingate et al., 2015).

Remote-sensing of phenology via satellites is another possibility (Fu et al., 2014; Jeganathan et al., 2014; Jeong et al., 2011), and could provide large-scale links between vegetation and CO_2 cycles (Barichivich et al., 2013). However, the correspondence to ground observations is differing by plant species and season (Klosterman et al., 2014; Liang et al., 2011; Misra et al., 2016), and this is where phenocams could fill the gap between automated satellite and manual field observations. Phenocams can also be used to monitor events at the species level, or even for single individual trees (Menzel et al., 2015). Thus, they can provide much higher spatial information than integrated measures, such as satellite observations or turbulent flux measurements.

Phenology is climate sensitive (Dose and Menzel, 2006; Menzel et al., 2006; Richardson et al., 2013), so climatological growing season indices (Linderholm, 2006) seem like another natural choice to estimate the vegetation season (Menzel et al., 2003; Zhang et al., 2004) or carbon uptake (Barford et al., 2001). Bark beetle flight activity was also linked to phenology (Zang et al., 2015) and climate (Baier et al., 2007), and bark beetle induced tree mortality can have severe consequences on forest leaf area index and gross primary production (Bright et al., 2013).

But how climatological indices, phenological observations, phenological estimates derived from near-surface and satellite remote-sensing, bark beetle flight and turbulent carbon exchange are interrelated in disturbed ecosystems is rarely addressed.

To this end, we combined time series of digital camera images with satellite-derived vegetation indices, eddy-covariance measurements of CO_2, climate, phenological observations and bark beetle counts in a windthrow disturbed forest in order to analyze (1) whether it is possible to observe succession using digital camera images, (2) if and to which degree webcam greenness, satellite retrieved vegetation indices, and turbulent CO_2 exchange observations match, (3) how their seasonality is related amongst each other and to climatological growing season indices or phenological observations.

2. Materials and Methods

2.1. Study site

The study site Lackenberg (Fig. 1) is located in the Bavarian Forest National Park (Bayerischer Wald) in south-eastern Germany (13.305°E, 49.100°N, 1308 m a.s.l.). The national park is forested on 98% of its area with a mixed forest dominated by spruce, fir and beech. However, at the altitude of the Lackenberg site, nearly all trees are Norway spruce (*Picea abies* (L.) H. Karst). The area has been heavily damaged by the storm Kyrill on January 18, 2007, and has not been cleared thereafter because of the forest management policy of the national park. The windthrow area at this site is approximately 26.8 ha. Almost all larger trees were uprooted during the storm. The main vegetation, besides surviving spruce trees and newly emerging young trees, consists of grasses (*Deschampia flexuosa* (L.) Trin., *Luzula sylvatica* (Huds.) Gaudin, *Juncus effuses* L.), fern (*Athyrium distentifolium* Tausch ex Opiz), few blue berries (*Vaccinium myrtillus* L.) and very few rowan berries (*Sorbus aucuparia* L.). In 2009 a tower was set up in the middle of the windthrow area, with instruments to measure turbulent CO_2 exchange (Lindauer et al., 2014), and in 2010 a webcam was mounted.

2.2. Webcam images setup

From May 2010 to July 2016, digital images were taken by a dual-sensor security webcam Mobotix M12 (Mobotix AG, Langmeil, Germany), which records near-infrared (NIR) and standard RGB images at the same time with slightly different fields of view. The camera was run in full automatic mode (exposure, aperture, and white balance) and was set up according to standard recommendations (Richardson et al., 2007; Sonnentag et al., 2012): camera facing north; gray scale reflectance panel (Fluorilon, Avian Technologies, New London, NH, USA) in field of view; multiple images taken each day between 12am and 1pm CET. We hoped to use the gray panel and the NIR image to calculate a pseudo-NDVI (normalized difference vegetation index), which, however, did not yield any sensible results. Because of hardware failure, at the end, only one backup image per day, taken at midday, with 640 × 480 pixels was available for analyses throughout the whole period. Additionally, not all images were (fully) transmitted due to network failures and we discarded all images that were empty or only partially transmitted.

The camera was moved multiple times during the study period, resulting in different views of the study site. Images were registered using open-source image-processing software Fiji (www.fiji.sc) in order to show the same view over the whole study period (see Fig. S1). Then, images were cropped to the common region excluding the gray panel, which was not registered successfully because it was too near to the camera compared to the background forest.

2.3. Automatic extraction of webcam image regions of interest (ROI)

For further analyses the webcam images were segmented into regions of interest (ROIs) with an approach proposed by Bothmann et al. (2017), which defines ROIs in an automated and data-driven way. The so-called 'unsupervised ROI approach' (uROI) is implemented in the R package phenofun (Bothmann, 2016) and works as follows.

Let x_t denote a three-color RGB image with $m*n$ pixels at time t (with a total of T images), $x_t \in \mathbb{R}^{m\times n\times 3}$that is $\overline{x_t} \in \mathbb{R}^{3mn}$First, each image is rearranged into a long vector $\overline{x_t} \in \mathbb{R}^{3mn}$. Then the entire image data is stored in a matrix X, where each column of X corresponds to one image, that is $X = (\overline{x_1},\ldots,\overline{x_T}) \in \mathbb{R}^{3mn\times T}$. Then, a truncated version of a singular value decomposition (SVD) of X is carried out to reduce dimensionality by only computing the first p singular vectors. This leads to a decomposition of X into $X = UDV'$, with $U \in \mathbb{R}^{3mn\times p}$, $D \in \mathbb{R}^{p\times p}$, $V' \in \mathbb{R}^{p\times T}$, where the columns of U are the eigenvectors of XX' and may be called eigenimages. Then, U is rearranged into a matrix $\overline{U} \in \mathbb{R}^{mn\times 3p}$, such that each pixel is described by $3p$ variables. Based on $\overline{U}$, the pixels are clustered with a k-means clustering algorithm leading to a pre-specified number of K clusters. After testing

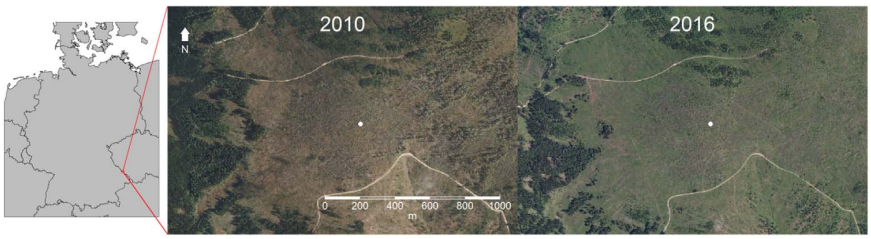

Fig. 1. Aerial images of the study site (courtesy of the Bavarian Forest National Park). The white dot in the middle is the location of the tower, where the webcam and other instruments were mounted. The windthrow area is located between the two roads, roughly a circle with 400 m radius around the tower. The strip left of the windthrow area besides the dense forests, was cleared in 2009 and 2010 after a massive bark beetle infestation in order to prevent a further spreading.

multiple values for p and K, $p = 24$ and $K = 3$ were found to show the most cohesive and meaningful clustering results.

2.4. Extracting greenness from webcam images

To adjust for the varying scene illumination, we used the green chromatic coordinate (GCC = green/[red + green + blue]) as measure of greenness (Sonnentag et al., 2012) and applied the spline-filtering procedure described in Migliavacca et al. (2011), using 2 (instead of 3) standard deviations for thresholding.

The study site is prone to fog and snow, which renders measures of greenness inadequate. To account for snow, we used snow depth from a meteorological station nearby (see below) and the blue chromatic coordinate (BCC = blue/[red + green + blue]). High BCC values occur if pixels are saturated or over-exposed, which is the case for snow. Manually inspecting the images, we found a BCC threshold of 0.3 good for indicating snow. Since snow melts faster if on trees than if on ground, we evaluated the BCC for each ROI, and masked GCC values, if snow depth was $>$ 0 cm and the BCC of the respective ROI was $>$ 0.3.

To account for fog, we calculated the blurriness of each image, by applying an edge-finding algorithm, and counting the edge pixels. For this we applied the "Find Edges" tool in software ImageJ, which uses a Sobel edge detector (see also ImageJ online documentation for details on the convolution kernels used). This resulted in a rough measure of the quality of the images, with low values indicating fog (few edges) and high values indicating sharp images. This blur metric was used as weights for modelling as shown below.

2.5. Vegetation indices from remote sensing

Based on MODIS it was possible to extract vegetation indices from January 2001 to June 2016, thus also covering the period before the storm. Three vegetation indices were derived from MODIS collection version 5, the NDVI (normalized difference vegetation index), EVI (enhanced vegetation index) and PPI (plant phenology index), which are all differently affected by snow (Jin and Eklundh, 2014). NDVI and EVI were available in 16 day time intervals at 250 m spatial resolution from product MOD13Q1, which also comprises their pixel reliability (QA Code). Values with QA codes 2 and 3, that is snow and clouds, were masked out. PPI was calculated according to Jin and Eklundh (2014), using nadir-viewing reflectances from product MCD43A4, which are available in 8 day time intervals at 500 m spatial resolution. Solar zenith angle, necessary to calculate the PPI, was available from ancillary data set MCD43A2, which also comprises a quality code, and a snow flag. Only snow-free values were used for modelling below. Other constants in the PPI formula were set as to the same values as in Jin and Eklundh (2014).

To minimize random error in MODIS values and ensure better comparability to the flux footprint of the site, NDVI and EVI values were averaged over a 3 × 3 pixel area centered on the location of the tower, and PPI values over a 2 × 2 pixel area. Fig. S2 compares average values to single pixel and 5 × 5 (NDVI and EVI) and 3 × 3 (PPI) pixel areas.

2.6. Estimating gross primary production (GPP) from turbulent CO_2 exchange

For assessing net ecosystem exchange (NEE) for the years 2010 to 2015 the setup described by Lindauer et al. (2014) was used. NEE (originally in mmol/m^{2}s, then converted to gC/m^{2}s) was calculated according to Foken et al. (2012) using the measured eddy-covariance data processed by the data analysis software TK3 (Mauder et al., 2013). Only high quality data (flagged 0 or 1 in TK3) was retained. For outlier removal, the data was split into 1.5 hour intervals over 25 consecutive days, yielding up to 75 values of 30 min fluxes. For each of these sets, flux values were removed that were 3*MAD (median absolute deviation, adjusted by 1.4826 for asymptotic normality) above or below the median.

Further processing of the flux data was performed using standard procedures (Reichstein et al., 2005) implemented in the REddyProc package in R (Reichstein and Moffat, 2015) in 2-year blocks (2010–2011, 2012–2013, and 2014–2015) to account for succession. These included ustar filtering (with estimated thresholds 0.35, 0.36, 0.28 m s^{-1} for the three periods, while Lindauer et al. (2014) used 0.3 m s^{-1} as threshold for the same site, however, for a different period: 2009–2013), gap-filling of net-ecosystem-exchange (NEE), and partitioning into gross primary production (GPP) and ecosystem respiration (R_{eco}) using soil temperature to estimate R_{eco}. Finally, daily means were calculated.

2.7. Meteorological data and climatological growing season indices

Auxiliary daily air temperature, precipitation and snow depth was available in approximately 12 km distance at similar altitude at the climate station Großer Arber (49.113°N, 13.134°R, 1436 m a.s.l.) from the German Meteorological Service (DWD). From June 2014 onwards, snow depth was available only every second day; the missing values were interpolated as mean of the previous and next day.

Over the last 30 years, the mean annual temperature was 3.67 °C and mean annual precipitation was 1480 mm. The region is covered with snow throughout December to March/April, but snow might start as early as October and stay until May (see Fig. S3 for meteorology during the study period).

Temperature was also directly measured at the study site, but it contained several gaps during the study period, so we decided to use the complete station data from the DWD to calculate climatological growing season indices. There is no universal definition for climatological growing season indices (Walther and Linderholm, 2006), so our choice fell on the most widely used ones: Last frost (after which no minimum temperature below 0 °C), first five consecutive days above 5 °C mean temperature, first frost, and first five consecutive days below 5 °C. As snow is also a major influence at this site, we calculated two indices based on the snow depth data: first and last day of continuous snow cover, where continuous means at least 20 days of snow depth $>$ 0 cm in order to remove short snow episodes before or after the main snow season.

2.8. Phenological data

Data from a bark beetle trap (pheromone-baited slot trap) near the study site (Bampferfleck, 49.094°N, 13.302°E, 1228 m a.s.l.), was made available from the national park administration (contact: Franz Baierl) for the years 2010 to 2015. The trap with *Ips typographus* bark beetles was usually emptied once a week from start/mid of May to mid of September, depending on snow and weather conditions.

Phenological data on May sprouting of Norway spruce, first flowering of meadow foxtail (*Alopecurus pratensis* L.) and full flowering of cock's-foot/orchard grass (*Dactylis glomerata* L.) were also provided by the German Meteorological Service for Großer Arber.

2.9. Modelling time series of GCC, NDVI, EVI, PPI and GPP, and extracting phenological dates

GCC, NDVI, EVI, PPI and GPP were modelled with penalized splines (Wood, 2016) using all available years. Weights were included for GCC (the blur metric), and for NDVI, EVI and PPI (mean of all pixel quality codes in reverse order times the number of pixels available per value). The function space for the penalized splines was set to have 12 degrees of freedom per year (or 1 df per 30 days) as maximum basis dimension (similar to the values in Bradley et al., 2007), as this threshold was low enough to capture the seasonal dynamics but not too high to include short-term variability. The penalized spline approach was chosen over

fitting parametric functions, such as double-logistic curves (as e.g. in Gu et al., 2009; Klosterman et al., 2014), because it allowed the incorporation of weights, was more flexible, and allowed a continuous signal over multiple years (the parametric double-log have to be fit separately to each year). Fig. S4 shows a comparison of the different approaches to model the time series, in which the estimated curves are similar in standard cases, but differ for more complicated seasons, and where the double-log curves fit the underlying data worse than the penalized splines.

From the modelled time series the days of start (SOS), end (EOS), and peak of season (POP) were extracted using the threshold method (White et al., 1997). SOS and EOS are defined as the time, when 50% of the maximum amplitude, that is difference between annual maxima and minima, are reached. While other methods exist to extract phenological dates, for example based on first derivatives or more complicated heuristics (Gu et al., 2009; Klosterman et al., 2014), we chose the threshold approach, because it yielded the most robust and meaningful estimates for all variables (GCC, NDVI, EVI, PPI and GPP) in all years (see Fig. S5 for a comparison).

2.10. Intra- and interannual correlations of GPP with proxies

Intraannual correlations of GPP with satellite vegetation indices and webcam GCC were performed by taking 16 day means of GPP, GCC, and PPI to match the temporal resolution of NDVI and EVI. Then Pearson correlation coefficients were calculated between all variables using all values from all years available.

To check how well remotely sensed vegetation indices and webcam greenness capture interannual variation in GPP, seasonal (Apr–Oct, May–Sep) means were calculated for the six years (2010–2015). As the webcam suffered from multiple hardware and connection failures, Apr-Oct means were only available for 2011 and 2014, and May-Sep means only for 2011–2014.

3. Results

3.1. Succession

The data-driven clustering of the webcam images resulted in identifying three distinct image regions (ROIs, see Fig. 2). The first cluster corresponds to the area that was covered by spruce trees during the whole study period. The second cluster was initially showing grass and became successively overgrown by spruce trees (and parts of a deciduous broadleaf in the bottom-right corner of the image). The third cluster corresponds to grass that remained visible until the end of the study period, however, a small fraction of pixels in this cluster also were covered with spruce at the end. The proportions of the three clusters to the total image area are 39% (spruce), 39% (grass to spruce), and 22% (grass).

The remotely sensed vegetation indices (NDVI, EVI and PPI) were available also before the storm, and show a clear break after the windthrow (Fig. 3). NDVI annual maxima after the storm were lower than before, but steadily increased afterwards with a significant linear trend ($p < 0.05$). EVI values did not depict a clear seasonality before the storm, only afterwards. Annual maxima of EVI stayed constant until 2010 and increased steadily thereafter. PPI also showed a clear increasing trend in annual maxima after the storm ($p < 0.05$).

The recovery of the forest stand after the windthrow resulted in an increased primary production, going from 603 gC m^{-2} y^{-1} in 2010 to 862 gC m^{-2} y^{-1} in 2015, while at same time net ecosystem exchange decreased from 285 gC m^{-2} y^{-1} in 2010 to -26 gC m^{-2} y^{-1} in 2015, thus indicating a switch in the ecosystem from carbon source to sink from 2014 to 2015.

At the same time, peak annual GPP increased from 4.182 gC m^{-2} d^{-1} in 2010 to 6.939 gC m^{-2} d^{-1} in 2015 (Table 1). This trend was mirrored in increasing annual maxima of NDVI, EVI, and PPI. Also the webcam derived index (GCC) showed an increase in annual maxima for the grass-to-spruce transition ROI from 0.368 in 2010 to 0.378 in 2015, while the other two ROIs had no apparent trend.

3.2. The seasonal course of GCC, NDVI, EVI, PPI, GPP and bark beetles

Time series of webcam GCC showed a strong seasonality for all three ROIs (Fig. 4). In general, the spruce ROI time series showed an increase early in the year around doy (day of year) 100, when the snow season ended, and a second smaller increase after May sprouting. After reaching its annual peak, GCC decreased slowly until the snow season started again, after which came a steep decrease to the annual minimum.

Grass GCC had a more pronounced peak-shape, with a steeper increase, that was later than the spruce increase, followed by a steeper decrease, which was earlier than the spruce decrease. In 2012 and 2014 the decrease was not as steep as in the other years.

The grass-to-spruce GCC time series resembled a mixture of the grass and spruce GCC time series with changing weights: In 2010 it had more of a peak shape like the grass GCC time series, and year after year it became more similar to the spruce GCC time series.

Remotely sensed vegetation activity (NDVI, EVI and PPI) also showed a strong seasonality. NDVI and EVI were similar and resembled the spruce GCC time series. PPI showed shorter seasons, which started later and ended earlier than NDVI and EVI, and resembled a mixture of the grass and spruce GCC series.

Gross primary production (GPP) seasonality matched the greenness seasonality with its steep increase in spring and a less steep decrease after reaching its peak. In 2014, it showed a longer lasting productive summer, which was mirrored also in NDVI, EVI, PPI and GCC time series. However, GPP was in general more similar to PPI than NDVI or EVI.

Bark beetle counts were high from 2010 to 2013, and then decreased sharply in 2014 and 2015. In 2010 and 2011 one major peak was attained in early July and end of May, respectively. For 2012 to 2014 two peaks corresponding to two beetle generations were visible: The first was end of June and the second beginning of August for 2012 and 2013, and two weeks earlier for 2014. In 2015 counts were much lower and no peaks obviously visible. This interannual variability was not matched by either GCC, satellite vegetation indices or GPP.

The common seasonality induced high correlations between GCC time series, satellite vegetation indices and GPP (Fig. S6). NDVI correlated similarly to all GCC ROIs (0.71-0.74), EVI correlated higher with grass (0.79) and grass-to-spruce (0.77) than spruce (0.67), and PPI more with grass and grass-to-spruce (both 0.84) than with spruce (0.67). GPP correlated highest with grass-to-spruce GCC (0.87), followed by PPI (0.82), grass GCC (0.82) and EVI (0.80).

3.3. Interannual variation in GPP and vegetation indices

Seasonal GPP was compared to satellite and webcam proxies (Fig. 5). GPP increased from year to year in the study period due to the succession, as did remotely sensed vegetation indices and the grass-to-spruce GCC (see Table 1), resulting in high correspondence of seasonal GPP with seasonal NDVI, EVI, PPI, grass-to-spruce GCC, and grass GCC. Only spruce GCC showed a negative relationship to GPP, due to a decreasing trend in seasonal spruce GCC.

3.4. Comparison of growing season indices

Estimates of start (SOS) and end of season (EOS) dates varied considerably within visual GCC derived indices, but also compared to GPP, climatological indices, or traditional phenological observations (Fig. 6; see also Figs. S7 and S8 for scatterplots comparing all SOS and EOS dates). GCC derived SOS of spruce was 20–48 days earlier than grass, while spruce-EOS was 28–99 days later than grass-EOS. Grass-to-

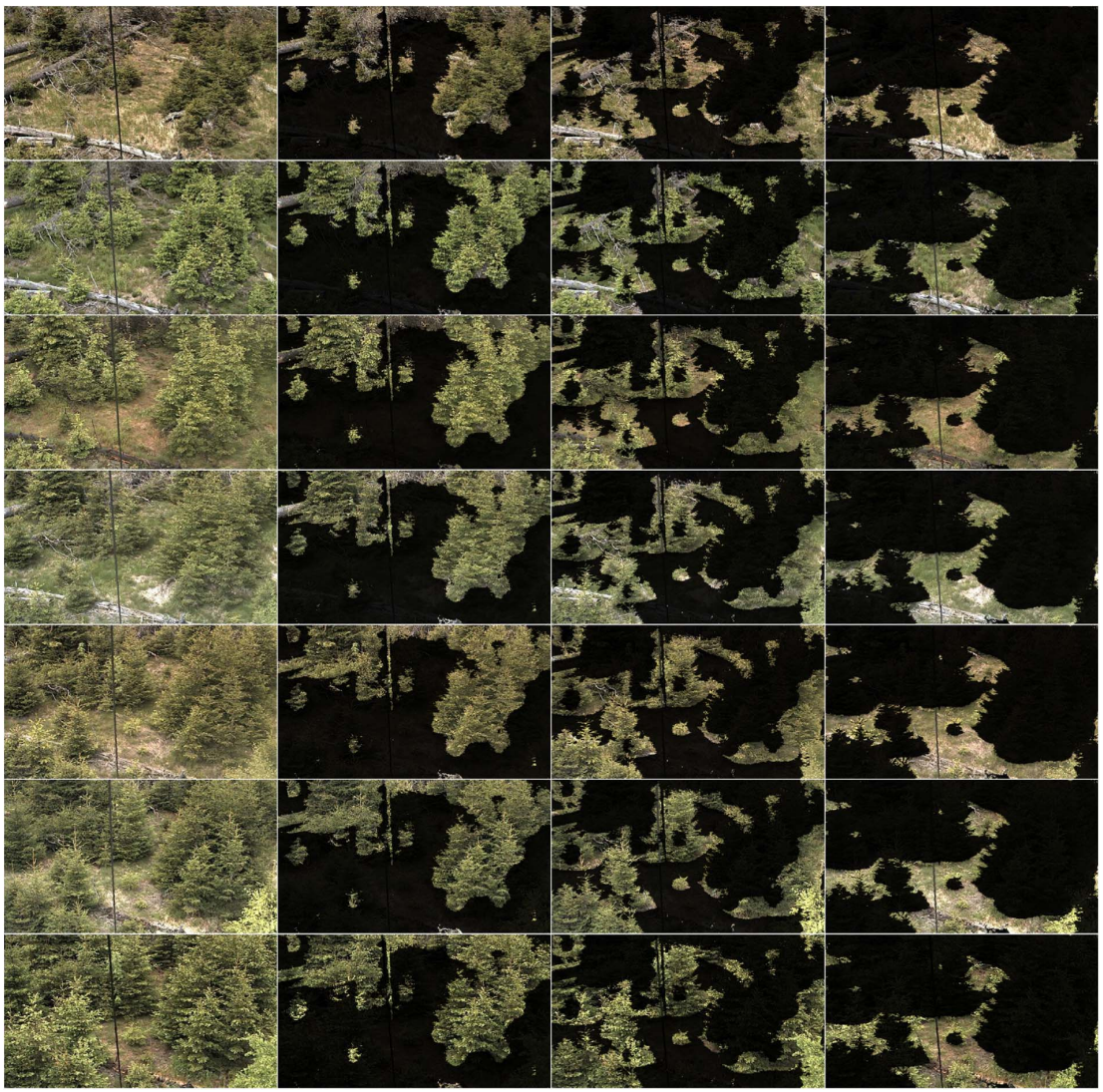

Fig. 2. Sample images from June of each year (2010–2016, top to bottom) showing the succession in the study site (first column). The other images show overlays of the three automatically extracted regions of interest (ROI) for each sample image. The three ROIs represent, from left to right, spruce, grass to spruce, and grass.

spruce-SOS was closer to grass-SOS for 2011 and 2012 and closer to spruce-SOS for 2014 and 2015. In each year the order in SOS was spruce, grass-to-spruce and grass. For EOS the order was reversed.

SOS of NDVI, EVI and PPI were most similar to grass, with NDVI-SOS on average 7 days earlier, EVI-SOS 2 days earlier, and PPI-SOS 7 days later than grass-SOS; while for EOS no correspondence was found. SOS of GPP matched best with PPI, which was on average 4 days later, and grass, which was 1 day earlier, while GPP-EOS had no correspondence to other EOS dates.

Of the climatological indices for SOS, the 5-days-above–5 °C date and the last day of continuous snow cover were good indicators of spruce-SOS, while the last frost corresponded best to grass-SOS, albeit being on average 9 days after grass-SOS. For EOS climatological indices, the only correspondence was between spruce-EOS and the 5-days-below–5 °C date.

The phenological observations of *P. abies*, *A. pratensis*, and *D. glomerata* were highly correlated with each other within years, where *P. abies* was on average 20 days earlier than *A. pratensis*, and *A. pratensis* 15 days earlier than *D. glomerata*. They were also correlated to GPP-SOS, where *P. abies* was on average 8 days later than GPP-SOS, and the other two accordingly to their difference to *P. abies*.

Start of bark beetle flight matched the phenology of *P. abies* very good for 2011, 2013, 2014 and 2015 (differences less than 6 days), but in 2010 and 2012 differences were 21 and 30 days. Climatological indices and the other variables had no apparent relationship to start dates of bark beetle flight.

Length of season (LOS = EOS minus SOS) had no apparent correspondence between the variables, except for a high correlation between the length of the snow-free season and the LOS determined by the 5-days–5 °C rules.

4. Discussion

Our study showed the benefits of webcam observations in monitoring the succession of a windthrow disturbed forest. The windthrow-caused uprooting of the taller spruce trees has left space for grasses and other vegetation to grow between the dead-wood (Fig. 2) causing a clearer seasonality of remotely sensed NDVI and EVI than before

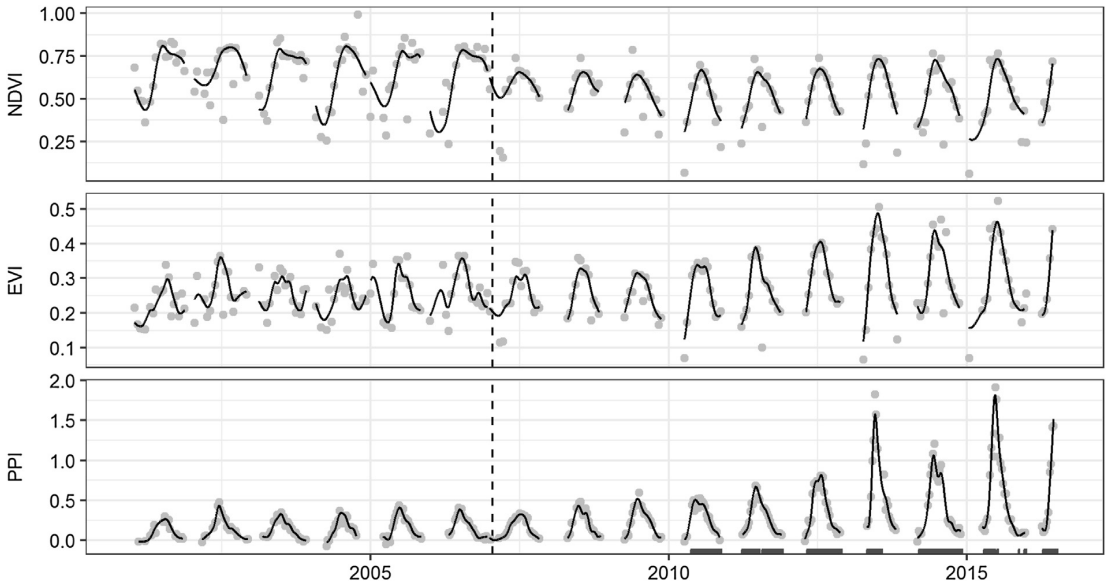

Fig. 3. Remotely sensed normalized difference vegetation index (NDVI), enhanced vegetation index (EVI) and plant phenology index (PPI) at study site. Solid line is the modelled time series (see Methods for details). Dashed vertical line is when the storm hit the area (January 2007). Small lines at the bottom indicate when the webcam was operational.

Table 1
Annual maxima of GPP (gross primary production, gC m^{-2} d^{-1}), NDVI (normalized difference vegetation index), EVI (enhanced vegetation index), PPI (plant phenology index), and GCC (green chromatic coordinate) of the three automatically derived image regions. The maximum value is taken from the modelled time series, which are lower than the original measured values.

Year	GPP	NDVI	EVI	PPI	GCC Spruce	Grass-to-spruce	Grass
2010	4.182	0.670	0.339	0.510	0.375	0.368	0.364
2011	4.063	0.657	0.389	0.672	0.381	0.374	0.363
2012	4.724	0.676	0.405	0.817	0.378	0.373	0.357
2013	5.621	0.733	0.488	1.579	0.378	0.376	0.364
2014	6.181	0.728	0.439	1.065	0.377	0.377	0.359
2015	6.939	0.734	0.463	1.817	0.376	0.378	0.372

(Fig. 3). Furthermore, younger spruce trees and emerged seedlings now made use of the more favorable growth conditions as mirrored in increasing trends of GPP. Since the spruce needles are greener (in terms of GCC) than grasses, also the webcam derived index GCC showed an increasing trend.

While GPP, NDVI, EVI, PPI and webcam indices all showed an increasing trend in productivity and greenness following the recovery of the forest (Table 1), only by GPP measurements it is possible to estimate the carbon sink/source strength, as well as the time when the ecosystem switches from source to sink or vice versa. Our estimates of annual net ecosystem exchange (NEE) for the years 2010 to 2013 are 286, 239, 272, and 118 gC m^{-2}, which are slightly different from the estimates in Lindauer et al. (2014): 255, 221, 240, and 167 gC m^{-2} but well within their uncertainty ranges. The differences may arise from different time windows used to calculate the ecosystem respiration as well as from the gap-filling. Thus our estimated values of NEE for 2014 and 2015 (47 and -26 gC m^{-2}) indicate that the windthrow area changed from carbon source to a sink around 2015 or shortly thereafter.

The three satellite-derived vegetation indices, NDVI, EVI, and PPI, differed considerably in their seasonal time series (Fig. 4) as well as in the estimated start and end of season dates (Fig. 6). NDVI and EVI are more similar to each other than compared to the PPI, which may be because of the different spatial and temporal resolutions (NDVI and EVI have 250 m pixels in 16 day intervals, and PPI has 500 m in 8 day intervals) and spatial aggregation (3×3 pixels for NDVI and EVI, and 2×2 pixels for PPI). However, the snow masked pixels agree in all three indices (Fig. 4) during the study period 2010–2016. This is not the case for the period before the storm hit the area (Fig. 3), during which the indices differed even more, and also NDVI and EVI were less similar to each other than in the period after the storm. So it is likely that these differences arise rather from the different algorithms used to calculate the indices (Jin and Eklundh, 2014; Klosterman et al., 2014) and their varying performance for different land covers (Huete et al., 2002).

The interannual variability of seasonal GPP values was positively associated to the NDVI, EVI, PPI, grass-to-spruce GCC, and grass GCC proxies in this study because of concurrent trends due to the succession (Fig. 5), while GPP was negatively associated to spruce GCC because of opposite trends. The seasonality of GPP matched best to the PPI, especially compared to NDVI or EVI, which confirms the findings of Jin and Eklundh (2014) that the PPI correlates better with GPP than NDVI or EVI for evergreen needleleaf forests.

The fraction of the webcam images showing grass was initially 61% in 2010 and declined to 22% in 2016. The surrounding of the study area is dominated by spruce trees, and the actual proportion of grass in the surroundings is smaller than in the webcam images (inferred from site knowledge), which explains why NDVI, EVI, and partly also PPI, were so closely related to the spruce part of the image concerning seasonality (Fig. 4). However, concerning SOS dates, NDVI, EVI, and PPI were more similar to the grass part (Fig. 6). So although the image composition might not depict the true proportion of the surrounding vegetation, by using different ROIs also underrepresented vegetation types could be analyzed, which is not yet possible with satellite measurements. An interesting question for further research would be if CO_2 fluxes could be attributed to different species by using webcam information.

The timing of the first bark beetle flight was not related to webcam, NDVI or climatological indices. Bark beetles start flying when daytime temperatures are above 16.5° and weather conditions (for example no precipitation) are suitable (Baier et al., 2007). Climatological indices derived from snow or 5 °C threshold were thus not useful in determining first flight, and neither was the onset of photosynthesis, derived from GCC, satellite vegetation indices, or GPP time series. However, phenological observations on spruce were useful in predicting bark beetle flight for 4 out of 6 six years. Zang et al. (2015) also showed

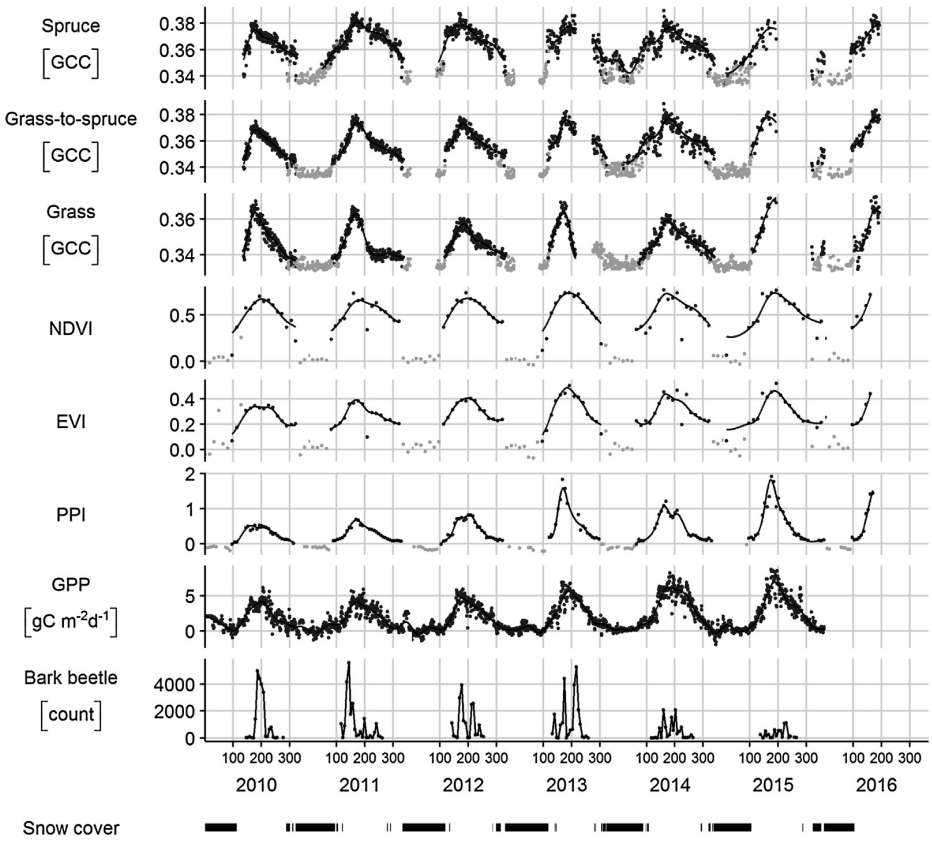

Fig. 4. Time series of green chromatic coordinate (GCC) of webcam image regions; remotely sensed normalized difference vegetation index (NDVI), enhanced vegetation index (EVI) and plant phenology index (PPI); gross primary production (GPP); bark beetle counts; and snow cover (black if snow depth > 0 cm). Grey points in the GCC, NDVI, EVI, and PPI time series indicate values with snow, which were masked out.

that phenology predicted flight activity better than thermal sums.

While bark beetles can have significant impacts on GPP and leaf area index (Bright et al., 2013), we could not detect any links between bark beetle occurrence and GPP or vegetation indices. However, initial infestation with bark beetles started soon after the windthrow and was followed by efforts from the national park to control the outbreak at its boundaries. The succession definitively overweighs the influence of the bark beetle infestation on GPP and vegetation indices.

The use of climatological growing season indices is based on temperature being a limiting factor for vegetation (Walther and Linderholm, 2006). However, depending on the region, other factors, such as photoperiod, precipitation, frost, or snow, might be more important. The limiting factors for this study site were depending on the species, since temperature and snow were correlated to spruce

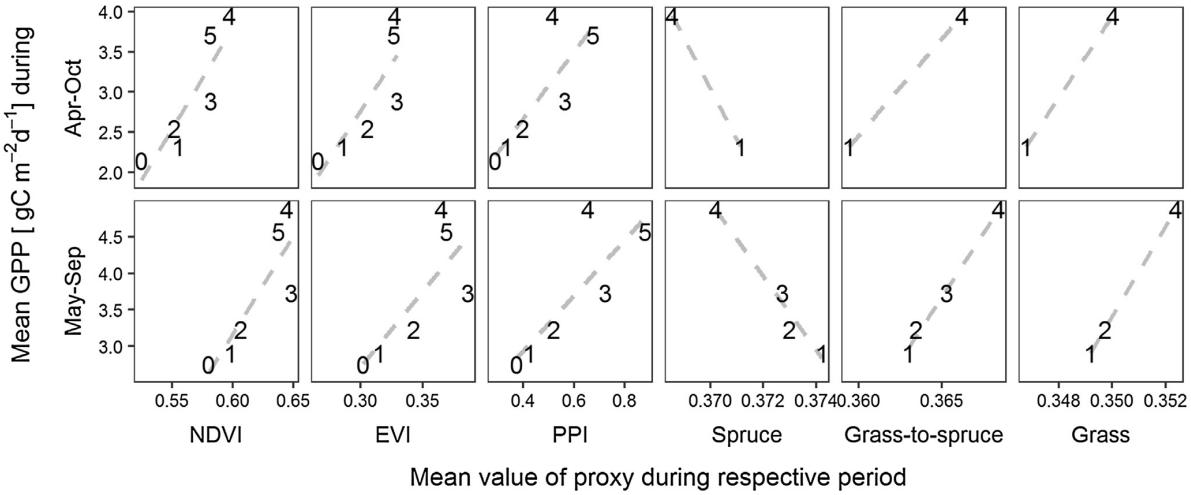

Fig. 5. Mean seasonal values of GPP (gross primary production) versus satellite and webcam proxies. Points are labelled with last digit of the year (that is 0 = 2010,…, 5 = 2015). Grey dashed line represents a linear regression. Missing points in the webcam proxies (spruce, grass-to-spruce, grass) are due to lack of data. Other abbrevations: normalized difference vegetation index (NDVI), enhanced vegetation index (EVI), plant phenology index (PPI).

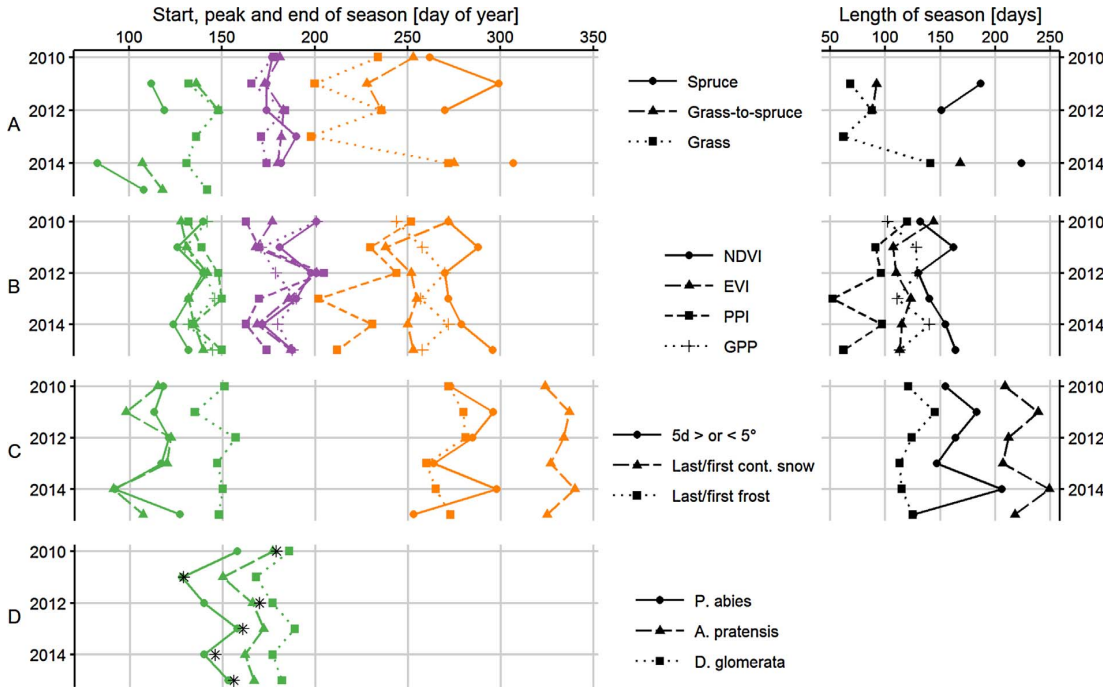

Fig. 6. Start (green), peak (purple), end (orange), and length (black) of season derived from (A) webcam image ROIs, (B) satellite and flux measurements, (C) abiotic proxies, and (D) phenology. Stars in panel (D) denote start of bark beetle flight. Phenological observations (D) are on May sprouting of *Picea abies*, first flowering of *Alopecurus pratensis* and full flowering of *Dactylis glomerata*. Abbreviations: NDVI (normalized difference vegetation index), EVI (enhanced vegetation index), PPI (plant phenology index), GPP (gross primary production), 5d > or < 5° (first occurrence of five consecutive days above or below 5 °C mean temperature), Last/first cont. snow (last and first day of continuous snow cover), Last/first frost (last or first day < 0 °C minimum temperature).

greenness, whereas frost was correlated to grass greenness.

5. Summary and conclusion

Webcam images were used to monitor the succession in a windthrow disturbed spruce forest. By automatically splitting the image in three regions of interest – spruce, grass, and grass grown over by spruce – the development of each vegetation class could be tracked separately, thus supplementing integrated observations derived from satellite or turbulent CO_2 exchange.

From the field of view of the camera 39% of the pixels showed grass in 2010 and became overgrown by spruce in 2016. This transition ROI showed an increasing trend in GCC, which was mirrored in increasing trends of GPP and satellite NDVI, EVI, and PPI. The seasonality of GPP was best matched by grass-to-spruce GCC and PPI. Interannual variation of seasonal GPP was positively correlated to grass-to-spruce GCC, NDVI, EVI and PPI, due to common trends induced by the succession. Climatological growing season indices based on temperature and snow could indicate SOS and EOS of spruce, while phenological observations correlated with GPP-SOS and timing of bark beetle flight.

An extensive network of scientific cameras is currently documenting the phenological development and is steadily growing into a global network (Brown et al., 2016), which could be further extended by tapping into the even wider availability of public non-scientific webcams (Graham et al., 2010; Jacobs et al., 2009; Morris et al., 2013). These phenocams and webcams could supplement satellite phenology to offer an unprecedentedly detailed look at our earth in order to observe phenology, infer vegetation activity, monitor disturbances and assess a possible recovery.

Acknowledgements

We thank the Bavarian Forest National Park for the opportunity to conduct this study within their boundaries, for their assistance, and for providing additional data. We much appreciate the efforts of R. Helm, M. Lindauer and C. Schunk in setting up and maintaining the camera. We thank G. Misra and S. Asam for fruitful ideas and discussions. This research has received funding from the European Research Council under the European Union's Seventh Framework Programme (FP7/2007-2013) [ERC grant number 282250]. It was performed with the support of the Technische Universität München – Institute for Advanced Study, funded by the German Excellence Initiative. Further, we acknowledge the funding from the Helmholtz Association and the Federal Ministry of Education and Research, Germany (BMBF) in the framework of TERENO (Terrestrial Environmental Observatories).

Appendix A. Supplementary data

Supplementary data associated with this article can be found, in the online version, at http://dx.doi.org/10.1016/j.agrformet.2017.05.020.

References

Baier, P., Pennerstorfer, J., Schopf, A., 2007. PHENIPS—A comprehensive phenology model of Ips typographus (L.) (Col., Scolytinae) as a tool for hazard rating of bark beetle infestation. For. Ecol. Manag. 249, 171–186. http://dx.doi.org/10.1016/j.foreco.2007.05.020.

Barford, C.C., Wofsy, S.C., Goulden, M.L., Munger, J.W., Pyle, E.H., Urbanski, S.P., Hutyra, L., Saleska, S.R., Fitzjarrald, D., Moore, K., 2001. Factors Controlling Long- and Short-Term Sequestration of Atmospheric CO2 in a Mid-latitude Forest. Science 294, 1688–1691. http://dx.doi.org/10.1126/science.1062962.

Barichivich, J., Briffa, K.R., Myneni, R.B., Osborn, T.J., Melvin, T.M., Ciais, P., Piao, S., Tucker, C., 2013. Large-scale variations in the vegetation growing season and annual cycle of atmospheric CO2 at high northern latitudes from 1950 to 2011. Glob. Change Biol. 19, 3167–3183. http://dx.doi.org/10.1111/gcb.12283.

Bothmann, L., 2016. phenofun: Automated Processing of Webcam Images for Phenological Classification R package version 0.0.3.

Bothmann, L., Menzel, A., Menze, B.H., Schunk, C., Kauermann, G., 2017. Automated Processing of Webcam Images for Phenological Classification. PLOS One 12 http://

dx.doi.org/10.1371/journal.pone.0171918.
Bradley, B.A., Jacob, R.W., Hermance, J.F., Mustard, J.F., 2007. A curve fitting procedure to derive inter-annual phenologies from time series of noisy satellite NDVI data. Remote Sens. Environ. 106, 137–145. http://dx.doi.org/10.1016/j.rse.2006.08.002.
Bright, B.C., Hicke, J.A., Meddens, A.J.H., 2013. Effects of bark beetle-caused tree mortality on biogeochemical and biogeophysical MODIS products. J. Geophys. Res. Biogeosciences 118, 974–982. http://dx.doi.org/10.1002/jgrg.20078.
Brown, T.B., Hultine, K.R., Steltzer, H., Denny, E.G., Denslow, M.W., Granados, J., Henderson, S., Moore, D., Nagai, S., SanClements, M., Sánchez-Azofeifa, A., Sonnentag, O., Tazik, D., Richardson, A.D., 2016. Using phenocams to monitor our changing Earth: toward a global phenocam network. Front. Ecol. Environ. 14, 84–93. http://dx.doi.org/10.1002/fee.1222.
Dixon, R.K., Solomon, A.M., Brown, S., Houghton, R.A., Trexier, M.C., Wisniewski, J., 1994. Carbon Pools and Flux of Global Forest Ecosystems. Science 263, 185–190. http://dx.doi.org/10.1126/science.263.5144.185.
Dose, V., Menzel, A., 2006. Bayesian correlation between temperature and blossom onset data. Glob. Change Biol. 12, 1451–1459. http://dx.doi.org/10.1111/j. 1365-2486.2006.01160. x.
Dragoni, D., Schmid, H.P., Wayson, C.A., Potter, H., Grimmond, C.S.B., Randolph, J.C., 2011. Evidence of increased net ecosystem productivity associated with a longer vegetated season in a deciduous forest in south-central Indiana. USA. Glob. Change Biol. 17, 886–897. http://dx.doi.org/10.1111/j. 1365-2486.2010.02281. x.
Foken, T., Aubinet, M., Leuning, R., 2012. The Eddy Covariance Method. In: Aubinet, M., Vesala, T., Papale, D. (Eds.), Eddy Covariance, Springer Atmospheric Sciences. Springer, Netherlands, pp. 1–19. http://dx.doi.org/10.1007/978-94-007-2351-1_1.
Fu, Y.H., Piao, S., Op de Beeck, M., Cong, N., Zhao, H., Zhang, Y., Menzel, A., Janssens, I.A., 2014. Recent spring phenology shifts in western Central Europe based on multiscale observations. Glob. Ecol. Biogeogr. 23, 1255–1263. http://dx.doi.org/10.1111/geb.12210.
Graham, E.A., Riordan, E.C., Yuen, E.M., Estrin, D., Rundel, P.W., 2010. Public Internet-connected cameras used as a cross-continental ground-based plant phenology monitoring system. Glob. Change Biol. 16, 3014–3023. http://dx.doi.org/10.1111/j. 1365-2486.2010.02164. x.
Grünwald, T., Bernhofer, C., 2007. A decade of carbon, water and energy flux measurements of an old spruce forest at the Anchor Station Tharandt. Tellus B 59. http://dx.doi.org/10.3402/tellusb.v59i3.17000.
Gu, L., Post, W., Baldoucchi, D., Black, A., Suyker, A., Verma, S., Vesala, T., 2009. Characterizing the Seasonal Dynamics of Plant Community Photosynthesis Across a Range of Vegetation Types. Phenology of Ecosystem Processes: Applications in Global Change Research. Springer New York, New York, NY.
Henneken, R., Dose, V., Schleip, C., Menzel, A., 2013. Detecting plant seasonality from webcams using Bayesian multiple change point analysis. Agric. For. Meteorol. 168, 177–185. http://dx.doi.org/10.1016/j.agrformet.2012.09.001.
Huete, A., Didan, K., Miura, T., Rodriguez, E.P., Gao, X., Ferreira, L.G., 2002. Overview of the radiometric and biophysical performance of the MODIS vegetation indices. Remote Sens. Environ. 83, 195–213. http://dx.doi.org/10.1016/s0034-4257(02)00096-2.
Jacobs, N., Burgin, W., Fridrich, N., Abrams, A., Miskell, K., Braswell, B.H., Richardson, A.D., Pless, R., 2009. The global network of outdoor webcams: properties and applications. ACM Presshttp://dx.doi.org/10.1145/1653771.1653789. p. 111.
Jeganathan, C., Dash, J., Atkinson, P.M., 2014. Remotely sensed trends in the phenology of northern high latitude terrestrial vegetation, controlling for land cover change and vegetation type. Remote Sens. Environ. 143, 154–170. http://dx.doi.org/10.1016/j.rse.2013.11.020.
Jeong, S.-J., Ho, C.-H., Gim, H.-J., Brown, M.E., 2011. Phenology shifts at start vs. end of growing season in temperate vegetation over the Northern Hemisphere for the period 1982-2008. Glob. Change Biol. 17, 2385–2399. http://dx.doi.org/10.1111/j. 1365-2486.2011.02397. x.
Jin, H., Eklundh, L., 2014. A physically based vegetation index for improved monitoring of plant phenology. Remote Sens. Environ. 152, 512–525. http://dx.doi.org/10.1016/j.rse.2014.07.010.
Julitta, T., Cremonese, E., Migliavacca, M., Colombo, R., Galvagno, M., Siniscalco, C., Rossini, M., Fava, F., Cogliati, S., Morra di Cella, U., Menzel, A., 2014. Using digital camera images to analyse snowmelt and phenology of a subalpine grassland. Agric. For. Meteorol. 198–199, 116–125. http://dx.doi.org/10.1016/j.agrformet.2014.08.007.
Keenan, T.F., Darby, B., Felts, E., Sonnentag, O., Friedl, M.A., Hufkens, K., O'Keefe, J., Klosterman, S., Munger, J.W., Toomey, M., Richardson, A.D., 2014. Tracking forest phenology and seasonal physiology using digital repeat photography: a critical assessment. Ecol. Appl. 24, 1478–1489. http://dx.doi.org/10.1890/13-0652.1.
Klosterman, S.T., Hufkens, K., Gray, J.M., Melaas, E., Sonnentag, O., Lavine, I., Mitchell, L., Norman, R., Friedl, M.A., Richardson, A.D., 2014. Evaluating remote sensing of deciduous forest phenology at multiple spatial scales using PhenoCam imagery. Biogeosciences 11, 4305–4320. http://dx.doi.org/10.5194/bg-11-4305-2014.
Liang, L., Schwartz, M.D., Fei, S., 2011. Validating satellite phenology through intensive ground observation and landscape scaling in a mixed seasonal forest. Remote Sens. Environ. 115, 143–157. http://dx.doi.org/10.1016/j.rse.2010.08.013.
Lindauer, M., Schmid, H.P., Grote, R., Mauder, M., Steinbrecher, R., Wolpert, B., 2014. Net ecosystem exchange over a non-cleared wind-throw-disturbed upland spruce forest—Measurements and simulations. Agric. For. Meteorol. 197, 219–234. http://dx.doi.org/10.1016/j.agrformet.2014.07.005.
Linderholm, H.W., 2006. Growing season changes in the last century. Agric. For. Meteorol. 137, 1–14. http://dx.doi.org/10.1016/j.agrformet.2006.03.006.
Luyssaert, S., Ciais, P., Piao, S.L., Schulze, E.-D., Jung, M., Zaehle, S., Schelhaas, M.J., Reichstein, M., Churkina, G., Papale, D., Abril, G., Beer, C., Grace, J., Loustau, D., Matteucci, G., Magnani, F., Nabuurs, G.J., Verbeeck, H., Sulkava, M., Van Der WERF, G.R., Janssens, I.A., Members of the CARBOEUROPE-IP SYNTHESIS TEAM, 2010. The European carbon balance. Part 3: forests. Glob. Change Biol. 16, 1429–1450. http://dx.doi.org/10.1111/j. 1365-2486.2009.02056. x.
Mauder, M., Cuntz, M., Drüe, C., Graf, A., Rebmann, C., Schmid, H.P., Schmidt, M., Steinbrecher, R., 2013. A strategy for quality and uncertainty assessment of long-term eddy-covariance measurements. Agric. For. Meteorol. 169, 122–135. http://dx.doi.org/10.1016/j.agrformet.2012.09.006.
Menzel, A., Helm, R., Zang, C., 2015. Patterns of late spring frost leaf damage and recovery in a European beech (Fagus sylvatica L.) stand in south-eastern Germany based on repeated digital photographs. Front. Plant Sci. 6, 110. http://dx.doi.org/10.3389/fpls.2015.00110.
Menzel, A., Jakobi, G., Ahas, R., Scheifinger, H., Estrella, N., 2003. Variations of the climatological growing season (1951-2000) in Germany compared with other countries. Int. J. Climatol. 23, 793–812. http://dx.doi.org/10.1002/joc.915.
Menzel, A., Sparks, T.H., Estrella, N., Koch, E., Aasa, A., Ahas, R., Alm-Kübler, K., Bissolli, P., Braslavská, O., Briede, A., Chmielewski, F.M., Crepinsek, Z., Curnel, Y., Dahl, Å., Defila, C., Donnelly, A., Filella, Y., Jatczak, K., Måge, F., Mestre, A., Nordli, Ø., Peñuelas, J., Pirinen, P., Remišová, V., Scheifinger, H., Striz, M., Susnik, A., Van Vliet, A.J.H., Wielgolaski, F.-E., Zach, S., Zust, A., 2006. European phenological response to climate change matches the warming pattern. Glob. Change Biol. 12, 1969–1976. http://dx.doi.org/10.1111/j. 1365-2486.2006.01193. x.
Migliavacca, M., Galvagno, M., Cremonese, E., Rossini, M., Meroni, M., Sonnentag, O., Cogliati, S., Manca, G., Diotri, F., Busetto, L., Cescatti, A., Colombo, R., Fava, F., Morra di Cella, U., Pari, E., Siniscalco, C., Richardson, A.D., 2011. Using digital repeat photography and eddy covariance data to model grassland phenology and photosynthetic CO2 uptake. Agric. For. Meteorol. 151, 1325–1337. http://dx.doi.org/10.1016/j.agrformet.2011.05.012.
Misra, G., Buras, A., Menzel, A., 2016. Effects of Different Methods on the Comparison between Land Surface and Ground Phenology—A Methodological Case Study from South-Western Germany. Remote Sens. 8, 753 10.3390/rs8090753.
Morris, D.E., Boyd, D.S., Crowe, J.A., Johnson, C.S., Smith, K.L., 2013. Exploring the Potential for Automatic Extraction of Vegetation Phenological Metrics from Traffic Webcams. Remote Sens. 5, 2200–2218. http://dx.doi.org/10.3390/rs5052200.
Nijland, W., de Jong, R., de Jong, S.M., Wulder, M.A., Bater, C.W., Coops, N.C., 2014. Monitoring plant condition and phenology using infrared sensitive consumer grade digital cameras. Agric. For. Meteorol. 184, 98–106. http://dx.doi.org/10.1016/j.agrformet.2013.09.007.
Petach, A.R., Toomey, M., Aubrecht, D.M., Richardson, A.D., 2014. Monitoring vegetation phenology using an infrared-enabled security camera. Agric. For. Meteorol. 195–196, 143–151. http://dx.doi.org/10.1016/j.agrformet.2014.05.008.
Reichstein, M., Falge, E., Baldocchi, D., Papale, D., Aubinet, M., Berbigier, P., Bernhofer, C., Buchmann, N., Gilmanov, T., Granier, A., Grünwald, T., Havránková, K., Ilvesniemi, H., Janous, D., Knohl, A., Laurila, T., Lohila, A., Loustau, D., Matteucci, G., Meyers, T., Miglietta, F., Ourcival, J.-M., Pumpanen, J., Rambal, S., Rotenberg, E., Sanz, M., Tenhunen, J., Seufert, G., Vaccari, F., Vesala, T., Yakir, D., Valentini, R., 2005. On the separation of net ecosystem exchange into assimilation and ecosystem respiration: review and improved algorithm. Glob. Change Biol. 11, 1424–1439. http://dx.doi.org/10.1111/j. 1365-2486.2005.001002. x.
Reichstein, M., Moffat, A.M., 2015. REddyProc: Data processing and plotting utilities of (half-)hourly eddy-covariance measurements R package version 0.7-1/r13.
Richardson, A.D., Jenkins, J.P., Braswell, B.H., Hollinger, D.Y., Ollinger, S.V., Smith, M.-L., 2007. Use of digital webcam images to track spring green-up in a deciduous broadleaf forest. Oecologia 152, 323–334. http://dx.doi.org/10.1007/s00442-006-0657-z.
Richardson, A.D., Keenan, T.F., Migliavacca, M., Ryu, Y., Sonnentag, O., Toomey, M., 2013. Climate change, phenology, and phenological control of vegetation feedbacks to the climate system. Agric. For. Meteorol. 169, 156–173. http://dx.doi.org/10.1016/j.agrformet.2012.09.012.
Seidl, R., Schelhaas, M.-J., Lexer, M.J., 2011. Unraveling the drivers of intensifying forest disturbance regimes in Europe. Glob. Change Biol. 17, 2842–2852. http://dx.doi.org/10.1111/j. 1365-2486.2011.02452. x.
Seidl, R., Schelhaas, M.-J., Rammer, W., Verkerk, P.J., 2014. Increasing forest disturbances in Europe and their impact on carbon storage. Nat. Clim. Change 4, 806–810. http://dx.doi.org/10.1038/nclimate2318.
Sonnentag, O., Hufkens, K., Teshera-Sterne, C., Young, A.M., Friedl, M., Braswell, B.H., Milliman, T., O'Keefe, J., Richardson, A.D., 2012. Digital repeat photography for phenological research in forest ecosystems. Agric. For. Meteorol. 152, 159–177. http://dx.doi.org/10.1016/j.agrformet.2011.09.009.
Toomey, M., Friedl, M.A., Frolking, S., Hufkens, K., Klosterman, S., Sonnentag, O., Baldocchi, D.D., Bernacchi, C.J., Biraud, S.C., Bohrer, G., Brzostek, E., Burns, S.P., Coursolle, C., Hollinger, D.Y., Margolis, H.A., McCaughey, H., Monson, R.K., Munger, J.W., Pallardy, S., Phillips, R.P., Torn, M.S., Wharton, S., Zeri, M., Richardson, A.D., 2015. Greenness indices from digital cameras predict the timing and seasonal dynamics of canopy-scale photosynthesis. Ecol. Appl. 25, 99–115. http://dx.doi.org/10.1890/14-0005.1.
Walther, A., Linderholm, H.W., 2006. A comparison of growing season indices for the Greater Baltic Area. Int. J. Biometeorol. 51, 107–118. http://dx.doi.org/10.1007/s00484-006-0048-5.
White, M.A., Thornton, P.E., Running, S.W., 1997. A continental phenology model for monitoring vegetation responses to interannual climatic variability. Glob. Biogeochem. Cycles 11, 217–234. http://dx.doi.org/10.1029/97GB00330.
Wingate, L., Ogée, J., Cremonese, E., Filippa, G., Mizunuma, T., Migliavacca, M., Moisy, C., Wilkinson, M., Moureaux, C., Wohlfahrt, G., Hammerle, A., Hörtnagl, L., Gimeno, C., Porcar-Castell, A., Galvagno, M., Nakaji, T., Morison, J., Kolle, O., Knohl, A., Kutsch, W., Kolari, P., Nikinmaa, E., Ibrom, A., Gielen, B., Eugster, W., Balzarolo, M., Papale, D., Klumpp, K., Köstner, B., Grünwald, T., Joffre, R., Ourcival, J.-M.,

Hellstrom, M., Lindroth, A., George, C., Longdoz, B., Genty, B., Levula, J., Heinesch, B., Sprintsin, M., Yakir, D., Manise, T., Guyon, D., Ahrends, H., Plaza-Aguilar, A., Guan, J.H., Grace, J., 2015. Interpreting canopy development and physiology using a European phenology camera network at flux sites. Biogeosciences 12, 5995–6015. http://dx.doi.org/10.5194/bg-12-5995-2015.

Wood, S., 2016. mgcv: Mixed GAM Computation Vehicle with GCV/AIC/REML Smoothness Estimation. R package version 1, 8–12.

Zang, C., Helm, R., Sparks, T.H., Menzel, A., 2015. Forecasting bark beetle early flight activity with plant phenology. Clim. Res. 66, 161–170. http://dx.doi.org/10.3354/cr01346.

Zhang, X., Friedl, M.A., Schaaf, C.B., Strahler, A.H., 2004. Climate controls on vegetation phenological patterns in northern mid- and high latitudes inferred from MODIS data. Glob. Change Biol. 10, 1133–1145. http://dx.doi.org/10.1111/j. 1529-8817.2003.00784. x.